

DIVERGENT APPLICATIONS OF FREE BASE CORROLES AND MANGANESE(III) CORROLES

Thesis Submitted to the Delhi Technological University
for the award of the degree of

DOCTOR OF PHILOSOPHY IN CHEMISTRY

By

ATUL VARSHNEY
(2k17/Ph.D/AC/05)

Under the supervision of:
Prof. (Dr.) ANIL KUMAR



**DEPARTMENT OF APPLIED CHEMISTRY
DELHI TECHNOLOGICAL UNIVERSITY
DELHI-110042 (INDIA)**

2023

©DELHI TECHNOLOGICAL UNIVERSITY-2023

ALL RIGHTS RESERVED

Dedication

*To my Parents
Mr. and Mrs. Varshney*

*To my siblings
Deeksha & Pash*

*To my wife
Shikha*

*To my son
Ayansh*

*Thanks for your endless sacrifices, love, support and
prayers*



**DEPARTMENT OF APPLIED CHEMISTRY
DELHI TECHNOLOGICAL UNIVERSITY
DELHI-110042 (INDIA)**

DECLARATION

I declare that the research work reported in the thesis entitled "**Divergent Applications of Free Base Corroles and Manganese(III) Corroles**" for the award of degree of **Doctoral of Philosophy** in Chemistry has been carried out by me under the supervision of **Prof. (Dr.) Anil Kumar**, Department of Applied Chemistry, Delhi Technological University, India.

The research work embodied in this thesis, except where otherwise indicate, is my original research. This thesis has not been submitted by me in part or full to any other University for the award of any degree or diploma. This thesis does not contain other person's data, graphs or other information, unless specifically acknowledged.

Atul Varshney
Candidate
2k17/Ph.D/AC/05

Prof. (Dr.) Anil Kumar
Supervisor

Prof. (Dr.) Anil Kumar
Head of Department
Applied Chemistry, DTU



**DEPARTMENT OF APPLIED CHEMISTRY
DELHI TECHNOLOGICAL UNIVERSITY
DELHI-110042 (INDIA)**

CERTIFICATE

This is to certify that the Ph.D. thesis entitled "**Divergent Applications of Free Base Corroles and Manganese(III) Corroles**" submitted to Delhi Technological University, Delhi, for the award of Doctoral of Philosophy in Chemistry, is based on original research work carried out by me, under the supervision of Prof. Anil Kumar, Department of Applied Chemistry, Delhi Technological University, Delhi, India. It is further certified that the work embodied in this thesis has neither partially or fully submitted to any other university or institution for the award of any degree or diploma.

Atul Varshney
Candidate
2k17/Ph.D/AC/05

This is to certify that the above statement made by the candidate is correct to the best of our knowledge.

Prof. (Dr.) Anil Kumar
Supervisor

Prof. (Dr.) Anil Kumar
Head of Department
Applied Chemistry, DTU

ACKNOWLEDGEMENTS

Foremost, I would like to express my sincere gratitude to my mentor Prof. Anil Kumar for the continuous support of my research work, for his patience, motivation, enthusiasm, and immense knowledge. His guidance helped me in all the time of research and writing of this thesis. I could not have imagined having a better advisor and mentor for my Ph.D.

I am extremely grateful to Prof. Yogesh Singh, former Honourable Vice-Chancellor and Prof. Jai Prakash Saini, Honourable Vice-Chancellor, Delhi Technological University for the kind permission for doing Ph.D. from DTU. Also my gratitude extends to Prof. Sudhir G. Warkar, former Head, Department of Applied Chemistry and Prof. Anil Kumar, Head, Department of Applied Chemistry, DTU for providing me the necessary facilities to carry out this research work. I wish to express my sincere thanks to whole faculty members of Department of Applied Chemistry, DTU for their help and support during this research work.

I am also thankful to the member of my Ph.D. SRC Committee, Prof. A. K. Singh (IIT Roorkee), Prof. S. Kukreti (University of Delhi), Prof. Sudhir G. Warkar (DTU), Dr. Mohan Singh Mehta (DTU) for approving my research proposal and evaluating the progress of my research work.

I am thankful to the members of my Ph.D. DRC Committee, DRC members (Applied Chemistry, DTU), Prof. S. S. Umare, VNIT, Nagpur (DRC member), Prof. Sreedevi Upadhyayula, IIT Delhi (DRC member) for their valuable suggestions and assessment of my research work.

Thanks to my senior Dr. Om Prakash Yadav who helped in the initial synthetic work in the exploration of corrole synthesis. Thanks to my labmates Deepali Ahluwalia, Jyoti, Sachin Kumar, Ritika and others for helping me in DFT calculation and analysis the compound structures.

Thanks to Dr. Sunil Yadav, Shivaji College, Delhi University for CV and Dr. Mohan Singh Mehta Sir and Dr. Mritunjay, Department of Applied Physics, Delhi Technological University, Delhi who helped me taking all Photophysical data of all synthesized free

base corroles. I would like to thank Dr. Vivek Kumar Agrawal, Department of Applied Mathematics, DTU for encouraging me all the time during in my research work.

I am extremely grateful to my parents for their love, prayers, caring and sacrifices for educating and preparing me for my future. I am very much thankful to Mrs. Shikha Varshney (wife) and Ayansh Varshney (son) for their love, understanding, prayers and continuing support to complete this research work. Also I express my thanks to my sister, brother, cousin brothers and brothers in law for their support. I would also like to give thanks to my friends Dr. Akash Kumar (Postdoctoral researcher at Gothenburg), Dr. Gyanendra Kumar and Ashish Yadav for the keen interest shown to complete this thesis successfully.

I would like to thank God Almighty for granting me wisdom, health and strength to accept the challenges of the life.

(Atul Varshney)

LIST OF CONTENTS

<i>Title</i>	<i>Page No.</i>
<i>Declaration</i>	<i>i</i>
<i>Certificate</i>	<i>ii</i>
<i>Acknowledgements</i>	<i>iii-iv</i>
<i>List of Contents</i>	<i>v-vii</i>
<i>List of Tables</i>	<i>viii</i>
<i>List of Schemes</i>	<i>ix</i>
<i>List of Figures</i>	<i>x-xi</i>
<i>List of Abbreviations</i>	<i>xii</i>
<i>Abstract</i>	<i>xiii</i>
 CHAPTER 1: INTRODUCTION	1-42
1.1. Corroles in chemistry	1
1.2. Types of corrole	3
1.2.1. A ₃ corrole	3
1.2.2. <i>cis</i> -A ₂ B corrole	5
1.2.3. <i>trans</i> -A ₂ B corrole	5
1.2.4. ABC corrole	6
1.3. Transition metals used in metal complex of corrole	7
1.4. Applications of corrole	12
1.4.1. Catalysis	12
1.4.2. Solar cells	14
1.4.3. Chemical sensors and sensor arrays	15
1.4.4. Biological applications	18
References	20
 CHAPTER 2: SCOPE OF THE WORK	43-44
 CHAPTER 3: OXIDATIVE CATALYTIC ACTIVITY OF ISOLATED (OXO)MANGANESE(V) CORROLE TO SULFIDES	45-72
3.1. Introduction	45
3.2. Significance and mechanism of sulfoxidation reactions	46
3.3. Experimental section	47
3.3.1. Chemicals	47

<i>Title</i>	<i>Page No.</i>
3.3.2. Common scheme for the synthesis of A ₂ B corrole (free base)	47
3.3.2.1. 5,15-Bis-nitrophenyl-10-(2,3,4,5,6-pentafluorophenyl) A ₂ B corrole 1	48
3.3.2.2. 5,15-Bis-nitrophenyl-10-(2,6-difluorophenyl) A ₂ B corrole 2	48
3.3.2.3. 5,15-Bis-nitrophenyl-10-phenyl A ₂ B corrole 3	48
3.3.2.4. 5,15-Bis-nitrophenyl-10-(4-methylphenyl) A ₂ B corrole 4	49
3.3.2.5. 5,15-Bis-nitrophenyl-10-(4-methoxyphenyl) A ₂ B corrole 5	49
3.3.3. Common method of synthesis of Manganese(III) A ₂ B corrole	49
3.3.3.1. Mn(III)5,15-bis-nitrophenyl-10-(pentafluorophenyl)-corrole 1	49
3.3.3.2. Mn(III)5,15-bis-nitrophenyl-10-(2,6-difluorophenyl)-corrole 2	50
3.3.3.3. Mn(III)5,15-bis-nitrophenyl-10-(phenyl)-corrole 3	50
3.3.3.4. Mn(III) 5,15-bis-nitrophenyl-10-(4-methylphenyl)-corrole 4	50
3.3.3.5. Mn(III) 5,15-bis-nitrophenyl-10-(4-methoxyphenyl)-corrole 5	51
3.3.4. General procedure for synthesis of Mn ^V (O) corrole	51
3.3.4.1. Mn ^V (O) 5,15-bis-nitrophenyl-10-(2,3,4,5,6-pentafluorophenyl)-corrole 1	51
3.3.4.2. Mn ^V (O) 5,15-bis-nitrophenyl-10-(2,6-difluorophenyl)-corrole 2	51
3.3.4.3. Mn ^V (O)5,15-bis-nitrophenyl-10-(phenyl)-corrole 3	51
3.3.4.4. Mn ^V (O) 5,15-bis-nitrophenyl-10-(4-methylphenyl)-corrole 4	51
3.3.4.5. Mn ^V (O) 5,15-bis-nitrophenyl-10-(4-methoxyphenyl)-corrole 5	52
3.4. Spectral characterization	52
3.4.1. UV-vis spectra of A ₂ B corroles, Mn(III) corroles and Mn ^V (O) corroles	52
3.4.2. NMR spectroscopy	54
3.4.3. Mass spectra	55
3.5. Electrochemistry of Mn(III)corroles	56

<i>Title</i>	<i>Page No.</i>
3.6. Kinetic Studies of manganese corroles	58
3.6.1. Rate constant of (oxo)manganese(V) corrole during self-decay	59
3.6.2. Rate constant of oxygen atom transfer of (oxo)manganese(V) corrole to thioanisole	60
3.7. Density functional theory (DFT) calculations	64
3.8. Conclusion	66
<i>References</i>	67
CHAPTER 4:HALOGEN ATOM EFFECT ON THE SENSING OF BIS <i>p</i>-NITRO A₂B CORROLES TOWARDS Hg²⁺ ION	73-97
4.1. Introduction	73
4.2. Experimental section	75
4.3. Common method for the synthesis of <i>trans</i> -A ₂ B free base corrole	76
4.3.1. Synthesis of 10-(o,m,p,m',o'-Pentafluorophenyl)-5,15-bis(p-nitrophenyl) <i>trans</i> -A ₂ B corrole 1	76
4.3.2. Synthesis of 10-(o,o'-difluorophenyl)-5,15-bis(p-nitrophenyl) <i>trans</i> -A ₂ B corrole 2	77
4.3.3. Synthesis of 10-(o,o'-dichlorophenyl)-5,15-bis(p-nitrophenyl) <i>trans</i> -A ₂ B corrole 3	78
4.3.4. Synthesis of 10-(o,o'-dibromophenyl)-5,15-bis(p-nitrophenyl) <i>trans</i> -A ₂ B corrole 4	79
4.4. Characterization	81
4.4.1. ¹ H NMR spectrum of 10-(o,o'-dichlorophenyl)- 5,15-bis(p-nitrophenyl) <i>trans</i> -A ₂ B corrole 3 & 10-(o,o'-dibromophenyl)- 5,15-bis(p-nitrophenyl) <i>trans</i> -A ₂ B corrole 4	81
4.4.2. Mass spectra of 10-(o,o'-dichlorophenyl)-5,15-bis(p-nitrophenyl) <i>trans</i> -A ₂ B corrole 3 & 10-(o,o'-dibromophenyl)- 5,15-bis(p-nitrophenyl) <i>trans</i> -A ₂ B corrole 4	83
4.5. Results and discussion	83
4.6. Conclusion	93
<i>References</i>	94
CHAPTER 5: CONCLUSION AND FUTURE SCOPE	98-100
5.1. Conclusion	98
5.2. Future scope	99
LIST OF PUBLICATIONS	101
LIST OF CONFERENCES AND WORKSHOP	102
ABOUT THE AUTHOR	103

LIST OF TABLES

<i>Table No.</i>	<i>Descriptions</i>	<i>Page No.</i>
3.1	Oxidation potential of Mn(III) A ₂ B corroles in acetonitrile with using TBAP as electrolyte	58
3.2	First order rate constant (k) of self-decay and pseudo-first-order rate constants (k_{obs}) of oxygen atom transfer to thioanisole (1-Mn^{V(O)} , 2-Mn^{V(O)} in ethyl acetate and 3-Mn^{V(O)} to 5-Mn^{V(O)} in acetonitrile)	64
3.3	Concentration of thioanisole used for kinetic study	64
3.4	DFT optimized molecules structural parameters and frontier molecular orbital energy	66
4.1	Photophysical data of 1-4 trans-A₂B corroles in toluene at room temperature	86
4.2	Comparison of the LoD with other reported sensors	92
4.3	Comparison of 1-4 probes for Hg ²⁺ sensing	92

LIST OF SCHEMES

<i>Scheme No.</i>	<i>Descriptions</i>	<i>Page No.</i>
1.1	Synthesis of A ₃ corrole	4
1.2	Synthesis of <i>cis</i> -A ₂ B corrole	5
1.3	Synthesis of <i>trans</i> -A ₂ B corrole	6
1.4	Synthesis of ABC corrole	6
3.1	Proposed Mechanism for Direct OAT of (Oxo)manganese(V) corrole to sulphides	47
3.2	Free base <i>trans</i> -A ₂ B corroles, Mn(III) corroles and their Mn ^V (O) complexes	52
4.1	Synthesis of 10-(o,m,p,m',o'-Pentafluorophenyl)-5,15-bis(p-nitrophenyl)corrole	77
4.2	Synthesis of 10-(o,o'-difluorophenyl)-5,15-bis(p-nitrophenyl)corrole	78
4.3	Synthesis of 10-(o,o'-dichlorophenyl)-5,15-bis(p-nitrophenyl)corrole	79
4.4	Synthesis of 10-(o,o'-dibromophenyl)-5,15-bis(p-nitrophenyl)corrole	80

LIST OF FIGURES

<i>Figure No.</i>	<i>Descriptions</i>	<i>Page No.</i>
1.1	Skeleton structure of porphyrin, corrin, corrolazine and corrole	1
1.2	Number of corrole-related publications since 1960	2
1.3	Structure of A ₃ , <i>cis</i> -A ₂ B, <i>trans</i> -A ₂ B and ABC corrole	3
1.4	Transition metals used in corrole chemistry	11
3.1	Graphical representation of oxygen atom transfer reaction of manganese corrole	46
3.2	UV-vis spectra of 1–5 <i>trans</i> -A ₂ B corroles in DCM	53
3.3	UV-vis spectra of 1-Mn(III) to 5-Mn(III) complexes of A ₂ B corroles in ethyl acetate	53
3.4	UV-vis spectra of 1-Mn^V(O) to 2-Mn^V(O) complexes in ethyl acetate and 3-Mn^V(O) to 5-Mn^V(O) in acetonitrile	54
3.5	¹ H NMR spectra (room temperature, CDCl ₃) of 5,15-Bis-nitrophenyl-10-(4-methoxyphenyl) A ₂ B corrole 5	55
3.6	HRMS of Mn(III) 5,15-bis-nitrophenyl-10-(phenyl)-corrole 3	55
3.7	HRMS of Mn(III) 5,15-bis-nitrophenyl-10-(4-methylphenyl)-corrole 4	56
3.8	Cyclic voltammogram of 1-Mn to 5-Mn	57
3.9	UV-vis spectra change of self-decay of (oxo)manganese(V) corrole (1-Mn(O) , 2-Mn(O)) in ethyl acetate while 3-Mn(O) to 5-Mn(O) in acetonitrile)	60
3.10	UV-vis spectral changes upon oxygen atom transfers from (oxo)manganese(V) corrole to thioanisole (1-Mn(O) and 2-Mn(O)) in ethyl acetate while 3-Mn(O) to 5-Mn(O) in acetonitrile)	62
3.11	UV-vis spectral changes upon oxygen atom transfers from (oxo)manganese(V) corrole to <i>para</i> -methoxy thioanisole (1-Mn(O) , 2-Mn(O)) in ethyl acetate and 3-Mn(O) to 5-Mn(O) in acetonitrile)	62
3.12	UV-vis spectral changes upon oxygen atom transfers from (oxo)manganese(V) corrole to <i>para</i> -fluoro thioanisole (1-Mn(O) , 2-Mn(O)) in ethyl acetate and 3-Mn(O) to 5-Mn(O) in acetonitrile)	63

<i>Figure No.</i>	<i>Descriptions</i>	<i>Page No.</i>
3.13	UV-vis spectral changes upon oxygen atom transfers from (oxo)manganese(V) corrole to para-(methylthio) benzonitrile, 1-Mn(O) , 2-Mn(O) in ethyl acetate and 3-Mn(O) to 5-Mn(O) in acetonitrile)	63
3.14	FMO (frontier molecular orbital) of 1-Mn to 5-Mn corrole, (Isosurface value= 0.02)	65
4.1	Graphical representation of Hg^{2+} ion sensor by <i>trans</i> -A ₂ B free base corrole	73
4.2	¹ H NMR spectrum of 10-(o,o'-dichlorophenyl)-5,15-bis(p-nitrophenyl) <i>trans</i> -A ₂ B corrole 3 in CDCl ₃	81
4.3	¹ H NMR spectrum of 10-(o,o'-dibromophenyl)- 5,15-bis(p-nitrophenyl) <i>trans</i> -A ₂ B corrole 4 in CDCl ₃	82
4.4	HRMS Spectra of 10-(o,o'-dichlorophenyl)-5,15-bis(p-nitrophenyl) <i>trans</i> -A ₂ B corrole 3	83
4.5	HRMS Spectra of 10-(o,o'-dibromophenyl)- 5,15-bis(p-nitrophenyl) <i>trans</i> -A ₂ B corrole 4	83
4.6	UV-visible spectra of 1-4 <i>trans</i> -A ₂ B corroles in toluene (9.9 μM).	84
4.7	Emission spectra of 1-4 A ₂ B corroles in toluene at 440 nm excitation	85
4.8	Fluorescence response of, 1-4 of 9.9×10^{-6} M to various cations (3.3×10^{-7} M) in toluene represented as a-d , respectively	87
4.9	Change in UV-visible spectrum during the addition of ethanol solution of Hg(II) acetate in toluene solution of 1-4 A ₂ B corroles in aerobic condition represented as a, b, c, d respectively	88
4.10	The decay in fluorescence emission intensity during the titration of methanolic solution of Hg(II) acetate (3.3×10^{-7} M) in toluene solution of 1-4 A ₂ B corroles (9.9×10^{-6} M) respectively under the excitation at $\lambda=440$ nm in aerobic condition	89
4.11	The Stern–Volmer plot of compounds 1-4 A ₂ B corroles respectively with positive deviation during increasing the concentration of methanolic solution of Hg(II) acetate inset the value of linearity constant (R^2)	91

LIST OF ABBREVIATIONS

OAT	:	Oxygen atom transfer
DDQ	:	2,3-Dichloro-5,6-dicyano-1,4-benzoquinone
DMF	:	Dimethylformamide
HCl	:	Hydrochloric acid
DSSC	:	Dye-sensitized solar cell
PVC	:	Poly vinyl chloride
DFT	:	Density functional theory
CV	:	Cyclic Voltammetry
UV-vis	:	Ultra violet-visible
NMR	:	Nuclear magnetic resonance
HRMS	:	High resolution mass spectroscopy
HOMO	:	Highest occupied molecular orbital
LUMO	:	Lowest unoccupied molecular orbital
DCM	:	Dichloromethane
FMO	:	Frontier molecular orbital
LoD	:	Limit of detection
TLC	:	Thin layer chromatography
λ	:	Wavelength (nm)
S-V	:	Stern-Volmer relation
PL	:	Photoluminescence
QY	:	Quantum yield
FWHM	:	Full width half maxima
ppm	:	Parts per million
μM	:	Micro molar
Λ	:	Wavelength (nm)
THF	:	Tetrahydrofuran
ϵ	:	Molar extinction coefficient
A	:	Absorbance
TPFCor	:	Tris(2,3,4,5,6-pentafluorophenyl)corrole
py	:	Pyridine
PPh_3	:	Triphenylphosphine

ABSTRACT

Corroles are non-natural aromatic tetra-pyrrolic systems, often kept in mind as contracted porphyrin systems. Corroles have received widespread attention especially in the past 20 years. Nobel Laureate Dorothy C. Hodgkin reported the first X-ray crystal structure of free base corrole. Free base corroles generally exists in three forms- A₃, A₂B (*cis* and *trans*) and ABC corroles. The present thesis encircles around one such free base form *viz.* *trans*-A₂B corrole and its manganese corroles and (oxo)manganese corroles. The thesis has been divided into five chapters. The literature survey including several reported applications of corrole are summarized as an introduction in **Chapter 1**. Scope and objectives of the research work discussed in **Chapter 2** of this thesis. In **Chpater 3**, synthesis of free base *trans*-A₂B corroles, and its manganese(III) corroles, (oxo) manganese(V) corroles and fully characterized by the UV-visible, NMR, Mass spectroscopy. Kinetics of self-decay and oxygen transfer reaction to thioanisole using ozonolysis of manganese(III) corroles, electrochemistry and calculated the HOMO-LUMO gap of manganese(III) corroles by DFT studies. The electron releasing and withdrawing group attached on phenyl group at C₁₀ position of corrole, which affect the rate constant of reactivity of 1-Mn^V(O) to 5-Mn^V(O) corroles. In **Chapter 4**, series of four free base *trans*-A₂B corroles (where A = para-nitrophenyl, and B = 2,3,4,5,6-pentafluorophenyl, 2,6-difluoro, 2,6-dichloro and 2,6-dibromophenyl group) have been synthesised and fully characterized by the UV-visible, NMR and mass spectrometry. These free base *trans*-A₂B corroles were tested for the sensing ability towards Hg²⁺ ion. The LoD for these corroles are comparable to reported sensors for Hg²⁺. All these four A₂B corroles exhibit different fluorescence quenching due to the electronic effect of the phenyl group at C₁₀ position, which has a different halogen atom at 2,6 position of the phenyl ring. **Chapter 5** discuss the conclusion and future scope of the work.

CHAPTER 1

INTRODUCTION

1.1 Corrole in chemistry

Corrole is an 18- π electrons macrocyclic molecule, which is fully conjugated and aromatic. Its skeleton structure resembles corrolazine, corrin (constituent of vitamin B₁₂) and porphyrin as shown in Figure 1.1. Porphyrin and corrole have tetrapyrrolic molecules but corrole having one less methine bridge (CH-20) as compared to porphyrin [1]. In the carbon skeleton of corrole C₅, C₁₀, C₁₅ shows the methine bridge (meso position), however in the case of porphyrin one more methine bridge present at C₂₀ positions as shown in Fig. 1.1. Due to one less methine bridge, corrole has lower symmetry group-C_{2v} and small cavity as compared with higher symmetry group-D_{4h} of porphyrin [2]. Corrole showed the higher N–H acidity because three protons present in the cavity of corrole, however one and two protons present in cavity of corrin and porphyrin, respectively [3]. Therefore, corrin and porphyrin worked as monoanionic and dianionic ligand respectively but corrole as trianionic ligand, which stabilize the metals in lower and higher oxidation states [4-7]. One of the most prominent feature of corrole is higher fluorescence level compare to similar porphyrinoids [8-10].

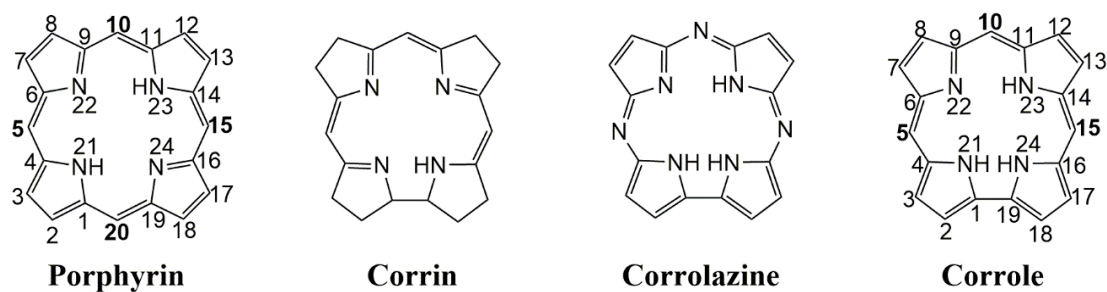


Fig. 1.1: Skeleton structure of porphyrin, corrin, corrolazine and corrole.

Corrole was first synthesized by the Johnson and Kay in 1965 [11]. Hodgkin and co-workers reported the first X-ray crystal of a free-base corrole [12]. Due to lower yield and synthesis of corrole from non-available starting material, the synthesis of corrole was difficult thus leading to lesser publications. Paolesse and Gross's group reported the one pot synthetic approach to corrole in 1999 [13-16]. After the discovery of this one pot synthetic approach, publications in corrole accelerated and are shown in Fig. 1.2.

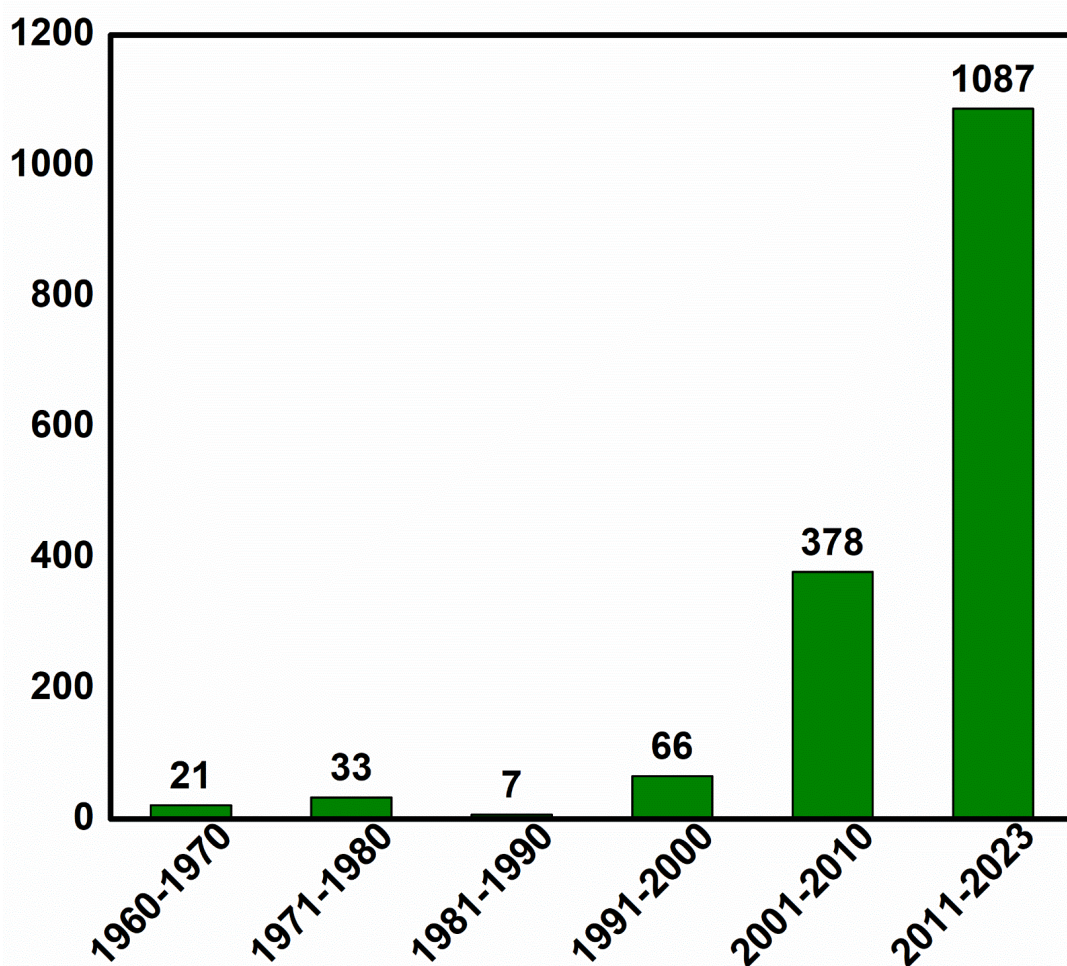


Fig 1.2: Number of corrole-related publications since 1960

Since 1999, corroles chemistry showed boom because of its synthetic accessibility (Fig1.2). Further, most of the research focused on the synthetic methodologies,

functionalisation and improving the yields. Nowadays, scientists are focusing on the application part of corroles in different fields like biological, environment, solar cell etc.

1.2 Types of corrole

Nomenclature of substituted corroles have same analogy like meso substituted porphyrin. According to the meso substituent, corroles are divided into four type such as A_3 , *cis*- A_2B , *trans*- A_2B and ABC corrole (Fig 1.3). If substituents are identical at C_5 , C_{10} and C_{15} positions that is called A_3 corrole. In *cis*- A_2B corrole, two substituents are same at C_5 and C_{10} but C_{15} different. But in *trans*- A_2B corrole, two substituents are same at C_5 and C_{15} but C_{10} different. In the case of ABC corrole, all substituent differ at C_5 , C_{10} and C_{15} positions.

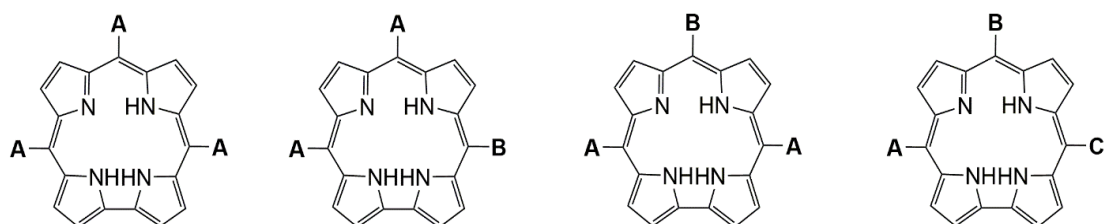
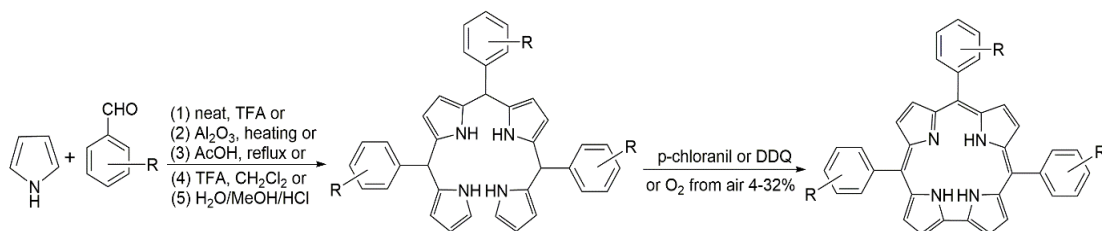


Fig. 1.3: Structure of A_3 , *cis*- A_2B , *trans*- A_2B and ABC corrole.

1.2.1 A_3 corrole

A_3 aryl corroles can be synthesized using aromatic aldehydes and pyrrole. Because of the oxidation potential of the electron-donating aliphatic substituents is too low to allow the stable product. The reactivity of carbonyl group depends on the attached substituents, which increase the positive charge on carbon atom of carbonyl group. In this way, Gross group synthesised first A_3 corrole by the reaction of pentafluorobenzaldehyde and pyrrole under neat conditions and added 2,3-dichloro-5,6-dicyano-1,4-benzoquinone (DDQ) for

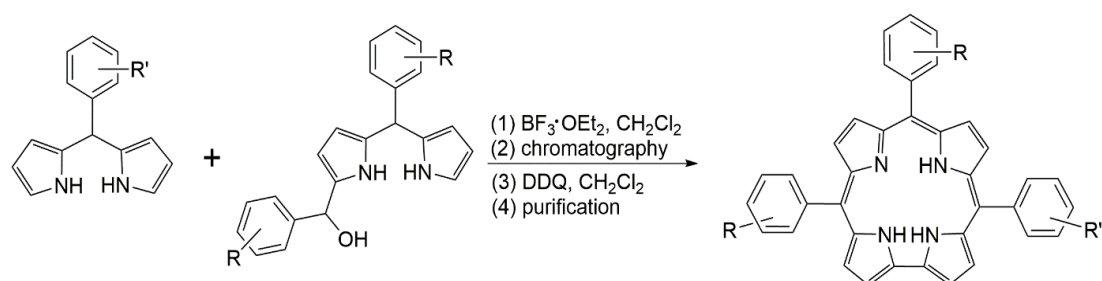
aromatization [14]. The 5,10,15-tris(pentafluorophenyl)corrole was obtained with 13% yield. Using the same procedure synthesis of the meso-alkyl-substituted corrole with 1% yield by the reaction hptafluorobutylaldehyde hydrate and pyrrole was carried out [17]. Gryko's group presented the facile route of synthesis of corroles [18]. In 2000, Lee and co-worker reported the bilanes in the literature [19]. In addition, Paolesse et al introduced the universal conditions with a pyrrole:aldehyde ratio of 10:1 for corrole synthesis with good yields [20]. Subsequently, Collman and Decreau used microwave for heating to improve the A₃ corroles yield [21]. Paolesse et al described the ratio of pyrrole and aldehyde for 5,10,15-triphenylcorrole [22]. Later 5,10,15-tris(4-nitrophenyl)corrole was synthesized by using the same methodology [23,24]. Virgil, Grubbs, and Gray reanalysed the both step first one tetrapyrrole and second corrole via removing the polymeric byproduct [25]. In 2006, Gryko and Koszarna introduced the different method to reduce the dipyrrane and tripyrrane impurity by using a mixture of water and methanol, and catalyzed by HCl [26,27]. Many scientists reported the synthesis of corrole by the contraction of porphyrin [28-30]. Vicente and co-workers synthesised the corrole by the condensation of dicarboranylaldehyde possessing two boron cages with pyrrole under Paolesse's conditions [31]. In practice, A₃ corroles can be synthesised by using any of the method shown in scheme 1.1.



Scheme 1.1: Synthesis of A₃ corrole.

1.2.2 *cis*-A₂B corrole

Tanaka and Osuka co-worker reported facile protocol for *cis*-A₂B corrole by acid catalyzed [2 + 2] condensation using carbinol and dipyrrane with DDQ [32]. In addition, they explored this method to synthesise the meso-free corrole (5,10 Bis(pentafluorophenyl)corrole) [33]. In 2002, Chandrashekhar et al proposed the first methodology of *cis*-A₂B corrole via [3+1] condensation of tripyrrane with pyrrole-2-carboxaldehyde [34]. The general procedure for the synthesis of *cis*-A₂B corrole is shown in below scheme1.2.

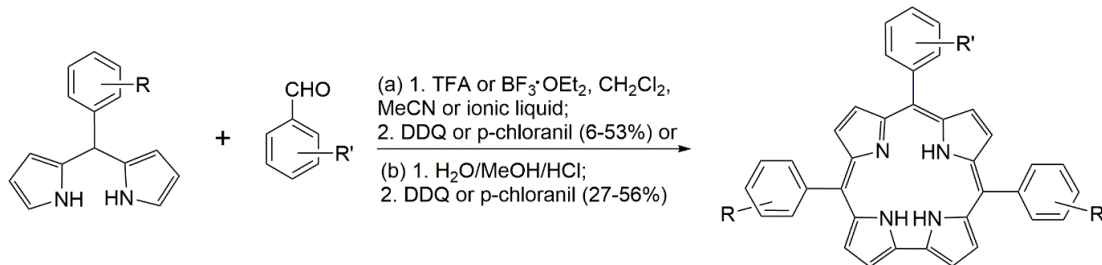


Scheme1.2: Synthesis of *cis*-A₂B corrole.

1.2.3 *trans*-A₂B corrole

The idea of synthesis of *trans*-A₂B corrole came from the Lindsey's work on *trans*-A₂B₂-porphyrins from dipyrranes and aldehydes [35,36]. In 2000, Gryko et al proposed the first method to synthesise the *trans*-A₂B corrole without acidic catalyst [37]. Later many research groups reported the methodology of *trans*-A₂B corrole using the aromatic aldehydes and dipyrrane [38-58]. Collman and Decreau synthesised *trans*-A₂B corrole by the condensation of dipyrromethane dicarbinols with 2,2'-bipyrrole [59]. In addition, Gryko and co-workers reported the synthesis of *trans*-A₂B-Corroles from ethyl oxalyl chloride and dipyrrane [60]. Later, Gryko and Geier et al synthesised of *trans*-A₂B-corroles from dipyrrane- Diols and Pyrrole [61,62].

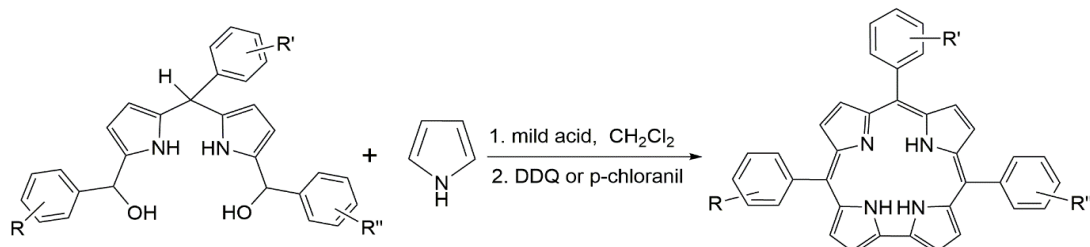
All these methodologies exist in the literature for the preparation for *trans*-A₂B corroles from aldehyde and dipyrranes. Numerous *trans*-A₂B-corrole were synthesised using the H₂O/MeOH/HCl. But the classical methodology with the use of TFA and CH₂Cl₂ is more efficient (scheme 1.3).



Scheme 1.3: Synthesis of *trans*-A₂B corrole.

1.2.4 ABC-corrole

Paolesse et al synthesised ABC-corroles by the condensation of two different dipyrranes with one aldehyde [20]. In addition, Guilard, Gryko, Geier et al described another method via condensation of a dipyrromethane-dicarbinol with pyrrole and acylation of mono-acylated dipyrromethanes under Vilsmeier condition [61-63]. Further, Churchill group synthesised the ABC corroles (5-(benzothien-2-yl)-15-(4-bromophenyl)-10-(pentafluorophenyl)-corrole) but purification of free base corrole was unsuccessful [64]. The scheme for synthesis of exemplary synthesis of ABC-Corrole (Scheme 1.4).



Scheme 1.4: Synthesis of ABC corrole.

1.3 Transition metals used in metal complex of corrole

With the ability to undergo metallation, the unique properties of corroles guide a huge impact on the formation of metallocorroles. Various different metal ions have been inserted into the corrole cavity. To date, a large library of transition metal ion binding arrangements has been assembled.

In group 4, oxotitanium corrolates were synthesised by reaction of free base corrole with titanyl acetylacetone [TiO(acac)₂] or titanocene or titanium(III) chloride (TiCl₃) in phenol [65]. In addition, titanium, zirconium and hafnium corrole complexes have been prepared via salt metathesis of lithium corrole [67,68].

In group 5, oxovanadium β -alkylcorrolates has been synthesised via freebase octaethylcorrole metalation with vanadium (III) acetylacetone [V(acac)₃] or Vanadium(III) chloride (VCl₃) [65].

In group 6, first chromium corrole was prepared as oxo (2,3,17,18-tetramethyl-7,8,12,13-tetraethylcorrolato)chromium(V) by the reaction the free-base corrole with anhydrous chromium(II) chloride (CrCl₂) in dry DMF [68,69]. In this way, oxo[tris(pentafluorophenyl)- corrolato]chromium(V) was obtained via aerobic reaction 5,10,15-tris-(pentafluorophenyl)corrole with chromium hexacarbonyl in toluene [70]. In addition, oxochromium (IV, V) complexes of tris(pentafluorophenyl) corrole were synthesised using chromium(II) chloride (CrCl₂) in pyridine [71,72]. Cr(V) and Cr(VI) nitrido complexes of tris(pentafluorophenyl) were obtained by the nitrogen transfer atom from stable (nitrido)manganese(V) complex of salophene to [tris(pentafluorophenyl)- corrolato]chromium(III) [73]. The first mononuclear chromium(V) imido corroles were synthesised by the reaction of Cr(TPFCor)(py)₂ with

mesityl azide under thermal or photochemical condition [74]. The first chiral ABC-metallocorrole (oxo[5-(4-bromophenyl)-10-(pentafluorophenyl)-15-(2-thianaphthyl)corrolato] chromium(V) synthesised through crude free base corrole via an aerobic oxidation using chromium hexacarbonyl [65]. Monomeric oxo(2,3,17,18-tetramethyl-7,8,12,13-tetraethylcorrolato)molybdenum(V) obtained by the reaction β -Octaalkylcorroles with molybdenum pentachloride or molybdenum hexacarbonyl in decalin [75]. In the same way, molybdenum corrole was prepared by the reaction of free base corroles (meso-triarylcorroles) with molybdenum hexacarbonyl in decalin or with tetrachlorobis(tetrahydrofuran)molybdate(III) in dicholomethane [76-80]. In addition, Gross et al developed the new methodology for the synthesis of low valent molybdenum corrole [81]. The first tungsten corrole was prepared via reaction of free base corrole with tungsten hexachloride in decalin, which was reported by Gross and co-workers [82]. The second example of tungsten(V) corrole was prepared through a metathesis of lithium corrole with tungsten hexachloride [83]. Bröring et al found unexpected air-stable corrole radical (3,17-dichloro-5,10,15-trimesitylcorrole) by the reaction of 5,10,15-trimesityl corrole with tungsten hexacarbonyl and tungsten hexachloride [84]. In this context, Ghosh and co-workers prepared the series of tungsten(VI) biscorroles by the meso-triarylcorroles with tungsten hexacarbonyl in decalin [85].

In group 7, manganese corrole has been synthesised by the different methodologies such as direct metalation with dimanganese decacarbonyl in toluene or with manganese(III) acetate in DMF or with manganese(II) acetate in DMF / methanol/pyridine [86-91]. Manganese (IV, V) corroles prepared by the different oxidation methods [90-93]. In addition, Kumar and co-workers synthesised a series of A₂B

manganese(III) corrole via green synthetic route [94]. Accidentally, rhenium corrole obtained by refluxing the porphyrin with dirhenium decacarbonyl in benzonitrile [28]. Ghosh's group reported the series of technetium corroles by the reaction of free base corrole with $[NEt_4]_2[^{99}\text{TcCl}_3(\text{CO})_3]$ in decalin [95].

In group 8, iron corroles have been synthesised by metalation of free base corrole with ferric chloride in DMF or iron pentacarbonyl in toluene or diiron nonacarbonyl in toluene or ferrous chloride in dry DMF [95-99]. In this context, $\text{Fe(III)(corrole)(NO)}$ prepared by the reaction of meso-triarylcorroles with hydrated ferrous chloride in mixture of pyridine and methanol via addition of an aqueous solution of sodium nitrite (NaNO_2) [100]. Walker et al were prepared corrolate π radical $[\text{Fe(III)(corrole}^{\bullet 2}]\text{Cl}^-$ [101-103]. Ghosh's group described π -cation radical character of chloroiron(IV) corroles [104]. Gross and co-workers observed no indication of corrole radical in chloroiron(IV) corrole and also explained the representation of corrole radicals in chloroiron(IV) corroles as $[\text{Fe(IV)(corrole}^3]\text{Cl}^-$ [105-107]. The existence of $[\text{Fe(III)(corrole}^{\bullet 2}]\text{Cl}^-$ has been proved theoretically as well as spectroscopically [107-109]. In recent years, several research group reported the iron corroles with different substituent [42, 110-115]. Monomer and dimer of ruthenium corroles obtained by the reaction of free base corrole with dichloro(1,5-cyclooctadiene)ruthenium(II) $[(\text{cod})\text{RuCl}_2]$ [116-119]. In 2014, Ghosh and co-workers were synthesised the first osmium corrole by the reaction meso-triarylcorroles with triosmium dodecacarbonyl $[\text{Os}_3(\text{CO})_{12}]$ / sodium azide in diethylene glycol monomethyl ether/glycol [120].

In group 9, cobalt corroles were synthesised by the reaction of free base corrole with cobalt acetate in pyridine at 100°C or in methanol in presence of PPh_3 [121-123].

Dimer, trimer, tetramer of cobalt corroles were also prepared by the reaction free-base oligomers with cobalt(II) acetate tetrahydrate in pyridine at 100 °C [123-126]. Cobalt corroles have been used as porphyrin-corrole dyads and biscorroles [127-137]. Gross and co-workers synthesised and characterised the first rhodium corrole by the reaction meso-triaryl corrole with $[\text{Rh}(\text{CO})_2\text{Cl}]_2$ (rhodium carbonyl chloride dimer) in benzene and in the presence of PPh_3 and K_2CO_3 (potassium carbonate) [123, 138-140]. In addition, Collman et al prepared the rhodium corrole via reaction free base corroles with $[\text{Rh}(\text{cod})_2\text{Cl}]_2$ (rhodium carbonyl chloride) in DCM or methanol in the presence of pyridine or diethylamine or trimethylamine at room temperature [141]. Iridium (III) corroles have been synthesised by the reaction TPFCor with $[\text{Ir}(\text{cod})\text{Cl}]_2$ (cyclooctadiene iridium chloride dimer) and K_2CO_3 (potassium carbonate) in THF also axially ligated by trimethylamine N-oxide or pyridine or substituted pyridine or triphenylphosphine or 4,4'-bipyridine or ammonia [142-148].

In group 10, Nickel corroles have been synthesised by reaction of β -octaalkylcorroles with nickel chloride (NiCl_2) in chloromethane (CH_3Cl) and methanol or $\text{Ni}(\text{OAc})_2$ (nickel(II) acetate) in DMF [4, 149]. Later, Guilard and co-workers prepared nickel biscorrole with anthracenyl spacer by heating biscorrole at 80 °C with $\text{Ni}(\text{OAc})_2$ (nickel(II) acetate) in pyridine or benzonitrile [150]. Gross and co-workers synthesised the palladium corrole from TPFCor via methylation of pyridine by methyl iodide [151]. Ghosh's synthesised the platinum corrole via reaction free base corrole with platinum acetate complex in benzonitrile [152].

In group 11, copper corrole was obtained by the reaction of free base corroles with copper acetate in hot DMF or pyridine at room temperature [4,20,149,153-160].

Further, 5,5'-linked and 10,10'-linked dimer of copper corrole was synthesised via metalation Cu(OAc)₂·H₂O (cupric acetate monohydrate) [126]. Also porphyrin-corrole dyads prepared by metalation with CuCl₂ (cupric chloride) in pyridine at 40°C [159]. Silver corroles were synthesised by the meso-triarylcorroles react with silver acetate in pyridine [161-168]. Dimer 5,5'-linked and 10,10'- linked silver corroles were prepared via metalation with silver acetate (AgOAc) [126]. Gold complexes of β-octabromo-meso-triarylcorrole have been prepared by free base β-octabromo-meso-triarylcorrole react with [MeAu(PPh₃)] or [ClAu(PPh₃)] in toluene or with chloroauric acid and trimethylamine in DCM [169, 170]. Simple gold corroles (i.e. without β-substituted) were synthesised by the reaction of free base corroles with gold(III) acetate in pyridine at room temperature [171-174].

Till now 22 transition metals used as central metal ion in corrole which are marked in periodic table (Fig.1.4). Transition metal complexes of corrole are utilising in different field. So research on transition metal corroles is interestingly going on.

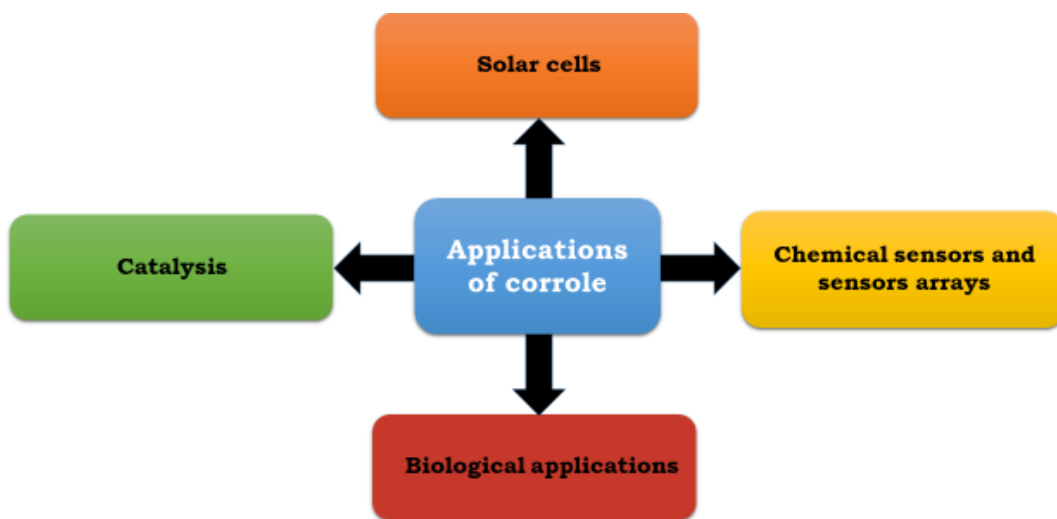
1	H													18	He	
	2															
Li	Be															
Na	Mg	3	4	5	6	7	8	9	10	11	12					
K	Ca	Sc	Ti	V	Cr	Mn	Fe	Co	Ni	Cu	Zn	Ga	Ge	As	Se	Br
Rb	Sr	Y	Zr	Nb	Mo	Tc	Ru	Rh	Pd	Ag	Cd	In	Sn	Sb	Te	I
Cs	Ba	Lu	Hf	Ta	W	Re	Os	Ir	Pt	Au	Hg	Tl	Pb	Bi	Po	At
Fr	Ra	Lr	Rf	Db	Sg	Bh	Hs	Mt	Ds	Rg	Cn	Nh	Fl	Mc	Lv	Ts
																Og

Fig. 1.4: Transition metals used in corrole chemistry

1.4 Applications of corrole

Corrole have a large number of applications and also having different features from parent porphyrin. With the age, scientists are exploring the corrole properties with its applications.

Some of the corrole's applications discussed below such as catalysis, solar cells, chemical sensors and sensor arrays, biological applications.



1.4.1 Catalysis

In 1999, first application of corrole and Metallocorrole is reported as oxidation catalyst [175]. 5,10,15-tris(pentafluorophenyl)corrolato iron(IV) chloride (TPFCorFeCl) has shown the catalytic oxidising (C–H bonds convert into C–OH bonds) behaviour with meta-chloroperoxybenzoic acid towards cyclohexane and adamantane [176]. Later, 5,10,15-tris(difluorophenyl)iron(IV) corrole was used as oxygenation of alkanes, alkenes, alkylbenzenes and alcohols with tert-butyl hydroperoxide (t-BuOOH) [177]. Further manganese corrole complexes 5,10,15-tris(pentafluorophenyl)manganese(III) corrole (TPFCorMn), 5,10,15-tris(2,6-difluorophenyl)manganese(III) corrole [T(2,6-

F₂)PCoMn] and perbrominated manganese(III) corrole were used as catalyst for the oxidation reactions [178,179]. Oxomanganese complex of octakis(para-tert-butylphenyl)corrolazinato³⁻) has been tested for oxidation of cyclohexane and alkylbanzenes [180]. Zhang and co-workers used iron(III) 5,10,15- tris(pentafluorophenyl) corrole (TPFCoFeIII) as olefin oxidising agent with iodobenzene diacetate [181]. In addition, iron(III) corrole was also used for the oxidation of sulphides to sulfoxide [182]. Later, same group manganese(III) and manganese(IV) corroles were tested as oxidant for sulphide to sulfone [183]. Recently, Kumar group observed the electronic and steric impact of C₁₀ substituent of oxo complex of manganese(V) corrole on the rate of OAT to thioanisole [184]. In this way, effect of N-base appended (oxo)manganese(V) corrole on epoxidation of alkenes are also reported in the literature [185].

Firstly, iron corrole complexes were used to copolymerization of carbon dioxide (CO₂) with cyclohexene oxide, propylene oxide and glycidyl phenyl ether [186]. In addition, same group explored the catalytic property of the manganese corroles for the copolymerization of epoxides with carbon dioxide (CO₂) and cyclic anhydrides [187]. In this way, manganese, iron, copper, cobalt, antimony and bismuth metal complexes of TPFCo were tested in the reaction of carbon dioxide with styrene oxide [188]. Manganese complex of TPFCo has been used as catalyst in the preparation of polyurethane [189]. Cobalt corroles worked as electrocatalyst for reduction of carbon dioxide (CO₂) [190,191]. Further, cobalt and iron corrole complexes and its β-brominated corroles has been used as electrocatalyst for oxygen reduction reaction in alkaline solutions [192-207]. Cobalt complex of TPFCo were also investigated for the oxygen evolution reactions and factor affecting the reaction [208-210]. Further, cobalt

corrole–carbon nanotube hybrids were synthesised and worked as catalyst for the investigation of the oxygen revolution reactions and hydrogen evolution reactions [211]. It was observed that the oxygen evolution reactions were greatly affected by the electronic factor of cobalt corroles [212-214]. Also, manganese corroles have been shown the promising catalyst character for oxygen evolution reactions [215]. Recently, iron corroles and its μ -oxo dimers, β - β' linked dimers were also tested for water oxidation electrocatalysis [216]. Further, cobalt, manganese, and copper complexes of TPFCor and T(2,6-F₂)PCorH₃ (5,10,15-tris-(2,6-difluorophenyl)corrole) have been explored as redox mediators for the oxygen evolution reactions in Li–O₂ (Lithium–air) batteries [217]. Cobalt corroles shows electrocatalytic efficiency towards hydrogen evolution reaction [218-228]. Cobalt and iron corroles were used as photoelectrocatalyst which increased the H₂ production [229]. Copper corroles has been investigated for hydrogen evolution reaction [230,231]. Kadish and co-workers reported the same CV behaviour of cobalt and copper corroles to support the hydrogen evolution reactions [232]. Even free-base corroles has been shown the electrocatalysts for the hydrogen evolution reactions [118,233]. Cobalt corroles have been also reported as a catalyst for the hydration of terminal alkynes and for the formation of heterocycles [234,235]. Iron complex of corrole–metal organic framework is used as catalyst for hetero Diels–Alder reactions between benzaldehydes and dienes [236]. Phosphorus corroles have been catalyzein ketone hydrosilylation, deoxygenation and bromination [228,237,238]. TPFCor complexes of aluminium and gallium used as catalysts for bromination [239].

1.4.2 Solar cells

Corroles were demonstrated as dye-sensitized solar cell (DSSC) and cells were prepared via the electron injection process from corrole to TiO₂ (titanium oxide) [240,241]. To

reduce the drawback of reported DSSC, gallium and phosphorous corroles have been explored as chromophores in DSSCs [242]. In addition, gold corroles were investigated as photosensitizers in DSSC [174]. Further, rhenium and osmium corroles were investigated as photosensitizer and compared the efficiency of gold corrole as photosensitizer [243]. To improve the efficiency, gold corrole decorated with good electron donor and sensitizer by the change substituent at corrole peripheral [244]. In addition, gallium complexes of corrole-BODIPY (4,4-difluoro-4-bora-3a,4a-diaza-s-indacene) were investigated as electron donor corrole [245]. Recently, copper corrole was utilised as a hole transporting material (HTM) in perovskite solar cells (PSCs) [246]. Very few examples of corrole have been demonstrated in the literature as solar cell device.

1.4.3 Chemical sensors and sensor arrays

Chemical sensors are the sensor used to detect compound and composition of complex in human being and environment [247]. Corrole is recently developing macromolecule to identify the analytes as quantitatively and qualitatively.

Free base corrole (5,15-Bis(pentafluorophenyl)-10-(4-methylphenyl)-corrole) used as oxygen sensor for gas detection [248]. To enhance the oxygen sensing property, gold corrole was combined with quantum dot [249]. Corrole and metallocorrole were investigated as anion sensor in pollutant and biological system. Gallium complexes of TPFCor showed anion sensing ability such as halides, cyanide, acetate, dihydrogen phosphate, caffeine and nicotine [250-252]. pH-sensitive “off-on-off” fluorescent sensor has been formed by Ga-corrole with an 8-hydroxyquinoline moiety [252].

Further, free base TPFCor corrole in polymethylmethacrylate (PMMA) and polyacrylamide has shown the sensitivity towards fluoride ion [251]. Later, trans-A₂B

corroles have been investigated to fluoride ion sensor [253]. Paolesse and co-workers explored the silicon-corrole as fluoride ion sensor [254,255]. Gallium complex of TPFCor has been demonstrated as the cyanide ion sensor spectrofluorometrically [251]. Cobalt corrole was also demonstrated as cyanide sensor using Whatman filter paper and imaged by a standard smartphone [256]. Also, β -brominated copper-corrole shown the sensing ability towards iodide [257]. Corrole and metallocorrole were used to detect the heavy metal ions. A corrole-based organic framework was used as metal ion sensor such as Ga^{3+} , Al^{3+} , Cr^{3+} and Fe^{3+} [258]. Free base corrole (TPFCorH₃) was combined with PVC (poly vinyl chloride) and dioctyl sebate as plasticizers to investigated the Hg^{2+} ion sensing [259]. In this order, *trans*-A₂B corrole was worked as cation sensor especially for Hg^{2+} ion, where A was nitrophenyl, and B was tridecyloxyphenyl [260].

Metallocorroles and corroles are also being used as chemical sensors based on electrochemical processes. The thin membrane was prepared using free base corrole (TPFCor) and 2-nitrophenyl octyl ether (o-NPOE) as a plasticizer and the additive sodium tetraphenylborate (NaTPB), which was highly selective for Ag^+ ion [261]. A combination of cobalt(II) porphyrin and cobalt(III) corrole was demonstrated for K^+ ion detection [262]. In addition, the same system has been developed as ion-selective electrode, which was prepared by coating the paper with a carbon nanotube layer [263]. Free base corrole-based liquid membrane electrodes are pH sensitive for salicylic acid and salicylate [264]. Cobalt complex of 5,10,15-tris(4-tert-butylphenyl)corrole has been shown binding affinity for nitrate via embedded in a PVC plasticizer membrane [265].

Corroles were used as resistive corrole sensors in donor–acceptor composites. Copper complexes of 10-(*p*-hydroxylphenyl)-5,15-diphenylcorrole and 5,10,15-tris(*p*-

carboxymethylphenyl)corrole have been used for the formation of self-arranging semiconducting nanostructure in nanoneedles and nanoribbons respectively, which shows an n-type response to NO₂ (nitrogen dioxide) [266]. Also, *meso*-tritolyl corrole was worked as sensor to detect NO₂ via non-covalently linked to singlewall carbon nanotubes [267]. In this order, 10-(4-chlorophenyl)-5,15-di(4-methylphenyl)-corrole and its cobalt complex were used as the organic framework with graphene oxide, which have limit of detection of NO₂ in ppm [268]. Light-activated gas sensors were prepared by the corrole with ZnO (zinc oxide) nanoparticles, which was tested for volatile compounds [269]. Copper corroles show more sensitivity towards donor ligands than copper porphyrin [269,270].

Corrole-based mass sensor prepared via deposition of Langmuir–Blodgett (LB) films of a manganese-corrole, which is sensitive towards amines, alcohols, alkanes, and aromatic aldehyde [271]. Similarly, solid-state films of cobalt(III) corroles adsorbed carbon monoxide, oxygen and nitrogen [272]. Cobalt(III) corroles incorporated in organic-inorganic hybrid Sol–Gel then cobalt-corrole have the selectivity for carbon monooxide [273,274]. Cobalt corroles and its β-acrolein substituted cobalt-corrole have shown sensitivity and selectivity for carbon mono oxide in porous organic polymer [275,276]. In this way, surface acoustic wave (SAW) device functionalized with cobalt and copper corroles were used for detection the carbon mono oxide [277]. Cobalt corroles, cobalt biscorroles and porphyrin-corroles having the binding affinity towards carbon mono oxide [128,278]. Free base 5,10,15-tris-(3,5-dihydroxyphenyl)corrole and its metal complexes of copper, iron, cobalt supramolecular porous solid layer bind the CO (carbon mono oxide) and NO (nitric oxide) [279].

Corrole-based gas sensor arrays of free base 5,10,15-triphenylcorrole and its iron and manganese complexes showed sensing affinity towards ethanol, ethyl acetate, dimethyl formamide and trimethylamine [280].

1.4.4 Biological applications

Corrole has been demonstrated as useful molecule in so many biological applications. Cu-corrole, Gd DOTA (1,4,7,10-tetraazacyclododecane-1,4,7,10-tetraacetic acid) complex was used as contrast agent for MRI and PET imaging [281]. In addition, a range of triazole linked corrole to DOTA/NOTA (1,4,7-triazacyclononane-1,4,7-triacetic acid) derivatives were prepared via copper(I)-catalysed Huisgen cycloaddition [282]. Metallocorroles were utilised as contrast-enhancing agent for MRI (magnetic resonance imaging) [23].

Zhou co-workers were synthesised the water soluble corroles, which shows the interaction with G-quadruplex [283]. Later, Zhou co-workers synthesised the five cationic methylpyridinium corroles for interactions with G-quadruplexes such as cmyc, htelo, and bcl2 [284]. Out of manganese and copper corroles, manganese corrole showed the higher stabilization to G-quadruplex [285]. Gallium(III) 5,10,15-(N-methyl-4-pyridyl)corrole bind with c-MYC G-quadruplex DNA, which used as antitumor drug [286].

Recently, corrole has been used as antiviral and shows inhibitory effects on hCMV (human cytomegalovirus) infection [287]. A library of corroles with nitro and fluoro substituent were prepared to study the antiviral activities [288,289]. In addition, 43 antiviral corrole-based molecules were studied for myxoma virus (Lausanne-like T1MYXV strain) [290].

Ga-corroles with ortho or para-methylpyridinium moieties were tested for antibacterial activities against the Gram-negative Bacterium A [291]. Sn- and P-corroles inhibited the germination of mold fungi spores [292]. Free base corrole (TPFCor) was used to prepare the Corrole-grafted-chitosan films, which shown bacteriostatic effect against *S. aureus* [293].

Further, gallium complexes of A_3 , and *trans*- A_2B corroles were demonstrated as photosensitizer in photodynamic therapy (PDT) [294-300]. In addition, for photodynamic therapy a phosphorus complex of 5,10,15-tris(ethoxylcarbonyl)corrole was used as non-toxic photosensitizer [301]. In addition, rhodium(V)-oxo triaryl corroles with methyl ester or carboxylic acid analogs were explored for photodynamic therapy [302, 303]. Tin complexes of tris-2-thienyl- and triphenyl corroles have shown the good candidature for photodynamic therapy [304-306]. Recently, Lemon and Marletta reported the phosphorus corroles which have been incorporated in to the HasA (heme acquisition system protein A) and H-NOX (heme nitric oxide/oxygen binding) protein for several biological applications [307].

References

1. Erben, C.; Will, S.; Kadish, K. M. In *The Porphyrin Handbook*; 1st ed.; Kadish, K. M., Smith, K. M., Guilard, R., Eds.; Academic Press: New York, **2000**; Vol. 2, p 233-300.
2. Gryko, D. T.; Fox, J. P.; Goldberg, D. P. *J. Porphyrins Phthalocyanines*. **2004**, 8, 1091 -1105.
3. Mahammed, A.; Weaver, J. J.; Gray, H. B.; Abelas, M.; Gross., Z. *Tetrahedron Lett.* **2003**, 44, 2077–2079.
4. Will, S.; Lex, J.; Vogel, E.; Schmickler, H.; Gisselbrecht, J. P.; Haubtmann, C.; Bernard, M.; Gross, M. *Angew. Chem. Int. Ed.* **1997**, 36, 357-361.
5. Gross, Z.; Gray, H. B. *Comments Inorg. Chem.* **2006**, 27, 61-72.
6. Gross, Z. *J. Biol. Inorg. Chem.* **2001**, 6, 733-738.
7. Paolesse, R.; Sagone, F.; Macagnano, A.; Boschi, T.; Prodi, L.; Mantalti, L.; Zaccheroni, N.; Bolettaand, F.; Smith, K. M. *J. Porph. Phthal.*, **1999**, 3, 364-370.
8. Bendix, J.; Dmochowski, I. J.; Gray, H. B.; Mahammed, A.; Simkhovich, L.; Gross, Z. *Angew. Chem. Int. Ed.* **2000**, 39, 4048-4051.
9. Shi, L.; Liu, H. Y.; Shen, H.; Hu, J.; Zhang, G. L.; Wang, H.; Ji, L. N.; Chang, C. K.; Jiang, H. F. *J. Porphyrins Phthalocyanines* **2009**, 13, 1221-1226.
10. Aviv-Harel, I.; Gross, Z. *Coord. Chem. Rev.* **2011**, 255, 717-736.
11. Johnson, A. W.; Kay, I. T. *Proc. R. Soc. London Ser. A* **1965**, 288, 334-341.
12. Harrison, H. R.; Hodder, O. J. R.; and Hodgkin, D.C. *J. Chem. Soc. B*, **1971**, 640–645.
13. Paolesse, R.; Jaquinod, L.; Nurco, D. J.; Mini, S.; Sagone, F.; Boschi, T.; Smith, K. M. *Chem. Commun.* **1999**, 1307-1308.
14. Gross, Z.; Galili, N.; Saltsman, I. *Angew. Chem. Int. Ed.* **1999**, 38, 1427-1429.

15. Gross, Z.; Galili, N.; Simkhovich, L.; Saltsman, I.; Botoshansky, M.; Blaser, D.; Boese, R.; Goldberg, I. *Org. Lett.* **1999**, *1*, 599-602.
16. Kumar, A.; Kim, D.; Kumar, S.; Mahammed, A.; Churchill, D. G.; and Gross Z. *Chem. Soc. Rev.* **2023**.
17. Simkhovich, L.; Goldberg, I.; Gross, Z. *J. Inorg. Biochem.* **2000**, *80*, 235-238.
18. Gryko, D. T.; Koszarna, B. *Org. Biomol. Chem.* **2003**, *1*, 350-357.
19. Ka, J.-W.; Cho, W.-S.; Lee, C.-H. *Tetrahedron Lett.* **2000**, *41*, 8121-8125.
20. Paolesse, R.; Marini, A.; Nardis, S.; Froiio, A.; Mandoj, F.; Nurco, D. J.; Prodi, L.; Montalti, M.; Smith, K. M. *J. Porphyrins Phthalocyanines* **2003**, *7*, 25-36.
21. Collman, J. P.; Decreau, R. A. *Tetrahedron Lett.* **2003**, *44*, 1207-1210.
22. Paolesse, R.; Nardis, S.; Sagone, F.; Khoury, R. G. *J. Org. Chem.* **2001**, *66*, 550-556.
23. Fu, B.; Huang, J.; Ren, L.; Weng, X.; Zhou, Y.; Du, Y.; Wu, X.; Zhou, X.; Yang, G. *Chem. Commun.* **2007**, 3264-3266.
24. Fryxelius, J.; Eilers, G.; Feyziyev, Y.; Magnuson, A.; Sun, L.; Lomoth, R. *J. Porphyrins Phthalocyanines* **2005**, *9*, 379-386.
25. Blumenfeld, C.; Fisher, K. J.; Henling, L. M.; Grubbs, R. H.; Gray, H. B.; Virgil, S. C. *Eur. J. Org. Chem.* **2015**, *2015*, 3022-3025.
26. Koszarna, B.; Gryko, D. T. *J. Org. Chem.* **2006**, *71*, 3707-3717.
27. Koszarna, B.; Gryko, D. T. *Tetrahedron Lett.* **2006**, *47*, 6205-6207.
28. Tse, M. K.; Zhang, Z.; Mak, T. C. W.; Chan, K. S. *Chem. Commun.* **1998**, 1199-1200.
29. Jeandon, C.; Ruppert, R.; Callot, H. J. *Chem. Commun.* **2004**, 1090-1091.
30. Jeandon, C.; Ruppert, R.; Callot, H. J. *J. Org. Chem.* **2006**, *71*, 3111-3120.
31. Luguya, R. J.; Fronczek, F. R.; Smith, K. M.; Vicente, M. G. H. *Tetrahedron Lett.* **2005**, *46*, 5365-5368.

32. Ooi, S.; Tanaka, T.; Osuka, A. *Eur. J. Org. Chem.* **2015**, 2015, 130-134.
33. Ooi, S.; Yoneda, T.; Tanaka, T.; Osuka, A. *Chem. - Eur. J.* **2015**, 21, 7772-7779.
34. Sankar, J.; Anand, V. G.; Venkatraman, S.; Rath, H.; Chandrashekhar, T. K. *Org. Lett.* **2002**, 4, 4233-4235.
35. (a) Lee, C.-H.; Lindsey, J. S. *Tetrahedron* **1994**, 50, 11427-11440; (b) Littler, B. J.; Ciringh, Y.; Lindsey, J. S. *J. Org. Chem.* **1999**, 64, 2864-2872.
36. Rao, P. D.; Littler, B. J.; Geier, G. R., III; Lindsey, J. S. *J. Org. Chem.* **2000**, 65, 1084-1092.
37. Gryko, D. T. *Chem. Commun.* **2000**, 2243-2244.
38. Brinás, R. P.; Brückner, C. *Synlett.* **2001**, 3, 442-444.
39. Asokan, C. V.; Smeets, S.; Dehaen, W. *Tetrahedron Lett.* **2001**, 42, 4483-4485.
40. Gryko, D. T.; Jadach, K. *J. Org. Chem.* **2001**, 66, 4267-4275.
41. Maiti, N.; Lee, J.; Kwon, S. J.; Kwak, J.; Do, Y.; Churchill, D. G. *Polyhedron* **2006**, 25, 1519-1530.
42. Gryko, D. T.; Koszarna, B. *Eur. J. Org. Chem.* **2005**, 2005, 3314-3318.
43. Bröring, M.; Milsmann, C.; Ruck, S.; Köhler, S. *J. Organomet. Chem.* **2009**, 694, 1011-1015.
44. Gryko, D. T.; Koszarna, B. *Synthesis* **2004**, 2004, 2205-2209.
45. Zhan, H.-Y.; Liu, H.-Y.; Chen, H.-J.; Jiang, H.-F. *Tetrahedron Lett.* **2009**, 50, 2196-2199.
46. Gryko, D. T.; Piechota, K. E. *J. Porphyrins Phthalocyanines* **2002**, 6, 81-97.
47. Saltsman, I.; Goldberg, I.; Gross, Z. *Org. Lett.* **2015**, 17, 3214-3217.
48. Maes, W.; Ngo, T. H.; Vanderhaeghen, J.; Dehaen, W. *Org. Lett.* **2007**, 9, 3165-3168.

49. Ngo, T. H.; Nastasi, F.; Puntoriero, F.; Campagna, S.; Dehaen, W.; Maes, W. *J. Org. Chem.* **2010**, *75*, 2127-2130.
50. Canard, G.; Gao, D.; D'Aleo, A.; Giorgi, M.; Dang, F.-X.; Balaban, T. S. *Chem. - Eur. J.* **2015**, *21*, 7760-7771.
51. Goldschmidt, R.; Goldberg, I.; Balazs, Y.; Gross, Z. *J. Porphyrins Phthalocyanines* **2006**, *10*, 76-86.
52. Barbe, J. M.; Stern, C.; Pacholska, E.; Espinosa, E.; Guilard, R. *J. Porphyrins Phthalocyanines* **2004**, *8*, 301-312.
53. El Ojaimi, M.; Gros, C. P.; Barbe, J. M. *Eur. J. Org. Chem.* **2008**, *2008*, 1181-1186.
54. Dogutan, D. K.; Stoian, S. A.; McGuire, R., Jr.; Schwalbe, M.; Teets, T. S.; Nocera, D. G. *J. Am. Chem. Soc.* **2011**, *133*, 131-140.
55. Barbe, J. M.; Burdet, F.; Espinosa, E.; Guilard, R. *Eur. J. Inorg. Chem.* **2005**, *2005*, 1032-1041.
56. Stefanelli, M.; Monti, D.; Venanzi, M.; Paolesse, R. *New J. Chem.* **2007**, *31*, 1722.
57. Orłowski, R.; Vakuliuk, O.; Gullo, M. P.; Danylyuk, O.; Ventura, B.; Koszarna, B.; Tarnowska, A.; Jaworska, N.; Barbieri, A.; Gryko, D. T. *Chem. Commun.* **2015**, *51*, 8284-8287.
58. van Hameren, R.; Elemans, J. A. A. W.; Wyrostek, D.; Tasior, M.; Gryko, D. T.; Rowan, A. E.; Nolte, R. J. M. *J. Mater. Chem.* **2009**, *19*, 66-69.
59. Decreau, R. A.; Collman, J. P. *Tetrahedron Lett.* **2003**, *44*, 3323-3327.
60. Koszarna, B.; Voloshchuk, R.; Gryko, D. T. *Synthesis* **2007**, *9*, 1339-1342.
61. Gryko, D. T.; Tasior, M.; Koszarna, B. *J. Porphyrins Phthalocyanines* **2003**, *7*, 239-248.

62. Geier, G. R., III; Chick, J. F. B.; Callinan, J. B.; Reid, C. G.; Auguscinski, W. P. *J. Org. Chem.* **2004**, *69*, 4159–4169.
63. Guillard, R.; Gryko, D. T.; Canard, G.; Barbe, J.-M.; Koszarna, B.; Brandes, S.; Tasior, M. *Org. Lett.* **2002**, *4*, 4491–4494.
64. Egorova, O. A.; Tsay, O. G.; Khatua, S.; Huh, J. O.; Churchill, D. G. *Inorg. Chem.* **2009**, *48*, 4634–4636.
65. Licoccia, S.; Paolesse, R.; Tassoni, E.; Polizio, F.; Boschi, T. *J. Chem. Soc., Dalton Trans.* **1995**, 3617–3621.
66. Buckley, H. L.; Chomitz, W.; Koszarna, B.; Tasior, M.; Gryko, D. T.; Brothers, P. J.; Arnold, J. *Chem. Commun.* **2012**, *48*, 10766–10768.
67. Padilla, R.; Buckley, H. L.; Ward, A. L.; Arnold, J. *Chem. Commun.* **2014**, *50*, 2922–2924.
68. Matsuda, Y.; Yamada, S.; Murakami, Y. *Inorg. Chim. Acta* **1980**, *44*, L309–L311.
69. Murakami, Y.; Matsuda, Y.; Yamada, S. *J. Chem. Soc., Dalton Trans.* **1981**, 855–861.
70. Meier-Callahan, A. E.; Gray, H. B.; Gross, Z. *Inorg. Chem.* **2000**, *39*, 3605–3607.
71. Meier-Callahan, A. E.; Di Bilio, A. J.; Simkhovich, L.; Mahammed, A.; Goldberg, I.; Gray, H. B.; Gross, Z. *Inorg. Chem.* **2001**, *40*, 6788–6793.
72. Czernuszewicz, R. S.; Mody, V.; Czader, A.; Gałezowski, M.; Gryko, D. T. *J. Am. Chem. Soc.* **2009**, *131*, 14214–14215.
73. Golubkov, G.; Gross, Z. *Angew. Chem., Int. Ed.* **2003**, *42*, 4507–4510.
74. Edwards, N. Y.; Eikey, R. A.; Loring, M. I.; Abu-Omar, M. M. *Inorg. Chem.* **2005**, *44*, 3700–3708.
75. Murakami, Y.; Matsuda, Y.; Yamada, S. *Chem. Lett.* **1977**, *6*, 689–692.

76. Luobeznova, I.; Raizman, M.; Goldberg, I.; Gross, Z. *Inorg. Chem.* **2006**, *45*, 386–394.
77. Johansen, I.; Norheim, H.-K.; Larsen, S.; Alemayehu, A. B.; Conradie, J.; Ghosh, A. *J. Porphyrins Phthalocyanines* **2011**, *15*, 1335–1344.
78. Mody, V. V.; Fitzpatrick, M. B.; Zabaneh, S. S.; Czernuszewicz, R. S.; Gałezowski, M.; Gryko, D. T. *J. Porphyrins Phthalocyanines* **2009**, *13*, 1040–1052.
79. Sashuk, V.; Koszarna, B.; Winiarek, P.; Gryko, D. T.; Grela, K. *Inorg. Chem. Commun.* **2004**, *7*, 871–875.
80. Czernuszewicz, R. S.; Mody, V.; Zareba, A. A.; Zaczek, M. B.; Gałezowski, M.; Sashuk, V.; Grela, K.; Gryko, D. T. *Inorg. Chem.* **2007**, *46*, 5616–5624.
81. Nigel-Etinger, I.; Goldberg, I.; Gross, Z. *Inorg. Chem.* **2013**, *52*, 4139–4141.
82. Nigel-Etinger, I.; Goldberg, I.; Gross, Z. *Inorg. Chem.* **2012**, *51*, 1983–1985.
83. Padilla, R.; Buckley, H. L.; Ward, A. L.; Arnold, J. J. *Porphyrins Phthalocyanines* **2015**, *19*, 150–153.
84. Schweyen, P.; Brandhorst, K.; Wicht, R.; Wolfram, B.; Brö ring, M. The Corrole Radical. *Angew. Chem., Int. Ed.* **2015**, *54*, 8213–8216.
85. Alemayehu, A. B.; Vazquez-Lima, H.; Gagnon, K. J.; Ghosh, A. *Chem. - Eur. J.* **2016**, *22*, 6914–6920.
86. Boschi, T.; Licoccia, S.; Paolesse, R.; Tagliatesta, P.; Tehran, M. A.; Pelizzi, G.; Vitali, F. *J. Chem. Soc., Dalton Trans.* **1990**, *9*, 463–468.
87. Kadish, K. M.; Adamian, V. A.; Van Caemelbecke, E.; Gueletii, E.; Will, S.; Erben, C.; Vogel, E. *J. Am. Chem. Soc.* **1998**, *120*, 11986–11993.
88. Gross, Z.; Golubkov, G.; Simkhovich, L. *Angew. Chem., Int. Ed.* **2000**, *39*, 4045–4047.

89. Gershman, Z.; Goldberg, I.; Gross, Z. *Angew. Chem., Int. Ed.* **2007**, *46*, 4320–4324.
90. Singh, P.; Dutta, G.; Goldberg, I.; Mahammed, A.; Gross, Z. *Inorg. Chem.* **2013**, *52*, 9349–9355.
91. Liu, H.; Lai, T.; Yeung, L.; Chang, C. K. *Org. Lett.* **2003**, *5*, 617–620.
92. Golubkov, G.; Bendix, J.; Gray, H. B.; Mahammed, A.; Goldberg, I.; DiBilio, A. J.; Gross, Z. *Angew. Chem., Int. Ed.* **2001**, *40*, 2132–2134.
93. Bröring, M.; Hell, C.; Brandt, C. D. *Chem. Commun.* **2007**, 1861–1862.
94. Yadav, O.; Varshney, A.; Kumar, A. *Inorg. Chem. Commun.* **2017**, *86*, 168-171.
95. Einrem, R. F.; Braband, H.; Fox, T.; Vazquez-Lima, H.; Alberto, R.; Ghosh, A. *Chem.Eur. J.* **2016**, *22*, 18747-18751.
96. Vogel, E.; Will, S.; Tilling, A. S.; Neumann, L.; Lex, J.; Bill, E.; Trautwein, A. X.; Wieghardt, K. *Angew. Chem., Int. Ed. Engl.* **1994**, *33*, 731–735.
97. Steene, E.; Wondimagegn, T.; Ghosh, A. *J. Phys. Chem. B* **2001**, *105*, 11406–11413.
98. Zhang, R.; Vanover, E.; Chen, T. H.; Thompson, H. *Appl. Catal., A* **2013**, *464–465*, 95–100.
99. Simkhovich, L.; Mahammed, A.; Goldberg, I.; Gross, Z. *Chem. - Eur. J.* **2001**, *7*, 1041–1055.
100. Sinha, W.; Deibel, N.; Agarwala, H.; Garai, A.; Schweinfurth, D.; Purohit, C. S.; Lahiri, G. K.; Sarkar, B.; Kar, S. *Inorg. Chem.* **2014**, *53*, 1417–1429.
101. Cai, S.; Walker, F. An.; Licoccia, S. *Inorg. Chem.* **2000**, *39*, 3466–3478.
102. Zakharieva, O.; Schonemann, V.; Gerdan, M.; Licoccia, S.; Cai, S.; Walker, F. A.; Trautwein, A. X. *J. Am. Chem. Soc.* **2002**, *124*, 6636–6648.
103. Walker, F. A.; Licoccia, S.; Paolesse, R. *J. Inorg. Biochem.* **2006**, *100*, 810–837.

104. Steene, E.; Dey, A.; Ghosh, A. *J. Am. Chem. Soc.* **2003**, *125*, 16300–16309.
105. Simkhovich, L.; Goldberg, I.; Gross, Z. *Inorg. Chem.* **2002**, *41*, 5433–5439.
106. Simkhovich, L.; Gross, Z. *Inorg. Chem.* **2004**, *43*, 6136–6138.
107. e, S.; Tuttle, T.; Bill, E.; Simkhovich, L.; Gross, Z.; Thiel, W.; Neese, F. *Chem. - Eur. J.* **2008**, *14*, 10839–10851.
108. Vazquez-Lima, H.; Norheim, H.-K.; Einrem, R. F.; Ghosh, A. *Dalton Trans.* **2015**, *44*, 10146–10151.
109. Norheim, H.-K.; Capar, J.; Einrem, R. F.; Gagnon, K. J.; Beavers, C. M.; Vazquez-Lima, H.; Ghosh, A. *Dalton Trans.* **2016**, *45*, 681–689.
110. Ganguly, S.; Vazquez-Lima, H.; Ghosh, A. *Chem. - Eur. J.* **2016**, *22*, 10336–10340.
111. Stefanelli, M.; Nardis, S.; Tortora, L.; Fronczek, F. R.; Smith, K. M.; Licoccia, S.; Paolesse, R. *Chem. Commun.* **2011**, *47*, 4255–4257.
112. Nardis, S.; Stefanelli, M.; Mohite, P.; Pomarico, G.; Tortora, L.; Manowong, M.; Chen, P.; Kadish, K. M.; Fronczek, F. R.; McCandless, G. T.; et al. *Inorg. Chem.* **2012**, *51*, 3910–3920.
113. Nardis, S.; Stefanelli, M.; Mohite, P.; Pomarico, G.; Tortora, L.; Manowong, M.; Ping Chen, P.; Kadish, K. M.; Fronczek, F. R.; McCandless, G. T.; Smith, K. M.; and Paolesse R. *Inorg. Chem.* **2014**, *53*, 4215–4227.
114. Schwalbe, M.; Dogutan, D. K.; Stoian, S. A.; Teets, T. S.; Nocera, D. G. *Inorg. Chem.* **2011**, *50*, 1368–1377.
115. Zyska, B.; Schwalbe, M. *Chem. Commun.* **2013**, *49*, 3799–3801.
116. Fischer, S.; Vestfrid, J.; Mahammed, A.; Herrmann-Westendorf, F.; Schulz, M.; Müller, J.; Kiesewetter, O.; Dietzek, B.; Gross, Z.; Presselt, M. *ChemPlusChem* **2016**, *81*, 594–603.

117. Jeróme, F.; Billier, B.; Barbe, J.; Espinosa, E.; Dahaoui, S.; Lecomte, C.; Guilard, R. *Angew. Chem., Int. Ed.* **2000**, *39* (22), 4051–4053.
118. Kadish, K. M.; Burdet, F.; Jeróme, F.; Barbe, J. M.; Ou, Z.; Shao, J.; Guilard, R. *J. Organomet. Chem.* **2002**, *652*, 69–76.
119. Simkhovich, L.; Luobeznova, I.; Goldberg, I.; Gross, Z. *Chem. - Eur. J.* **2003**, *9*, 201–208.
120. Alemayehu, A. B.; Gagnon, K. J.; Terner, J.; Ghosh, A. *Angew. Chem., Int. Ed.* **2014**, *53*, 14411–14414.
121. Conlon, M.; Johnson, A. W.; Overend, W. R.; Rajapaksa, D.; Elson, C. M. *J. Chem. Soc., Perkin Trans. I* **1973**, 2281–2288.
122. Pumarico, G.; Nardis, S.; Paolesse, R.; Ongayi, O. C.; Courtney, B. H.; Fronczek, F. R.; Vicente, M. G. H. *J. Org. Chem.* **2011**, *76*, 3765–3773.
123. Simkhovich, L.; Galili, N.; Saltsman, I.; Goldberg, I.; Gross, Z. *Inorg. Chem.* **2000**, *39*, 2704–2705.
124. Mohammed, A.; Giladi, I.; Goldberg, I.; Gross, Z. *Chem. - Eur. J.* **2001**, *7*, 4259–4265.
125. Hirabayashi, S.; Omote, M.; Aratani, N.; Osuka, A. *Bull. Chem. Soc. Jpn.* **2012**, *85*, 558–562.
126. Ooi, S.; Tanaka, T.; Osuka, A. *Inorg. Chem.* **2016**, *55*, 8920–8927.
127. Jeróme, F.; Gros, C. P.; Tardieu, C.; Barbe, J.; Guilard, R. *New J. Chem.* **1998**, *22*, 1327–1329.
128. Guilard, R.; Jerome, F.; Gros, C. P.; Barbe, J. M.; Ou, Z.; Shao, J.; Kadish, K. M. *C. R. Acad. Sci., Ser. IIc: Chim.* **2001**, *4*, 245–254.
129. Kadish, K. M.; Ou, Z.; Shao, J.; Gros, C. P.; Barbe, J. M.; Jeróme, F.; Bolze, F.; Burdet, F.; Guilard, R. *Inorg. Chem.* **2002**, *41*, 3990–4005.

130. Barbe, J.-M.; Burdet, F.; Espinosa, E.; Gros, C. P.; Guilard, R. *J. Porphyrins Phthalocyanines* **2003**, *7*, 365–374.
131. Guilard, R.; Burdet, F.; Barbe, J.-M.; Gros, C. P.; Espinosa, E.; Shao, J.; Ou, Z.; Zhan, R.; Kadish, K. M. *Inorg. Chem.* **2005**, *44*, 3972–3983.
132. Kadish, K. M.; Shao, J. G.; Ou, Z. P.; Fremond, L.; Zhan, R. Q.; Burdet, F.; Barbe, J. M.; Gros, C. P.; Guilard, R. *Inorg. Chem.* **2005**, *44*, 6744–6754.
133. Kadish, K. M.; Fremond, L.; Ou, Z.; Shao, J.; Shi, C.; Anson, F. C.; Burdet, F.; Gros, C. P.; Barbe, J.-M.; Guilard, R. *J. Am. Chem. Soc.* **2005**, *127*, 5625–5631.
134. Kadish, K. M.; Fremond, L.; Burdet, F.; Barbe, J. M.; Gros, C. P.; Guilard, R. *J. Inorg. Biochem.* **2006**, *100*, 858–868.
135. Kadish, K. M.; Fremond, L.; Shen, J.; Chen, P.; Ohkubo, K.; Fukuzumi, S.; El Ojaimi, M.; Gros, C. P.; Barbe, J. M.; Guilard, R. *Inorg. Chem.* **2009**, *48*, 2571–2582.
136. Jerome, F.; Gros, C. P.; Tardieu, C.; Barbe, J. M.; Guilard, R. *Chem. Commun.* **1998**, 2007–2008.
137. Guilard, R.; Jérôme, F.; Barbe, J. M.; Gros, C. P.; Ou, Z.; Shao, J.; Fischer, J.; Weiss, R.; Kadish, K. M. *Inorg. Chem.* **2001**, *40*, 4856–4865.
138. Simkhovich, L.; Iyer, P.; Goldberg, I.; Gross, Z. *Chem. - Eur. J.* **2002**, *8*, 2595–2601.
139. Saltsman, I.; Simkhovich, L.; Balazs, Y.; Goldberg, I.; Gross, Z. *Inorg. Chim. Acta* **2004**, *357*, 3038–3046.
140. Saltsman, I.; Balazs, Y.; Goldberg, I.; Gross, Z. *J. Mol. Catal. A: Chem.* **2006**, *251*, 263–269.
141. Collman, J. P.; Wang, H. J. H.; Decreau, R. A.; Eberspacher, T. A.; Sunderland, C. *J. Chem. Commun.* **2005**, 2497–2499.
142. Palmer, J. H.; Day, M. W.; Wilson, A. D.; Henling, L. M.; Gross, Z.; Gray, H. B. *J. Am. Chem. Soc.* **2008**, *130*, 7786–7787.

143. Palmer, J. H.; Mahammed, A.; Lancaster, K. M.; Gross, Z.; Gray, H. B. *Inorg. Chem.* **2009**, *48*, 9308–9315.
144. Palmer, J. H.; Lancaster, K. M. *Inorg. Chem.* **2012**, *51*, 12473–12482.
145. Sinha, W.; Ravotto, L.; Ceroni, P.; Kar, S. *Dalton Trans.* **2015**, *44*, 17767–17773.
146. Palmer, J. H.; Brock-Nannestad, T.; Mahammed, A.; Durrell, A. C.; Vandervelde, D.; Virgil, S.; Gross, Z.; Gray, H. B. *Angew. Chem., Int. Ed.* **2011**, *50*, 9433–9436.
147. Dong, S. S.; Nielsen, R. J.; Palmer, J. H.; Gray, H. B.; Gross, Z.; Dasgupta, S.; Goddard, W. A. *Inorg. Chem.* **2011**, *50*, 764–770.
148. Palmer, J. H.; Durrell, A. C.; Gross, Z.; Winkler, J. R.; Gray, H. B. *J. Am. Chem. Soc.* **2010**, *132*, 9230–9231.
149. Johnson, A. W.; Kay, I. T. *J. Chem. Soc.* **1965**, 1620–1629.
150. Jerôme, F.; Barbe, J.-M.; Gros, C. P.; Guillard, R.; Fischer, J.; Weiss, R. *New J. Chem.* **2001**, *25*, 93–101.
151. Chen, Q.-C.; Fridman, N.; Diskin-Posner, Y.; Gross, Z. *Chem. Eur. J.* **2020**, *26*, 9481–9485.
152. Alemayehu, A. B.; Vazquez-Lima, H.; Beavers, C. M.; Gagnon, K. J.; Bendix, J.; Ghosh, A. *2014*, *50*, 11093–11096.
153. Brückner, C.; Briñas, R. P.; Krause Bauer, J. A. *Inorg. Chem.* **2003**, *42*, 4495–4497.
154. Bröring, M.; Bregier, F.; Coñulsu Tejero, E.; Hell, C.; Holthausen, M. C. *Angew. Chem., Int. Ed.* **2007**, *46*, 445–448.
155. Alemayehu, A. B.; Gonzalez, E.; Hansen, L. K.; Ghosh, A. *Inorg. Chem.* **2009**, *48*, 7794–7799.
156. Alemayehu, A. B.; Hansen, L. K.; Ghosh, A. *Inorg. Chem.* **2010**, *49*, 7608–7610.

157. Thomas, K. E.; Conradie, J.; Hansen, L. K.; Ghosh, A. *Eur. J. Inorg. Chem.* **2011**, *2011*, 1865–1870.
158. Pierloot, K.; Zhao, H.; Vancoillie, S. *Inorg. Chem.* **2010**, *49*, 10316–10329.
159. Lemon, C. M.; Huynh, M.; Maher, A. G.; Anderson, B. L.; Bloch, E. D.; Powers, D. C.; Nocera, D. G. *Angew. Chem., Int. Ed.* **2016**, *55*, 2176–2180.
160. Guilard, R.; Gros, C. P.; Barbe, J.; Espinosa, E.; Jeróme, F.; Tabard, A.; Latour, J.; Shao, J.; Ou, Z.; Kadish, K. M. *Inorg. Chem.* **2004**, *43*, 7441–7455.
161. Brückner, C.; Barta, C. A.; Briñas, R. P.; Krause Bauer, J. A. *Inorg. Chem.* **2003**, *42*, 1673–1680.
162. Yadav, P.; Sankar, M. *Dalton Trans.* **2014**, *43*, 14680–14688.
163. Stefanelli, M.; Shen, J.; Zhu, W.; Mastroianni, M.; Mandoj, F.; Nardis, S.; Ou, Z.; Kadiah, K. M.; Fronczek, F. R.; Smith, K. M.; and Paolesse R. *Inorg. Chem.* **2009**, *48*, 6879–6887.
164. Sinha, W.; Sommer, M. G.; Deibel, N.; Ehret, F.; Sarkar, B.; Kar, S. *Chem. - Eur. J.* **2014**, *20*, 15920–15932.
165. Stefanelli, M.; Mastroianni, M.; Nardis, S.; Licoccia, S.; Fronczek, F. R.; Smith, K. M.; Zhu, W.; Ou, Z.; Kadish, K. M.; Paolesse, R. *Inorg. Chem.* **2007**, *46*, 10791–10799.
166. Thomas, K. E.; Vazquez-Lima, H.; Fang, Y.; Song, Y.; Gagnon, K. J.; Beavers, C. M.; Kadish, K. M.; Ghosh, A. *Chem. - Eur. J.* **2015**, *21*, 16839–16847.
167. Sarangi, R.; Giles, L. J.; Thomas, K. E.; Ghosh, A. *Eur. J. Inorg. Chem.* **2016**, *2016*, 3225–3227.
168. Pacholska, E.; Espinosa, E.; Guilard, R. *Dalton Trans.* **2004**, 3181–3183.
169. Rabinovich, E.; Goldberg, I.; Gross, Z. *Chem. - Eur. J.* **2011**, *17*, 12294–12301.
170. Alemayehu, A. B.; Ghosh, A. *J. Porphyrins Phthalocyanines* **2011**, *15*, 106–110.

171. Thomas, K. E.; Alemayehu, A. B.; Conradie, J.; Beavers, C.; Ghosh, A. *Inorg. Chem.* **2011**, *50*, 12844–12851.
172. Sinha, W.; Sommer, M. G.; van der Meer, M.; Plebst, S.; Sarkar, B.; Kar, S. *Dalton Trans.* **2016**, *45*, 2914–2923.
173. Teo, R. D.; Gray, H. B.; Lim, P.; Termini, J.; Domeshek, E.; Gross, Z. *Chem. Commun.* **2014**, *50*, 13789–13792.
174. Alemayehu, A. B.; Day, N. U.; Mani, T.; Rudine, A. B.; Thomas, K. E.; Gederaas, O. A.; Vinogradov, S. A.; Wamser, C. C.; Ghosh, A. *ACS Appl. Mater. Interfaces* **2016**, *8*, 18935–18942.
175. Gross, Z.; Simkhovich, L.; and Galili, N. *Chem. Commun.* **1999**, 599–600.
176. Biswas, A. N.; Das, P.; Agarwala, A.; Bandyopadhyay, D.; and Bandyopadhyay, P. *J. Mol. Catal. A: Chem.* **2010**, *326*, 94–98.
177. Pariyar, A.; Bose, S.; Biswas, A. N.; Das, P.; and Bandyopadhyay, P. *Catal. Commun.* **2013**, *32*, 23–27.
178. Bose, S.; Pariyar, A.; Biswas, A. N.; Das, P.; and Bandyopadhyay, P. *Catal. Commun.* **2011**, *12*, 1193–1197.
179. Bose, S.; Pariyar, A.; Biswas, A. N.; Das, P.; and Bandyopadhyay, P. *Catal. Commun.* **2011**, *12*, 446–449.
180. Lansky, D. E.; and Goldberg, D. P. *Inorg. Chem.* **2006**, *45*, 5119–5125.s
181. Chen, T.-H.; Kwong, K. W.; Carver, A.; Luo, W.; and Zhang, R. *Appl. Catal., A*. **2015**, *497*, 121–126.
182. Chen, T.-H.; Kwong, K. W.; Lee, N. F.; Ranburger, D.; and Zhang, R. *Inorg. Chim. Acta*. **2016**, *451*, 65–72.
183. Ranburger, D.; Willis, B.; Kash, B.; Jeddi, H.; Alcantar, C.; and Zhang, R. *Inorg. Chim. Acta*. **2019**, *487*, 41–49.
184. Varshney, A.; Kumar, A.; and Yadav, S. *Inorg. Chim. Acta*. **2021**, *514*, 120013.

185. Ng, N.-C.; Mahmood, M. H. R.; Liu, H.-Y.; Yam, F.; Yeung, L.-L.; and Chang, C.-K. *Chin. Chem. Lett.* **2014**, *25*, 571–574.
186. Nakano, K.; Kobayashi, K.; Ohkawara, T.; Imoto, H.; and Nozaki, K. *J. Am. Chem. Soc.* **2013**, *135*, 8456–8459.
187. Robert, C.; Ohkawara, T.; and Nozaki, K. *Chemistry*. **2014**, *20*, 4789–4795.
188. Tiffner, M.; Gonglach, S.; Haas, M.; Schofberger, W.; and Waser, M. *Chem. – Asian J.* **2017**, *12*, 1048–1051.
189. Malik, M.; and Kaur, R. *Polym. Adv. Technol.* **2018**, *29*, 1078–1085.
190. Gonglach, S.; Paul, S.; Haas, M.; Pillwein, F.; Sreejith, S. S.; Barman, S.; De, R.; Mullegger, S.; Gerschel, P.; Apfel, U. P.; Coskun, H.; Aljabour, A.; Stadler, P.; Schofberger, W.; and Roy, S. *Nat. Commun.* **2019**, *10*, 3864.
191. De, R.; Gonglach, S.; Paul, S.; Haas, M.; Sreejith, S. S.; Gerschel, P.; Apfel, U. P.; Vuong, T. H.; Rabeh, J.; Roy, S.; and Schofberger, W. *Angew. Chem., Int. Ed.* **2020**, *59*, 10527–10534.
192. Kosa, M.; Levy, N.; Elbaz, L.; and Major, D. T. *J. Phys. Chem. C*. **2018**, *122*, 17686–17694.
193. Levy, N.; Mahammed, A.; Friedman, A.; Gavriel, B.; Gross, Z.; and Elbaz, L. *ChemCatChem*. **2016**, *8*, 2832–2837.
194. Friedman, A.; Landau, L.; Gonen, S.; Gross, Z.; and Elbaz, L. *ACS Catal.* **2018**, *8*, 5024–5031.
195. Friedman, A.; Saltsman, I.; Gross, Z.; and Elbaz, L. *Electrochim. Acta*. **2019**, *310*, 13–19.
196. Levy, N.; Shpilman, J. S.; Honig, H. C.; Major, D. T.; and Elbaz, L. *Chem. Commun.* **2017**, *53*, 12942–12945.
197. Honig, H. C.; Krishnamurthy, C. B.; Borge-Dura'n, I.; Tasior, M.; Gryko, D. T.; Grinberg, I.; and Elbaz, L. *J. Phys. Chem. C*. **2019**, *123*, 26351–26357.

198. Friedman, A.; Reddy Samala, N.; Honig, H. C.; Tasior, M.; Gryko, D. T.; Elbaz, L.; and Grinberg, I. *ChemSusChem.* **2021**, *14*, 1886–1892.
199. Honig, H. C.; Friedman, A.; Zion, N.; and Elbaz, L. *Chem. Commun.* **2020**, *56*, 8627–8630.
200. Levy, N.; Lori, O.; Gonen, S.; Mizrahi, M.; Ruthstein, S.; and Elbaz, L. *Carbon.* **2020**, *158*, 238–243.
201. Lei, H.; Liu, C.; Wang, Z.; Zhang, Z.; Zhang, M.; Chang, X.; Zhang, W.; and Cao, R. *ACS Catal.* **2016**, *6*, 6429–6437.
202. Meng, J.; Lei, H.; Li, X.; Qi, J.; Zhang, W.; and Cao, R. *ACS Catal.* **2019**, *9*, 4551–4560.
203. Xie, L.; Li, X.; Wang, B.; Meng, J.; Lei, H.; Zhang, W.; and Cao, R. *Angew. Chem., Int. Ed.* **2019**, *58*, 18883–18887.
204. Meng, J.; Lei, H.; Li, X.; Zhang, W.; and Cao, R. *J. Phys. Chem. C.* **2020**, *124*, 16324–16331.
205. Raggio, M.; Mecheri, B.; Nardis, S.; D’Epifanio, A.; Licoccia, S.; and Paolesse, R. *Eur. J. Inorg. Chem.* **2019**, 4760–4765.
206. Wang, X.; Zheng, T.; Tang, Y.; Li, X.; Rykov, A. I.; Li, X.; Wang, J.; He, Q.; Cheng, J.; and Zhang, X. *J. Electrochem. Soc.* **2021**, *168*, 044506.
207. Rana, A.; Lee, Y.-M.; Li, X.; Cao, R.; Fukuzumi, S.; and Nam, W. *ACS Catal.* **2021**, *11*, 3073–3083.
208. Xu, L.; Lei, H.; Zhang, Z.; Yao, Z.; Li, J.; Yu, Z.; and Cao, R. *Phys. Chem. Chem. Phys.* **2017**, *19*, 9755–9761.
209. Sinha, W.; Mizrahi, A.; Mahammed, A.; Tumanskii, B.; and Gross, Z. *Inorg. Chem.* **2018**, *57*, 478–485.
210. Sun, H.; Han, Y.; Lei, H.; Chen, M.; and Cao, R. *Chem. Commun.* **2017**, *53*, 6195–6198.

211. Li, X.; Lei, H.; Liu, J.; Zhao, X.; Ding, S.; Zhang, Z.; Tao, X.; Zhang, W.; Wang, W.; Zheng, X. and Cao, R. *Angew. Chem., Int. Ed.* **2018**, *57*, 15070–15075.
212. `Kumar, A.; Sujesh, S.; Varshney, P.; Paul, A.; and Jeyaraman, S. *Dalton Trans.* **2019**, *48*, 11345–11351.
213. Neuman, N. I.; Albold, U.; Ferretti, E.; Chandra, S.; Steinhauer, S.; Rossner, P.; Meyer, F.; Doctorovich, F.; Vaillard, S. E.; and Sarkar, B.; *Inorg. Chem.* **2020**, *59*, 16622–16634.
214. Mondal, B.; Chattopadhyay, S.; Dey, S.; Mahammed, A.; Mittra, K.; Rana, A.; Gross, Z.; and Dey, A. *J. Am. Chem. Soc.* **2020**, *142*, 21040–21049.
215. Schofberger, W.; Faschinger, F.; Chattopadhyay, S.; Bhakta, S.; Mondal, B.; Elemans, J. A.; Mullegger, S.; Tebi, S.; Koch, R.; Klappenberger, F.; Paszkiewicz, M.; Barth, J. V.; Rauls, E.; Aldahhak, H.; Schmidt, W. G.; and Dey, A.; *Angew. Chem., Int. Ed.* **2016**, *55*, 2350–2355.
216. Sinha, W.; Mahammed, A.; Fridman, N.; and Gross, Z.; *ACS Catal.* **2020**, *10*, 3764–3772.
217. Kwak, W.-J.; Mahammed, A.; Kim, H.; Nguyen, T. T.; Gross, Z.; Aurbach, D.; and Sun, Y.-K. *Mater. Horiz.* **2020**, *7*, 214–222.
218. Li, X.; Lei, H.; Guo, X.; Zhao, X.; Ding, S.; Gao, X.; Zhang, W.; and Cao, R.; *ChemSusChem.* **2017**, *10*, 4632–4641.
219. Mondal, B.; Sengupta, K.; Rana, A.; Mahammed, A.; Botoshansky, M.; Dey, S. G.; Gross Z.; and Dey, A. *Inorg. Chem.* **2013**, *52*, 3381–3387.
220. Niu, Y.; Li, M.; Zhang, Q.; Zhu, W.; Mack, J.; Fomo, G.; Nyokong T.; and Liang, X. *Dyes Pigm.* **2017**, *142*, 416–428.
221. Liang, X.; Qiu, Y.; Zhang, X.; and Zhu, W. *Dalton Trans.* **2020**, *49*, 3326–3332.
222. Zhang, X.; Guo, W.; Zhu, W.; and Liang, X. *J. Porphyrins Phthalocyanines.* **2021**, *25*, 273–281.

223. Niu, Y.; Zhu, W.; Mack, J.; Dubazana, N.; Nyokong, T.; Fu, B.; Xu, H.; and Liang, X. *J. Porphyrins Phthalocyanines*. **2021**, *25*, 289–297.
224. Yuan, H. Q.; Wang, H. H.; Kandhadi, J.; Wang, H.; Zhan, S. Z.; and Liu, H. Y. *Appl. Organomet. Chem.* **2017**, *31*, e3773.
225. Chen, H.; Huang, D.-L.; Hossain, M. S.; Luo, G.-T.; and Liu, H.-Y. *J. Coord. Chem.* **2019**, *72*, 2791–2803.
226. Chen, Y.; Fan, Q.-H.; Hossain, M. S.; Zhan, S.-Z.; Liu, H.-Y.; and Si, L.-P. *Eur. J. Inorg. Chem.* **2020**, *491*–498.
227. Fang, J.-J.; Lan, J.; Yang, G.; Yuan, G.-Q.; Liu H.-Y.; and Si, L.-P. *New J. Chem.* **2021**, *45*, 5127–5136.
228. Li, M.; Niu, Y.; Zhu, W.; Mack, J.; Fomo, G.; Nyokong, T.; and Liang, X. *Dyes Pigm.* **2017**, *137*, 523–531.
229. Morales Va’squez, M. A.; Hamer, M.; Neuman, N. I. Tesio, A. Y.; Hunt, A.; Bogo, H.; Calvo, E. J.; and Doctorovich, F.; *ChemCatChem*. **2017**, *9*, 3259–3268.
230. Gu, T.; Wen, J.; Zhu, W.; and Liang, X. *Macroheterocycles*. **2019**, *12*, 129–134.
231. Sudhakar, K.; Mahammed, A.; Chen, Q.-C.; Fridman, N.; Tumanskii, B.; and Gross, Z. *ACS Appl. Energy Mater.* **2020**, *3*, 2828–2836.
232. Osterloh, W. R.; Desbois, N.; Quesneau, V.; Brandes, S.; Fleurat-Lessard, P.; Fang, Y.; Blondeau-Patissier, V.; Paolesse, R.; Gros, C. P.; and Kadish, K. M. *Inorg. Chem.* **2020**, *59*, 8562–8579.
233. Rodríguez-López, N.; Wu, Y.; Ge, Y.; and Villagrán, D. *J. Phys. Chem. C*. **2020**, *124*, 10265–10271.
234. Lai, J.-W.; Liu, Z.-Y.; Chen, X.-Y.; Zhang, H.; and Liu, H.-Y. *Tetrahedron Lett.* **2020**, *61*, 152426.
235. Goswami, M.; Geuijen, P.; Reek, J. N. H.; and de Bruin, B. *Eur. J. Inorg. Chem.* **2018**, *617*–626.

236. Zhao, Y.; Qi, S.; Niu, Z.; Peng, Y.; Shan, C.; Verma, G.; Wojtas, L.; Zhang, Z.; Zhang, B.; Feng, Y.; Chen, Y. S.; and Ma, S.; *J. Am. Chem. Soc.* **2019**, *141*, 14443–14450.
237. Gilhula, J. C.; and Radosevich, A. T. *Chem. Sci.* **2019**, *10*, 7177–7182.
238. Zhan, X.; Teplitzky, P.; Diskin-Posner, Y.; Sundararajan, M.; Ullah, Z.; Chen, Q. C.; Shimon, L. J. W.; Saltsman, I.; Mahammed, A.; Kosa, M.; Baik, M. H.; Churchill, D. G.; and Gross, Z. *Inorg. Chem.* **2019**, *58*, 6184–6198.
239. Zhan, X.; Yadav, P.; Diskin-Posner, Y.; Fridman, N.; Sundararajan, M.; Ullah, Z.; Chen, Q. C.; Shimon, L. J. W.; Mahammed, A.; Churchill, D. G.; Baik, M. H.; and Gross, Z. *Dalton Trans.* **2019**, *48*, 12279–12286.
240. Walker, D.; Chappel, S.; Mahammed, A.; Brunschwig, B. S.; Winkler, J. R.; Gray, H. B.; Zaban, A.; and Gross, Z. *J. Porphyrins Phthalocyanines.* **2012**, *10*, 1259–1262.
241. Sudhakar, K.; Giribabu, L.; Salvatori, P.; and Angelis, F. D. *Phys. Status Solidi A.* **2015**, *212*, 194–202.
242. Brennan, B.J.; Lam, Y. C.; Kim, P. M.; Zhang, X.; and Brudvig, G. W.; *ACS Appl. Mater. Interfaces.* **2015**, *7*, 16124–16130.
243. Higashino, T.; Kurumisawa, Y.; Alemayehu, A. B.; Einrem, R. F.; Sahu, D.; Packwood, D.; Kato, K.; Yamakata, A.; Ghosh, A.; and Imahori, H. *ACS Appl. Energy Mater.* **2020**, *3*, 12460–12467.
244. Lai, S.-L.; Wang, L.; Yang, C.; Chan, M.-Y.; Guan, X.; Kwok, C.-C.; and Che, C.-M.; *Adv. Funct. Mater.* **2014**, *24*, 4655–4665.
245. Mishra, R.; Basumatary, B.; Singhal, R.; Sharma, G. D.; and Sankar, J. *ACS Appl. Mater. Interfaces.* **2018**, *10*, 31462–31471.
246. Agresti, A.; Berionni Berna, B.; Pescetelli, S.; Catini, A.; Menchini, F.; Di Natale, C.; Paolesse, R.; and Di Carlo, A. *Adv. Funct. Mater.* **2020**, *30*, 2003790.

247. Hulanicki, A.; Glab, S.; and Ingman, F. *Pure Appl. Chem.* **1991**, *63*, 1247–1250.
248. Czechowski, N.; Nowak-Krol, A.; Gryko, D. T.; and Mac'kowski, S. *Phys. Scr.* **2013**, *T157*, 014009.
249. Santos, C. I. M.; Oliveira, E.; Barata, J. F. B.; Faustino, M. A. F.; Cavaleiro, J. A. S.; Neves, M. G. P. M. S. and Lodeiro, C. *Inorg. Chim. Acta*. **2014**, *417*, 148–154.
250. Santos, C. I. M.; Oliveira, E.; Barata, J. F. B.; Faustino, M. A. F.; Cavaleiro, J. A. S.; Neves, M. G. P. M. S.; and Lodeiro, C. *J. Mater. Chem.* **2012**, *22*, 13811–13819.
251. Santos, C. I. M.; Oliveira, E.; Menezes, J. C. J. M. D. S.; Barata, J. F. B.; Faustino, M. A. F.; Ferreira, V. F.; Cavaleiro, J. A. S.; Neves, M. G. P. M. S.; and Lodeiro, C. *Tetrahedron*. **2014**, *70*, 3361–3370.
252. Cai, F.; Xia, F.; Guo, Y.; Zhu, W.; Fu, B.; Liang, X.; Wang, S.; Cai, Z.; and Xu, H. *New J. Chem.* **2019**, *43*, 18012–18017.
253. Yadav, O.; Varshney, A.; Kumar, A.; Ratnesh, R. K.; and Mehata, M. S. *Spectrochim. Acta, Part A*. **2018**, *202*, 207–213.
254. Pomarico, G.; Monti, D.; Bischetti, M.; Savoldelli, A.; Fronczek, F. R.; Smith, K. M.; Genovese, D.; Prodi, L.; and Paolesse, R. *Chem. – Eur. J.* **2018**, *24*, 8438–8446.
255. Jaworska, E.; Caroleo, F.; Di Natale, C.; Maksymiuk, K.; Paolesse, R.; and Michalska, A.; *J. Porphyrins Phthalocyanines*. **2020**, *24*, 929–937.
256. Lvova, L.; Pomarico, G.; Mandoj, F.; Caroleo, F.; Di Natale, C.; Kadish, K. M.; and Nardis, S. *J. Porphyrins Phthalocyanines*. **2020**, *24*, 964–972.
257. Basumatary, B.; Ayoub Kaloo, M.; Singh, V. K.; Mishra, R.; Murugavel, M.; and Sankar, J. *RSC Adv.* **2014**, *4*, 28417–28420.
258. Li, Y.; Chen, M.; Han, Y.; Feng, Y.; Zhang, Z.; and Zhang, B. *Chem. Mater.* **2020**, *32*, 2532–2540.
259. He, C.-L.; Ren, F.-L.; Zhang, X.-B.; and Han, Z.-X.; *Talanta*. **2006**, *70*, 364–369.

260. Pariyar, A.; Bose, S.; Chhetri, S. S.; Biswas, A. N.; and Bandyopadhyay, P.; *Dalton Trans.* **2012**, *41*, 3826–3831.
261. Zhang, X.-B.; Han, Z.-X.; Fang, Z.-H.; Shen, G.-L.; and Yu, R.-Q.; *Anal. Chim. Acta*. **2006**, *562*, 210–215.
262. Jaworska, E.; Naitana, M. L.; Stelmach, E.; Pomarico, G.; Wojciechowski, M.; Bulska, E.; Maksymiuk, K.; Paolesse, R.; and A. Michalska, A. *Anal. Chem.* **2017**, *89*, 7107–7114.
263. Jaworska, E.; Pomarico, G.; Berna, B. B.; Maksymiuk, K.; Paolesse, R.; and Michalska, A. *Sens. Actuators, B.* **2018**, *277*, 306–311.
264. Radecki, J.; Stenka, I.; Dolusic, E.; and Dehaen, W. *Electrochim. Acta*. **2006**, *51*, 2282–2288.
265. Yang, S.; and Meyerhoff, M. E.; *Electroanalysis*. **2013**, *25*, 2579–2585.
266. Lu, G.; Sun, Q.; Zhang, T.; Kong, X.; Wang, Q.; and He, C. *Synth. Met.* **2019**, *252*, 69–75.
267. Wang, Y.; Akhigbe, J.; Ding, Y.; Brückner, C.; and Lei, Y. *Electroanalysis*. **2012**, *24*, 1348–1355.
268. Tang, J.; Chen, B.; Zhang, Y.; Lu, J.; Zhang, T.; Guo, Q.; and Zhang, J. *Funct. Mater. Lett.* **2019**, *12*, 1940001.
269. Magna, G.; Muduganti, M.; Stefanelli, M.; Sivalingam, Y.; Zurlo, F.; Di Bartolomeo, E.; Catini, A.; Martinelli, E.; Paolesse, R.; and Di Natale, C. *ACS Appl. Nano Mater.* **2021**, *4*, 414–424.
270. Ding, T.; Alema n, E. A.; Modarelli, D. A.; and Ziegler, C. J.; *J. Phys. Chem. A.* **2005**, *109*, 7411–7417.
271. Paolesse, R.; Di Natale, C.; Macagnano, A.; Sagone, F.; Scarselli, M. A.; Chiaradia, P.; Troitsky, V. I.; Berzina, T. S.; and D'Amico, A. *Langmuir*. **1999**, *15*, 1268–1274.

272. Barbe, J. M.; Canard, G.; Brandes, S.; Jerome, F.; Dubois, G.; and Guilard, R.; *Dalton Trans.* **2004**, 1208–1214.
273. Barbe, J.-M.; Canard, G.; Brande`s, S.; and Guilard, R. *Angew. Chem., Int. Ed.* **2005**, *44*, 3103–3106.
274. Barbe, J.-M.; Canard, G.; Brande`s, S.; and Guilard, R.; *Chem. – Eur. J.* **2007**, *13*, 2118–2129.
275. Brande`s, S.; Quesneau, V.; Fonquernie, O.; Desbois, N.; Blondeau-Patissier, V.; and Gros, C. P. *Dalton Trans.* **2019**, *48*, 11651–11662.
276. Savoldelli, A.; Magna, G.; Di Natale, C.; Catini, A.; Nardis, S.; Fronczek, F. R.; Smith, K. M.; and Paolesse, R. *Chem. – Eur. J.* **2017**, *23*, 14819–14826.
277. Vanotti, M.; Poisson, S.; Soumann, V.; Quesneau, V.; Brande`s, S.; Desbois, N.; Yang, J.; Andreacute, L.; Gros, C. P.; and Blondeau-Patissier, V. *Sens. Actuators, B.* **2021**, *332*, 129507.
278. Quesneau, V.; Shan, W.; Desbois, N.; Brande`s, S.; Rousselin, Y.; Vanotti, M.; Blondeau-Patissier, V.; Naitana, M.; FleuratLessard, P.; Van Caemelbecke, E.; Kadish, K. M.; and Gros, C. P. *Eur. J. Inorg. Chem.* **2018**, 4265–4277.
279. Tortora, L.; Pomarico, G.; Nardis, S.; Martinelli, E.; Catini, A.; D’Amico, A.; Di Natale, C.; and Paolesse, R.; *Sens. Actuators, B.* **2013**, *187*, 72–77.
280. Capuano, R.; Pomarico, G.; Paolesse, R.; and Di Natale, C. *Sensors.* **2015**, *15*, 8121–8130.
281. Desbois, N.; Michelin, C.; Chang, Y.; Stupar, V.; Bonnaud, M.; Pacquelet, S.; and Gros, C. P. *Tetrahedron Lett.* **2015**, *56*, 7128–7131.
282. Desbois, N.; Pacquelet, S.; Dubois, A.; Michelin, C.; and Gros, C. P. *Beilstein J. Org. Chem.* **2015**, *11*, 2202–2208.
283. Sims, J. D.; Hwang, J. Y.; Wagner, S.; Alonso-Valenteen, F.; Hanson, C.; Taguiam, J. M.; Polo, R.; Harutyunyan, I.; Karapetyan, G.; Sorasaenee, K.; Ibrahim, A.; Marban, E.; Moats, R.; Gray, H. B.; Gross, Z.; and Medina-Kauwe, L. K. *J. Controlled Release.* **2015**, *217*, 92–101.

284. Ma, H.; Zhang, M.; Zhang, D.; Huang, R.; Zhao, Y.; Yang, H.; Liu, Y.; Weng, X.; Zhou, Y.; Deng, M.; Xu, L.; and Zhou, X. *Chem. – Asian J.* **2010**, *5*, 114–122.
285. Fu, B.; Zhang, D.; Weng, X.; Zhang, M.; Ma, H.; Ma, Y.; and Zhou, X. *Chemistry*. **2008**, *14*, 9431–9441.
286. Zhang, Z.; Wen, J.-Y.; Lv, B.-B.; Li, X.; Ying, X.; Wang, Y.-J.; Zhang, H.-T.; Wang, H.; Liu, H.-Y.; and Chang, C. K. *Appl. Organomet. Chem.* **2016**, *30*, 132–139.
287. Gros, C. P.; Desbois, N.; Michelin, C.; Demilly, E.; TilkinMariame, A. F.; Mariame, B.; and Gallardo, F. *ACS Infect. Dis.* **2015**, *1*, 350–356.
288. Kappler-Gratias, S.; Bucher, L.; Desbois, N.; Rousselin, Y.; Bystricky, K.; Gros, C. P.; and Gallardo, F. *RSC Med. Chem.* **2020**, *11*, 783–801.
289. Bucher, L.; Kappler-Gratias, S.; Desbois, N.; Bystricky, K.; Gallardo, F.; and Gros, C. P. *RSC Med. Chem.* **2020**, *11*, 771–782.
290. Kappler-Gratias, S.; Bucher, L.; Top, S.; QuentinFroignant, C.; Desbois, N.; Bertagnoli, S.; Louison, M.; Monge, E.; Bousquet-Melou, A.; Lacroix, M.; Gros, C. P.; and F. Gallardo, F. *ACS Infect. Dis.* **2021**, *7*, 2370–2382.
291. Cardote, T. A. F.; Barata, J. F. B.; Amador, C.; Alves, E.; Neves, M.; Cavaleiro, J. A. S.; Cunha, A.; Almeida, A.; and Faustino, M. A. F. *An. Acad. Bras. Cienc.* **2018**, *90*, 1175–1185.
292. Preuss, A.; Saltsman, I.; Mahammed, A.; Pfitzner, M.; Goldberg, I.; Gross, Z.; and Roder, B. *J. Photochem. Photobiol. B*. **2014**, *133*, 39–46.
293. Barata, J. F.; Pinto, R. J.; Vaz Serra, V. I.; Silvestre, A. J.; Trindade, T.; Neves, M. G.; Cavaleiro, J. A.; Daina, S.; Sadocco, P.; and Freire, C. S.; *Biomacromolecules*. **2016**, *17*, 1395–1403.
294. Agadjanian, H.; Ma, J.; Rentsendorj, A.; Valluripalli, V.; Hwang, J. Y.; Mahammed, A.; Farkas, D. L.; Gray, H. B.; Gross, Z.; and Medina-Kauwe, L. K. *Proc. Natl. Acad. Sci. U. S. A.* **2009**, *106*, 6105–6110.

295. Zhang, Z.; Wang, H. H.; Yu, H. J.; Xiong, Y. Z.; Zhang, H. T.; Ji, L. N.; and Liu, H. Y.; *Dalton Trans.* **2017**, *46*, 9481–9490.
296. Hwang, J. Y.; Lubow, J.; Chu, D.; Ma, J.; Agadjanian, H.; Sims, J.; Gray, H. B.; Gross, Z.; Farkas, D. L.; and Medina-Kauwe, L. K.; *Mol. Pharmaceutics*. **2011**, *8*, 2233–2243.
297. Soll, M.; Chen, Q. C.; Zhitomirsky, B.; Lim, P. P.; Termini, J.; Gray, H. B.; Assaraf, Y. G. and Gross, Z. *Cell Death Discovery*. **2020**, *6*, 67.
298. Sharma, V. K.; Mahammed, A.; Soll, M.; Tumanskii, B.; and Gross, Z.; *Chem. Commun.* **2019**, *55*, 12789–12792.
299. Sun, Y. M.; Jiang, X.; Liu, Z. Y.; Liu, L. G.; Liao, Y. H.; Zeng, L.; Ye, Y.; and Liu, H. Y.; *Eur. J. Med. Chem.* **2020**, *208*, 112794.
300. Pribisko, M.; Palmer, J.; Grubbs, R. H.; Gray, H. B.; Termini, J.; and Lim, P. *Proc. Natl. Acad. Sci. U. S. A.* **2016**, *113*, E2258–E2266.
301. Zhang, Z.; Yu, H. J.; Huang, H.; Wang, H. H.; Wu, S.; Liu, H. Y.; and Zhang, H. T.; *Eur. J. Med. Chem.* **2019**, *163*, 779–786.
302. Einrem, R. F.; Alemayehu, A. B.; Borisov, S. M.; Ghosh, A.; and Gederaas, O. A. *ACS Omega*. **2020**, *5*, 10596–10601.
303. Alemayehu, A. B.; McCormick-McPherson, L. J.; Conradie, J.; and Ghosh, A.; *Inorg. Chem.* **2021**, *60*, 8315–8321.
304. Babu, B.; Prinsloo, E.; Mack, J.; and Nyokong, T.; *New J. Chem.* **2019**, *43*, 18805–18812.
305. Lai, S.-H.; Wang, L.-L.; Wan, B.; Lu, A.-W.; Wang, H.; and Liu, H.-Y. *J. Photochem. Photobiol., A*. **2020**, *390*, 112283.
306. Xie, A.-N.; Zhang, Z.; Wang, H.-H.; Ali, A.; Zhang, D.-X.; Wang, H.; Ji, L.-N.; and Liu, H.-Y. *J. Porphyrins Phthalocyanines* **2018**, *22*, 739–750.
307. Lemon, C. M.; and Marletta, M. A. *Inorg. Chem.* **2021**, *60*, 2716–2729.

CHAPTER 2

SCOPE OF THE WORK

2.1 Introduction

Corroles and metallocorroles show interesting properties such as catalysis and fluorescence. Many transition metals are used in corrole chemistry. Manganese corroles derived from the transition metal are used in a variety of fields including medicine, catalysis, the environment, and so on. As a result, the first goal was to synthesise five free base A_2B corroles ($A =$ nitrophenyl, and $B =$ pentafluorophenyl, 2,6-difluorophenyl, phenyl, 4-methylphenyl, and 4-methoxyphenyl groups) and later their manganese metalated corroles and oxo complexes of manganese corroles were synthesised. Rate of self-decay and rate of formation sulfide to sulfoxide via manganese corroles for the oxygen atom present on these oxomanganese (V) corroles was later determined. Then we observed the effect of the electronic factor of the substituted group (at the C-10 position of corrole) on the kinetic rate of the oxygen transfer reaction, which was justified by the cyclic voltammetry and DFT.

Nowadays, Corroles and metallocorroles are widely used for sensing the gaseous molecules, hazardous anions and cations. This led us to our second aim which was using free base A_2B corroles as cationic sensor. In this work, four A_2B free base corroles have been shown to have a higher sensing ability towards the Hg^{2+} ion out of Na^+ , Ag^+ , Ca^{2+} , Cd^{2+} , Pb^{2+} , Cu^{2+} , Zn^{2+} , Al^{3+} ions. The difference in four A_2B corroles by C-10 position (B) with $A =$ nitrophenyl and $B =$ pentafluorophenyl, 2, 6-difluoro, 2,6-dichloro and 2,6-dibromophenyl groups. All four free base corroles demonstrated the detection of mercury ions in toluene. Photophysical properties of all four A_2B corroles,

such as limit of detection and fluorescence quenching, show the effect of halogen atoms on the selectivity of metal ions.

2.2 Objectives

Synthesis of manganese corroles and its catalytic application. Synthesis of A₂B free base corroles and their different applications including cation sensors.

2.2.1 Specific objectives

- ❖ Synthesis of A₂B free base corroles, manganese(III) corroles and (oxo)-manganese(V) corroles and their characterization by the UV-visible, NMR and mass spectroscopy.
- ❖ Determination of the rate of self-decay and oxygen atom transfer through (oxo)manganese(V) corroles to sulfides.
- ❖ Electrochemistry of manganese(III) corroles.
- ❖ Determination of the HOMO-LUMO gap of Mn(III) corroles via DFT calculation.
- ❖ Study the effect of halogen atoms on the sensing ability of free base *trans*-A₂B corrole towards the mercury ion.
- ❖ Study of the photophysical properties of synthesized A₂B free base corroles.

CHAPTER 3

OXIDATIVE CATALYTIC ACTIVITY OF ISOLATED (OXO)MANGANESE(V) CORROLE TO SULFIDES

3.1 Introduction

Manganese corroles are widely used for oxygen atom transfer (OAT) reactions because manganese complexes have ability to acquire a wide range of oxidation state. Gross and co-workers in 2000, reported the Mn(III) corrole as an epoxidation and cyclopropanation catalyst using the iodosylbenzene as an oxygen source [1]. In this article, oxo-manganese(V) corroles and β -brminated oxo-manganese corroles were demonstrated for sulfoxidation under stoichiometric conditions [2]. Further, Bandyopadhyay and co-workers employed the manganese corroles and β -brominated manganese corroles for the oxidation of hydrocarbons and alcohol [3,4]. Liu and co-workers reported the DFT calculation of oxomanaganese(V) corroles [5]. The catalytic activity of manganese corrole was also affected by the solvent and axial ligands [6-8]. Liu and Chang's group studied the rate of oxygen atom transfer reactions from non-brominated and brominated $\text{Mn}^{\text{V}}(\text{O})$ corroles to styrene [9]. Zhang and co-workers described multiple oxidation pathways using $\text{Mn}^{\text{V}}(\text{O})$ corrole [10]. Mn(III) complexes of TPFC and TPFcCN have been previously used for dioxygen activation and the O – O bond formation [11]. Goldberg's group discovered that $\text{Mn}^{\text{IV}}(\text{OH})$ corrole has a higher rate of hydrogen atom transfer than $\text{Mn}^{\text{V}}(\text{O})$ corrole[12]. Manganese corrole is also used for CO_2 fixation with epoxides under mild conditions [13]. The non-isocyanate polyurethane was synthesised using manganese complexes of 5,10,15- tris(pentafluorophenyl) corrole as catalyst[14]. This work aims to illustrate the substituent effect on the efficiency of manganese corrole towards sulfoxidations under catalytic conditions.

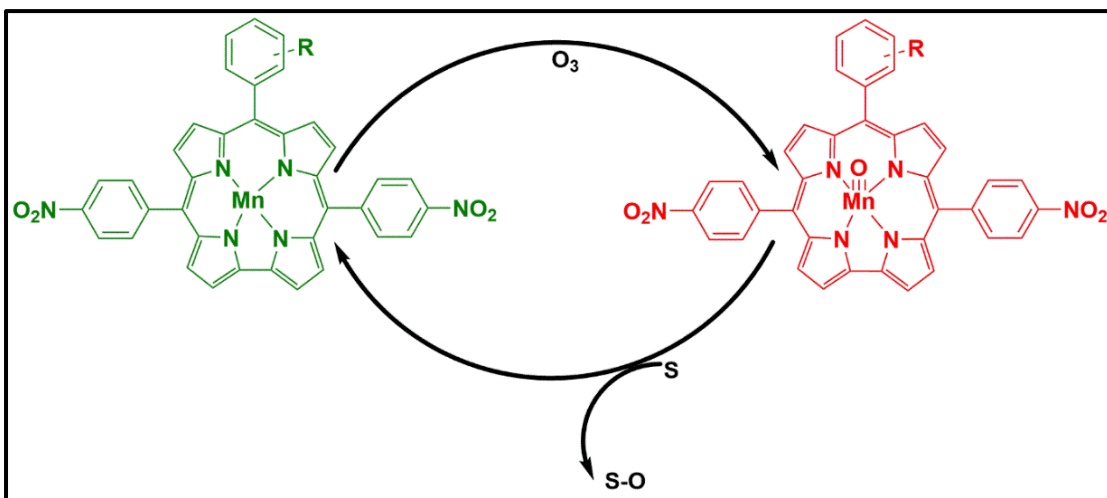


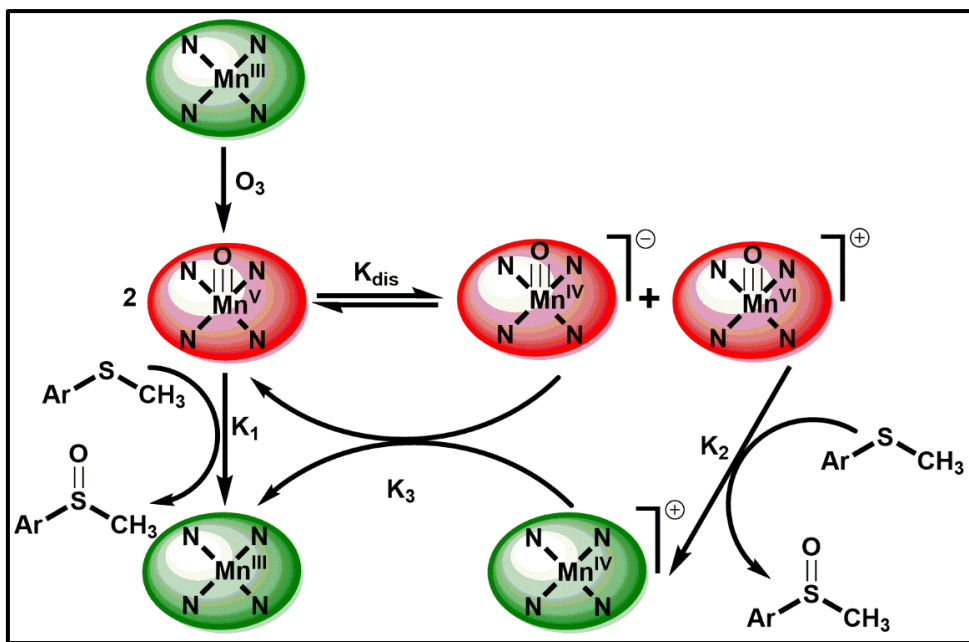
Fig. 3.1: Graphical representation of oxygen atom transfer reaction of manganese corrole

3.2 Significance and mechanism of sulfoxidation reactions

The sulfoxides are used in the pharmaceutical industry and the production of antifungal and antibacterial compounds [15,16]. The problem faces to production of sulfoxides in the synthesis of proton pump inhibitors, which are used to treat heartburn and ulcers [17].

In traditional method of oxidation of sulphides using the toxic heavy metal, peroxyacids or strong oxidant which are harmful to us [18,19]. Presently, eco-friendly sulfoxidation catalysis is a developing area of research [20].

OAT mechanism of the metal-oxo complex is complicated because both compropanation and disproportionation mechanisms can be used to explain the oxygen atom transfer phenomenon. Oxo-manganese(V) corroles have efficiently performed stoichiometric sulfoxidations, which depends on the electronic effects of the corrole.



Scheme 3.1: Proposed Mechanism for Direct OAT of (Oxo)manganese(V) corrole to sulfides.

3.3 Experimental section

3.3.1 Chemicals

All chemical solvents ($CH_3COOCH_2CH_3$, $CHCl_3$, CH_2Cl_2 , C_6H_{14} and CH_3OH) were purchased from E. Merck Ltd. All aldehydes were ordered from Sigma-Aldrich, which are used for syntheses without purification. But pyrrole was used after purification by distillation process. Deuterated solvents were purchased from Sigma-Aldrich. LOBA Chemie supplied silica gel (100-200 m mesh) and aluminium oxide active (basic) for *trans*- A_2B corrole (free base) and manganese corrole, respectively.

3.3.2 Common scheme for the synthesis of A_2B corrole (free base)

A_2B corroles were prepared using the reported method in the literature [21-24]. 1 mmol of DPM (5-(4-Nitrophenyl) dipyrromethane) and 0.5 mmol of the corresponding aldehyde were dissolved in 100 mL methanol and consequently, 5 mL of 36% HCl was

added. Then the solution was stirred at room temperature for 2 hours. Using chloroform, the solution was extracted, then washed with distilled water, dried over anhydrous sodium sulphate and filtered. Chloroform was used to dilute the reaction mixture, and 1.5 mmol of *p*-chloranil was added in it. The reaction mixture was stirred at room temperature overnight, and the progress of the reaction was monitored using TLC in the Hexane/DCM solvent system. The green-coloured solution of A₂B corrole was collected by column chromatography and recrystallized by a mixture of hexane and DCM [25].

3.3.2.1 5,15-Bis-nitrophenyl-10-(2,3,4,5,6-pentafluorophenyl) A₂B Corrole 1

The green crude A₂B corrole was purified using column chromatography with 4:6; DCM: hexane as eluent. The spectroscopy data matches the previous report [26]. UV-vis (CH₂Cl₂) λ_{max} , nm ($\epsilon \times 10^3 \text{ M}^{-1} \text{ cm}^{-1}$) 432 (**27.9**), 590 (**10.0**).

3.3.2.2 5,15-Bis-nitrophenyl-10-(2,6-difluorophenyl) A₂B corrole 2

This A₂B corrole was prepared by the, same procedure as above and the spectroscopy data matches the previous report [26]. UV-vis (CH₂Cl₂) λ_{max} , nm ($\epsilon \times 10^3 \text{ M}^{-1} \text{ cm}^{-1}$) 419 (**30.7**), 595 (**8.57**).

3.3.2.3 5,15-Bis-nitrophenyl-10-phenyl A₂B corrole 3

This A₂B corrole was also prepared using the same procedure as above, and the spectroscopy data matches the earlier report [27]. UV-vis (CH₂Cl₂) λ_{max} , nm ($\epsilon \times 10^3 \text{ M}^{-1} \text{ cm}^{-1}$) 426 (**22.2**), 584 (**7.39**).

3.3.2.4 5,15-Bis-nitrophenyl-10-(4-methylphenyl) A₂B corrole 4

This A₂B free base corrole was synthesised according to the reported procedure [26].

UV-vis (CH₂Cl₂) λ_{max} , nm ($\epsilon \times 10^3$ M⁻¹ cm⁻¹) 414 (**16.8**), 586 (**3.43**).

3.3.2.5 5,15-Bis-nitrophenyl-10-(4-methoxyphenyl) A₂B corrole 5

This A₂B free base corrole was synthesised using the reported method [26]. UV-vis

(CH₂Cl₂) λ_{max} , nm ($\epsilon \times 10^3$ M⁻¹ cm⁻¹) 416 (**15.4**), 584 (**4.24**).

3.3.3 Common method of synthesis of manganese(III) A₂B corrole

Mn(III) corroles were synthesised using the methods described previously [1, 2, 26].

The corresponding A₂B free base corrole was dissolved in DMF. Then 4 to 5 folds' excess manganese acetate salt was added to a 100 mL R.B. flask and refluxed for 10 min. The change in colour of the solution from green to green-brown was observed, and the progress of the reaction was checked via TLC with the hexane/ethyl acetate solvent system. The reaction mixture was evaporated to dryness and dissolved in a minimum amount of DCM with aluminium oxide. Crude Mn(III) corrole was purified using column chromatography (basic aluminium oxide) with hexane/ethyl acetate as solvent system and was recrystallized in n-hexane.

3.3.3.1 Mn(III) 5,15-bis-nitrophenyl-10-(pentafluorophenyl)-corrole 1

Solvent system hexane/ethyl acetate 10:1 was used for the purification of 1-Mn(III) corrole and the isolation of the green manganese complex of corrole. Recrystallization from hot n-hexane provided a pure complex (48.8 mg, 91%). UV-Visible (EtOAc) λ_{max} , nm ($\epsilon \times 10^3$ M⁻¹ cm⁻¹) : 420 (**60.7**), 473 (**73.0**), 639 (**28.1**). MS (HRMS): m/z observed [M+H]⁺

758.0521; calculated for C₃₇H₁₆F₅MnN₆O₄⁺ 758.0534. Elemental analysis: calculated (found) for C₃₇H₁₆F₅MnN₆O₄: C 58.59 (59.60), H 2.13 (2.23), N 11.08 (10.11).

3.3.3.2 Mn(III) 5,15-bis-nitrophenyl-10-(2,6-difluorophenyl)-corrole 2

2-Mn(III) corrole was purified by the hexane/ethyl acetate 7:3. UV-Visible (EtOAc) λ_{max} , nm ($\epsilon \times 10^3 \text{ M}^{-1} \text{ cm}^{-1}$) 418 (**44.1**), 469 (**44.2**), 585 (**15.7**), 642 (**18.3**). MS (HRMS): m/z observed [M+H]⁺ **705.0866**; calculated for C₃₇H₁₉F₂MnN₆O₄⁺ **705.0816**. Elemental analysis: calculated (found) for C₃₇H₁₉F₂MnN₆O₄: C 63.08 (**63.24**), H 2.72 (**2.90**), N 11.93 (**12.66**).

3.3.3.3 Mn(III) 5,15-bis-nitrophenyl-10-(phenyl)-corrole 3

3-Mn(III) corrole was purified by hexane/ethyl acetate 1:1. UV-Visible (EtOAc) λ_{max} , nm ($\epsilon \times 10^3 \text{ M}^{-1} \text{ cm}^{-1}$) 418 (**54.2**), 470 (**61.2**), 664 (**31.3**). MS (HRMS): m/z observed [M +H]⁺ **688.0990**; calculated for C₃₇H₂₁MnN₆O₄⁺ **668.1005**. Elemental analysis: calculated (found) for C₃₇H₂₁MnN₆O₄: C 66.47 (**66.11**), H 3.17 (**3.73**), N 12.57 (**12.93**).

3.3.3.4 Mn(III) 5,15-bis-nitrophenyl-10-(4-methylphenyl)-corrole 4

4-Mn(III) corrole was purified by hexane/ethyl acetate 2:3. UV-Visible (EtOAc) λ_{max} , nm ($\epsilon \times 10^3 \text{ M}^{-1} \text{ cm}^{-1}$) 420 (**63.9**), 473 (**81.9**), 665 (**42.3**). MS (HRMS): m/z observed [M +H]⁺ **682.1115**; calculated for C₃₈H₂₃MnN₆O₄⁺ **682.1161**. Elemental analysis: calculated (found) for C₃₈H₂₃MnN₆O₄: C 66.87 (**66.19**), H 3.40 (**3.39**), N 12.31 (**11.50**).

3.3.3.5 Mn(III) 5,15-bis-nitrophenyl-10-(4-methoxyphenyl)-corrole 5

5-Mn(III) corrole was purified by hexane and ethyl acetate 3:7. UV-Visible (EtOAc) λ_{max} , nm ($\epsilon \times 10^3 \text{ M}^{-1} \text{ cm}^{-1}$) 423 (**15.5**), 478 (**21.0**), 668 (**11.0**). MS (HRMS): m/z observed [M +H]⁺ **698.1122**; calculated for C₃₈H₂₃MnN₆O₅⁺ **698.1110**. Elemental analysis: calculated (found) for C₃₈H₂₃MnN₆O₅: C **65.33 (65.75)**, H **3.32 (3.50)**, N **12.03 (11.74)**.

3.3.4 General procedure for synthesis of Mn^V(O) corrole

Mn^V(O) corroles were synthesised by using the reported method [2]. The stock solution (14.56 to 28.30 μM) of all the Mn(III) corroles (**1-Mn** to **5-Mn**) were prepared. 10 mL aliquots of Mn(III) corrole stock solution were treated with a flushed flow of ozone and argon in dry ice until the colour changed from green to red for **1-Mn^V(O)** to **5-Mn^V(O)** corrole. UV-visible spectroscopy was utilised to analyse **1-Mn^V(O)** to **5-Mn^V(O)** corroles, which were then employed in further kinetic investigations.

3.3.4.1 Mn^V(O) 5,15-bis-nitrophenyl-10-(2,3,4,5,6-pentafluorophenyl)-corrole 1

UV-vis (ethyl acetate): λ_{max} , nm ($\epsilon \times 10^3 \text{ M}^{-1} \text{ cm}^{-1}$) 341 (**49.0**), 413 (**47.8**), 516 (**11.5**).

3.3.4.2 Mn^V(O) 5,15-bis-nitrophenyl-10-(2,6-difluorophenyl)-corrole 2

UV-vis (ethyl acetate): λ_{max} , nm ($\epsilon \times 10^3 \text{ M}^{-1} \text{ cm}^{-1}$) 338 (**29.9**), 412 (**28.0**), 517 (**80.1**).

3.3.4.3 Mn^V(O) 5,15-bis-nitrophenyl-10-(phenyl)-corrole 3

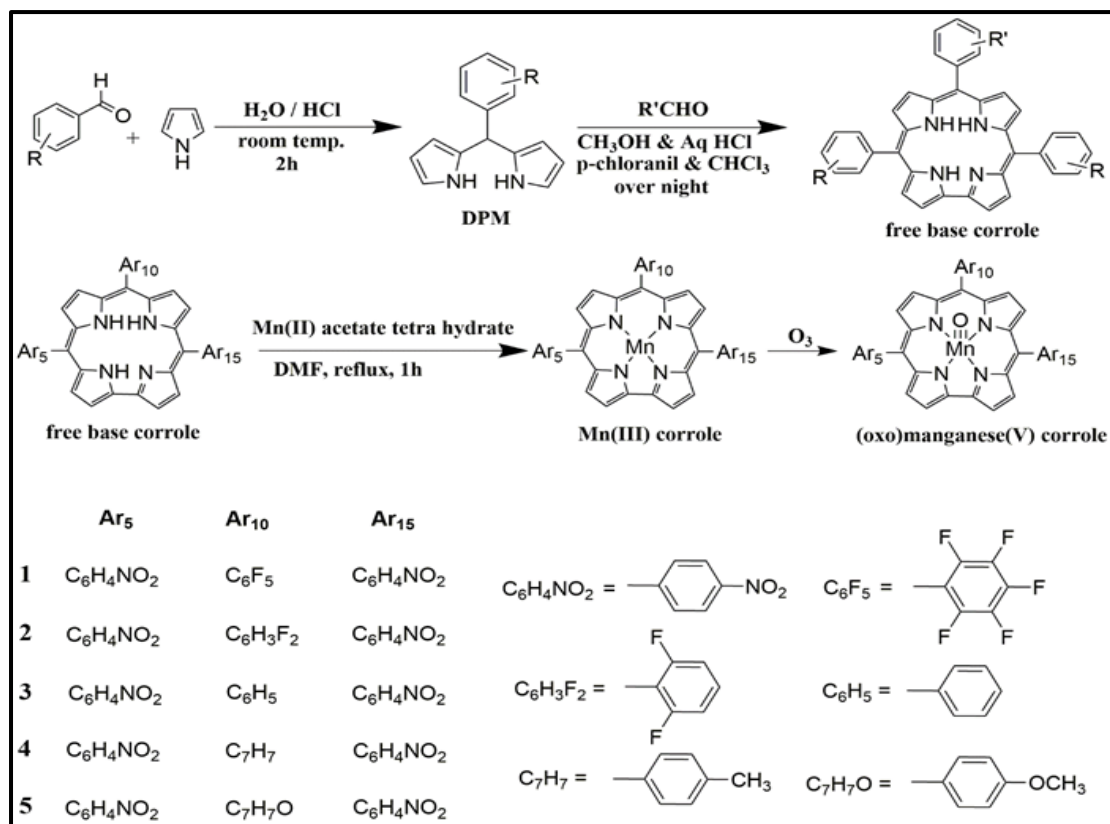
UV-vis (acetonitrile): λ_{max} , nm ($\epsilon \times 10^3 \text{ M}^{-1} \text{ cm}^{-1}$) 346 (**56.1**), 411 (**64.3**), 518 (**16.8**).

3.3.4.4 Mn^V(O) 5,15-bis-nitrophenyl-10-(4-methylphenyl)-corrole 4

UV-vis (acetonitrile): λ_{max} , nm ($\epsilon \times 10^3 \text{ M}^{-1} \text{ cm}^{-1}$) 347 (**42.0**), 412 (**59.1**), 607 (**53.4**).

3.3.4.5 Mn^V(O) 5,15-bis-nitrophenyl-10-(4-methoxyphenyl)-corrole 5

UV-vis (acetonitrile): λ_{max} , nm ($\varepsilon \times 10^3 \text{ M}^{-1} \text{ cm}^{-1}$) 349 (17.7), 413 (22.7), 542 (5.45).



Scheme 3.2: Free base *trans*-A₂B corroles, Mn(III) corroles and their Mn^V(O) complexes

3.4 Spectral characterization

3.4.1 UV-vis spectra of A₂B corroles, Mn(III) corroles and Mn^V(O) corroles

UV-1800 Shimadzu spectrophotometer was used to record the UV-Vis spectra. Solvents such as CH₂Cl₂, CH₃COOCH₂CH₃, and CH₃CN were used to calculate the molar absorptivity coefficients of A₂B corroles, Mn(III) corroles, and Mn^V(O) corroles.

The UV-vis spectra of A₂B corrole (free base), Mn(III) corrole and Mn^V(O) corrole were found to be similar to previously reported UV-vis spectra [1, 2, 9, 28]. B-bands were observed at 410-435 nm and Q-bands at 570-600 nm in UV-visible spectra of *trans*-A₂B

corroles (free base) (Fig. 3.2). Mn(III) corroles, on the other hand have two **B-band** in the region 410-480 nm and Q-band 635-645 nm (Fig. 3.3). In case of $\text{Mn}^{\text{V}}(\text{O})$ corroles, the Soret band split in the region of 335-415 nm and Q-band at 515-520 nm (Fig. 3.4).

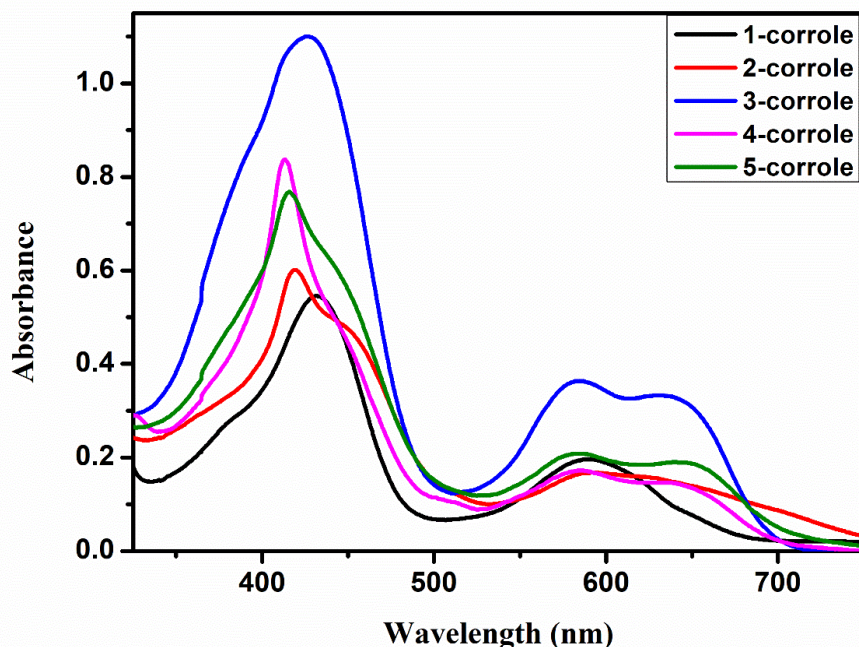


Fig. 3.2: UV-vis spectra of **1-5** *trans*-A₂B corroles in DCM.

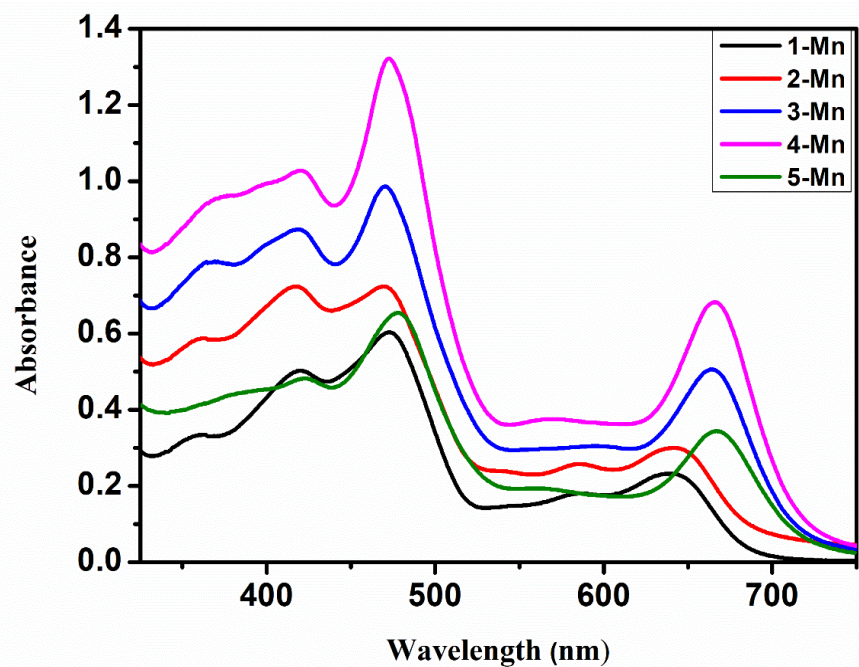


Fig. 3.3: UV-vis spectra of **1-Mn(III)** to **5-Mn(III)** complexes of A₂B corroles in ethyl acetate.

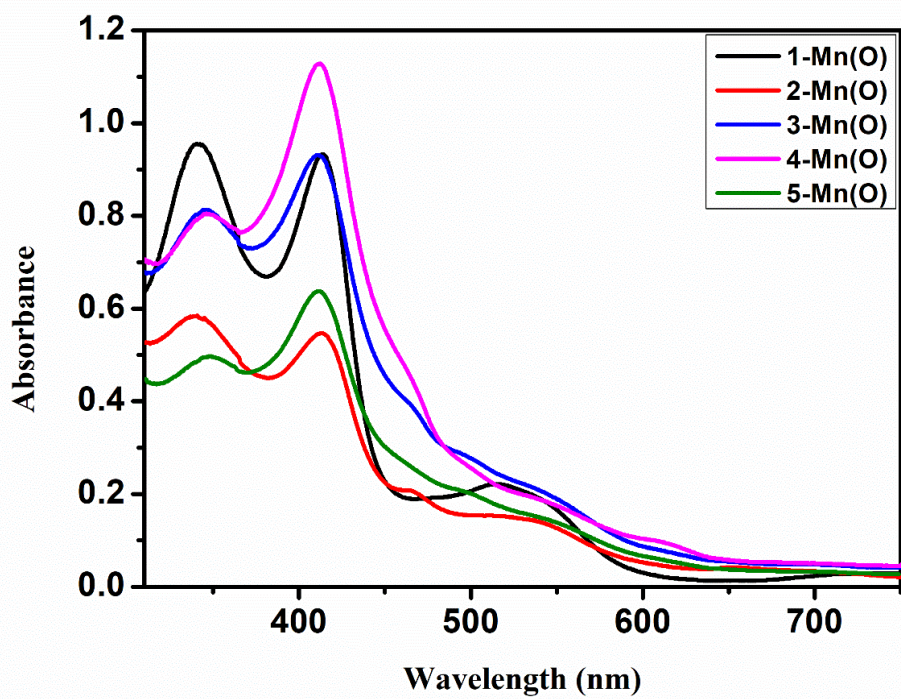


Fig. 3.4: UV-vis spectra of **1-Mn^{IV}(O)** to **2-Mn^{IV}(O)** complexes in ethyl acetate and **3-Mn^{IV}(O)** to **5-Mn^{IV}(O)** in acetonitrile.

3.4.2 NMR spectroscopy

Jeol, Model: JNM-EXCP 400 was used to record the ^1H NMR data at 400MHz. ^1H chemical shifts are observed at 7.26 ppm relative to the solvent (CDCl_3) peak. ^1H NMR spectra showed the signature of corrole [2,21,22,29-31]. We were unable to observe the NMR spectra of Mn(III) corroles because Mn(III) corroles have paramagnetic character. Figure 3.5 depicts the ^1H NMR of free base A₂B corrole 4. We observed the typical four set of doublets of pyrrolic hydrogens in the 8-9.1 ppm. The peak of $-\text{OCH}_3$ hydrogen was observed at 4.1 ppm.

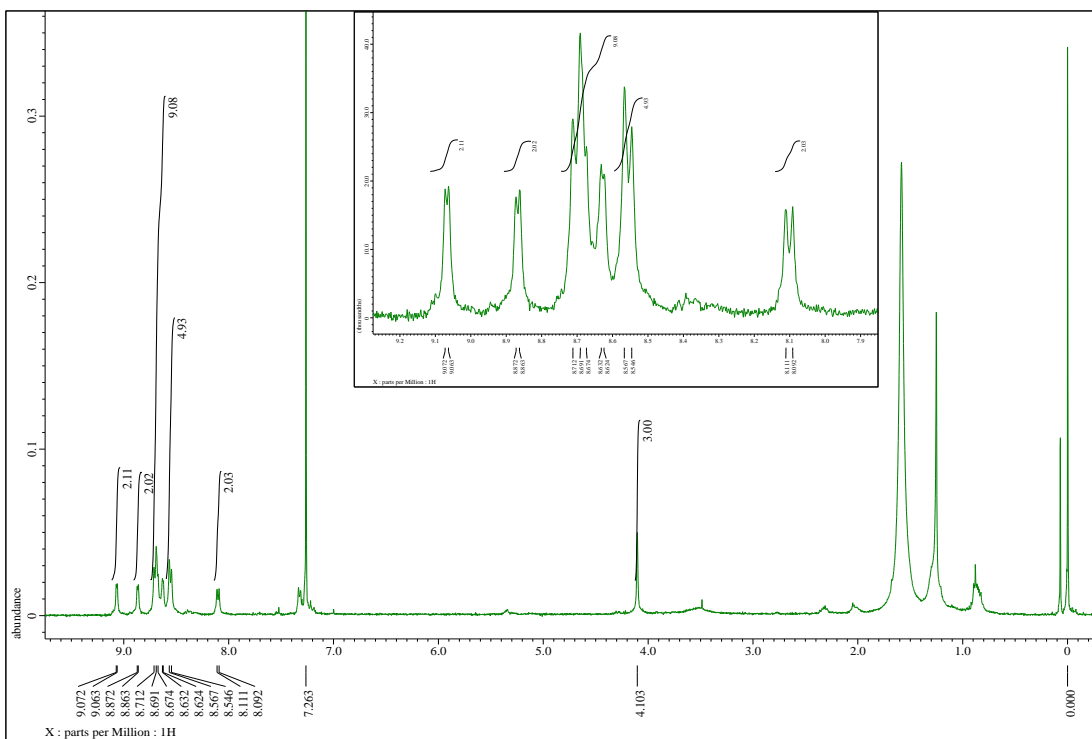


Fig. 3.5: ^1H NMR spectra (room temperature, CDCl_3) of 5,15-Bis-nitrophenyl-10-(4-methoxy phenyl) A_2B corrole **5**.

3.4.3 Mass spectra

The HRMS data of the Mn(III) complexes were recorded and found that the data matches with our earlier report. The HRMS data of 3-Mn(III) and 4-Mn(III) are shown below in Fig. 3.6 and 3.7.

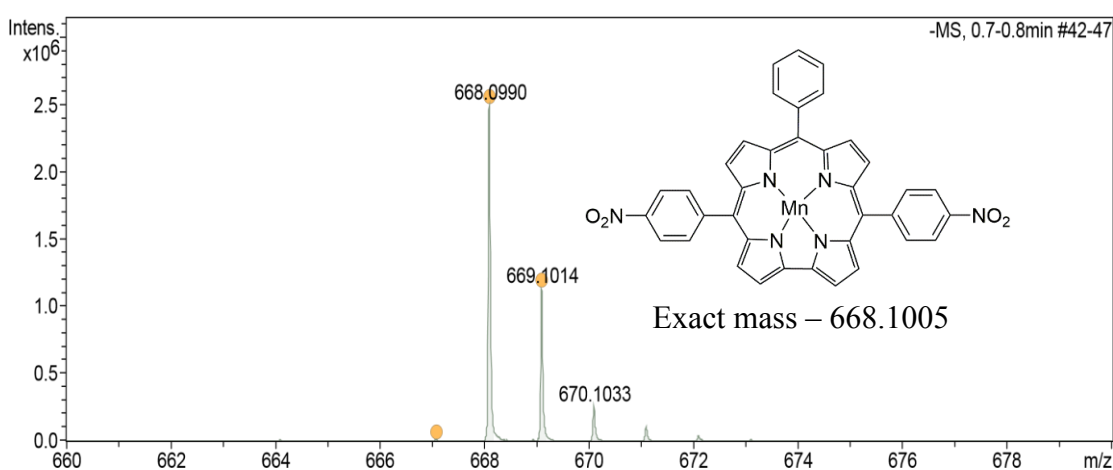


Fig. 3.6: HRMS of Mn(III) 5,15-bis-nitrophenyl-10-(phenyl)-corrole **3**

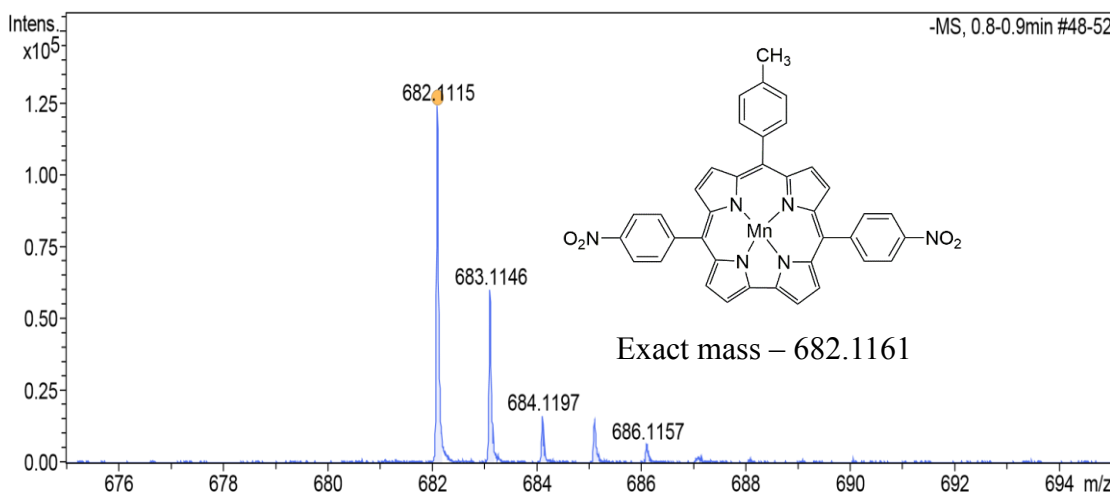


Fig. 3.7: HRMS of Mn(III) 5,15-bis-nitrophenyl-10-(4-methylphenyl)-corrole 4

3.5 Electrochemistry of Mn(III)corroles

CHI1120A instrument with its software CHI1120 Electrochemical Analyzer, was used to record the cyclic voltammogram data. For recording the cyclic voltammograms, glassy carbon, Ag/AgCl, platinum wire was used as the working electrode, reference electrode and counter electrode respectively. The electrolyte was Fluka-purchased tetrabutylammonium perchlorate (TBAP) mixed in acetonitrile, and the Mn-corrole concentration was 10^{-3} M. The scan rate was 100 mV/s, and the oxidation potential of ferrocene was 0.45 V. The oxidation of metallocorrole was observed to be much easier compared to metalloporphyrin [28]. Mn(III) corrole is stable in air but easily oxidised to Mn(IV) corrole at low potential and is affected by the electronic and steric factors of the substituents [1,2,9,28,32-39]. Coordination at the fifth position via a ligand such as OPPh_3 as well as halides such as Cl^- , Br^- and I^- stabilises the Mn^{IV} complex. [1,2,32-40]. The electron density of corrole π system is found dependent on the electron withdrawing and electron releasing groups attached to the meso substituents [41,42]. The cyclic voltammetry of **1-Mn** to **5-Mn** corroles was carried out using acetonitrile as solvent (Fig. 3.8).

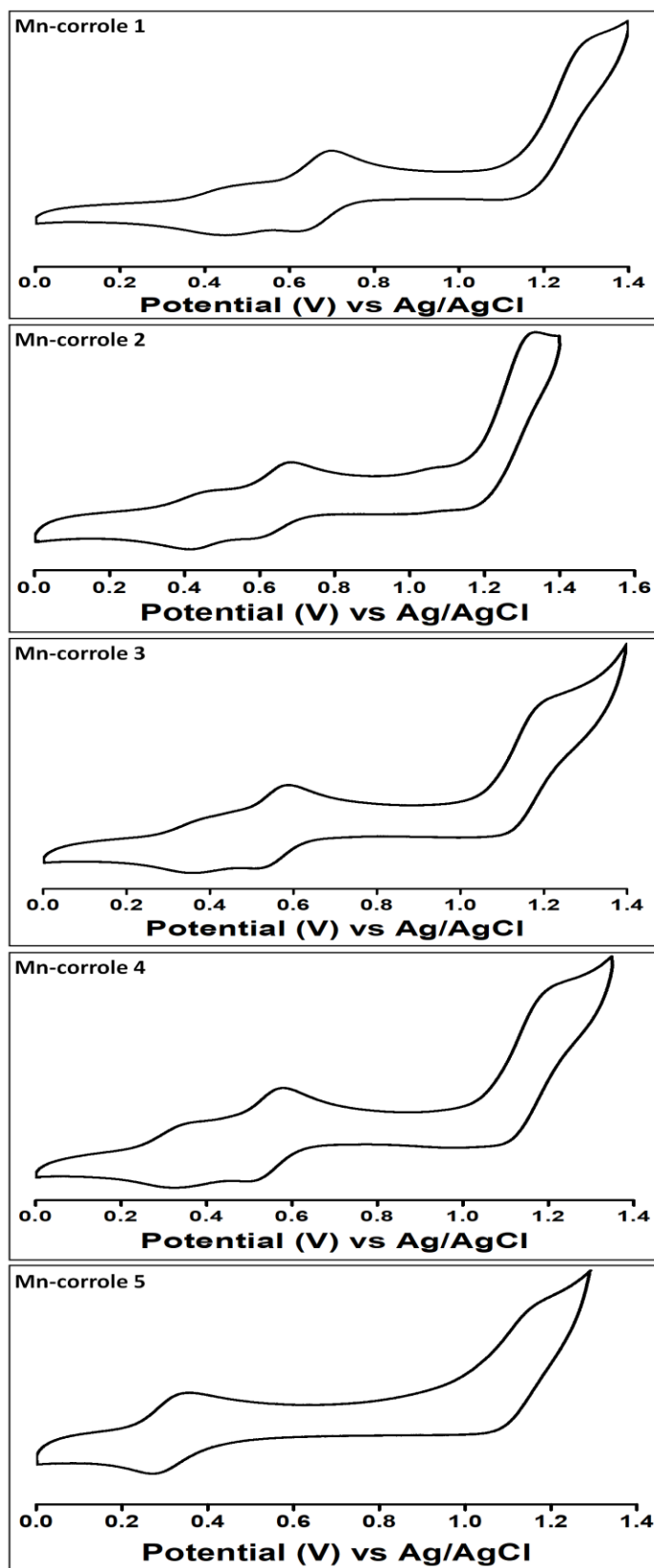


Fig. 3.8: Cyclic voltammogram of **1-Mn** to **5-Mn**.

All five Mn-corrole are distinguished by meso substituent at C-10 position of corrole. The $E_{1/2}$ value of couple $\text{Mn}^{\text{IV}}/\text{Mn}^{\text{III}}$ of **1-Mn** to **5-Mn** A_2B corroles was found to be in the range of 0.31 to 0.65 V (Table.3.1). **1-Mn**, **2-Mn** and **3-Mn** have a first oxidation potential that is 182-350 mV higher than Mn(III) OEC but 200 mV lower than Mn(III) TPP [2, 9, 34, 35]. The values of $E_{1/2}$ and ΔE of **1-Mn** to **5-Mn** A_2B corroles coincides with a gradual decrease as the electron donating tendency of phenyl substituent increases. However, we found that the value of $E_{1/2}$ and ΔE of **5-Mn** A_2B corrole decreased (0.31 V) and increased (97 mV), respectively. This unexpected result could be attributed to the -OCH₃ phenyl substituent at C-10 position of corrole. The same observations have also been reported in literature previously [2,9].

Table 3.1: Oxidation potential of Mn(III) A_2B corroles in acetonitrile with using TBAP as electrolyte

Corrole	$E_{1/2}$ (V)	ΔE (mV)
1-Mn	0.65	84
2-Mn	0.63	80
3-Mn	0.54	75
4-Mn	0.54	66
5-Mn	0.31	97

3.6 Kinetic studies of manganese corroles

At 20 °C, kinetic studies of **1-Mn^{V(O)}** to **5-Mn^{V(O)}** corroles were performed using a UV-1800 Shimadzu spectrophotometer. For kinetic experiments, freshly prepared (oxo)manganese(V) corroles were prepared by passing ozone through a stock solution of Mn(III) corrole [19.60 to 28.30 μM]. All kinetics experiments were

repeated three times for confirmation of the results at different wavelengths. The choice of solvent for a kinetic study depends on the stability of the manganese complex. So, we found that oxo complexes of **1-Mn** and **2-Mn** corroles are more stable in ethyl acetate, while oxo complexes of **3-Mn**, **4-Mn** and **5-Mn** corroles are most stable in acetonitrile. Gas chromatography was employed to analyse the formation of sulfoxides.

3.6.1 Rate constant of (oxo)manganese(V) corrole during self-decay

A UV-visible spectrophotometer was used to monitor the self-decay process. The colour change from red for Mn^V(O) corroles to green for Mn(III) corroles allowed us to easily observe the self-decay process. It was also confirmed by the spectral changes in UV-visible spectra with time. The oxo complex of the Mn corrole band in the range 340 to 360 nm disappears during the self-decay process, and an absorption peak at 480 nm appears. This process happened due to metal ligand charge transfer along with the absorption band of manganese(III) corrole monitored in the range of 550 to 600 nm [9]. A first-order reaction led to the self-decay of (oxo)manganese corrole. As a result, we calculated the rate constant of self-decay manganese corroles and the results are tabulated in Table 3.2. The rate constant of self-decay also confirmed the stability of **1-Mn^VO** and **2-Mn^VO** corroles in ethyl acetate, as well as **3-Mn^VO**, **4-Mn^VO** and **5-Mn^VO** in acetonitrile. So, we used acetonitrile and ethyl acetate as solvents for the investigation of reactivity of the (oxo)manganese corrole towards oxygen atom transfer at 20°C.

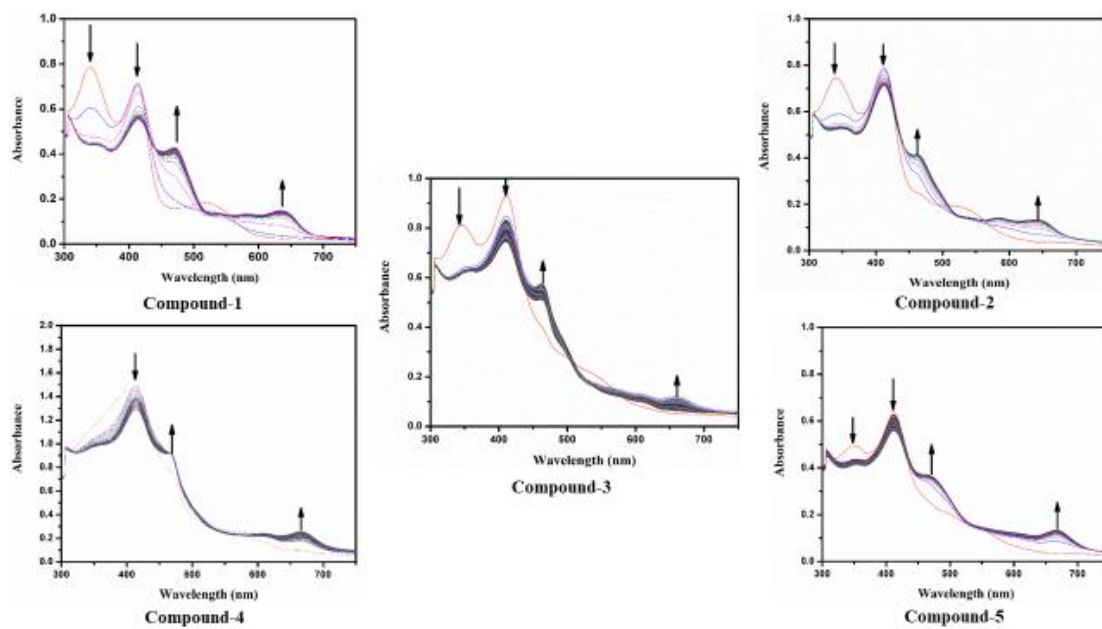


Fig. 3.9: UV-vis spectra change of self-decay of (oxo)manganese(V) corroles (**1-Mn(O)** and **2-Mn(O)** in ethyl acetate while **3-Mn(O)** to **5-Mn(O)** in acetonitrile)

3.6.2 Rate constant of oxygen atom transfer of (oxo)manganese(V) corrole to thioanisole

We determined the rate constant of oxygen transfer reactions by using the UV-visible spectrophotometer. The solutions of thioanisole were prepared in ethyl acetate, which has a 1000-fold higher concentration than (oxo)manganese(V) corrole and is tabulated in Table 3.3. The solution turned green when we added a solution of thioanisole derivatives to the (oxo)-Mn(V) corrole. This showed the oxygen atom transfer reaction of (oxo)manganese corrole to thioanisole.

The oxygen atom transfer reaction of (oxo)manganese corrole to thioanisole followed pseudo-order reactions. We determined the rate constant by employing a pseudo-order rate equation for track the disappearance and appearance of bands at 340 to 400 nm and 490 to 620 nm, respectively, with time. We calculated the pseudo-rate constant of **1-Mn^V(O)** to **5-Mn^V(O)** corrole, which is tabulated in Table 3.2. We discovered that in

the presence of thioanisole, decay rate increased continuously. For oxygen atom transfer towards thioanisole, the reactivity order was **1-Mn^V(O) > 2-Mn^V(O) > 5-Mn^V(O) > 3-Mn^V(O) > 4-Mn^V(O)** corrole for oxygen atom transfer towards thioanisole. When we go through previous years literature, the order is purely dependent on the electronic and steric factors [2-5,9,28,31,43-48]. The electron withdrawing substituent in **1-Mn** and **2-Mn** and the electron releasing substituent in **4-Mn**, **5-Mn** are present in the five Mn-corroles under investigation. At C₁₀ of corrole, there are five fluorine atoms in **1-Mn** corrole and two fluorine atoms in **2-Mn** corrole. Due to presence of fluorine atoms, **1-Mn** and **2-Mn** corrole have electron deficient environment. On the other side, **3-Mn**, **4-Mn**, **5-Mn** A₂B corroles have no fluorine atom on phenyl group at C₁₀ position and hence their reactivity is depending upon the electron releasing or hindering group present on *meso* positions. **3-Mn^V(O)** corrole have only phenyl group without any substituent at C₁₀ position of corrole. **4-Mn^V(O)** and **5-Mn^V(O)** have -CH₃ and -OCH₃ in the *para* positions of the *meso* phenyl group. We can easily attribute the reactivity order to the presence of pentafluoro, difluoro, methyl and methoxy phenyl groups. As a result, **1-Mn^V(O)** have five fluorine atoms, which makes it most hindered and electronically deficient corrole. **2-Mn^V(O)** has two fluorine atoms, which shows only steric protection, so the reactivity of OAT to thioanisole is lower than that of **1-Mn^V(O)** [2]. So, we observed that the reactivity does depend on only two factors: one is electron releasing and electron withdrawing and the other is steric protection. The rate constant of OAT also affected with -I effect of the different derivative of thioanisole. It is evident from the Table 3.3 the highest rate constant was observed with 4-(methylthio)benzonitrile. The rate constant of oxygen atom transfer reaction of reported corroles is depending on both the electronic and steric factors [2,9,46]. The electron

withdrawing group increases the reactivity of the OAT reaction, which was explained by the DFT calculation [5,47].

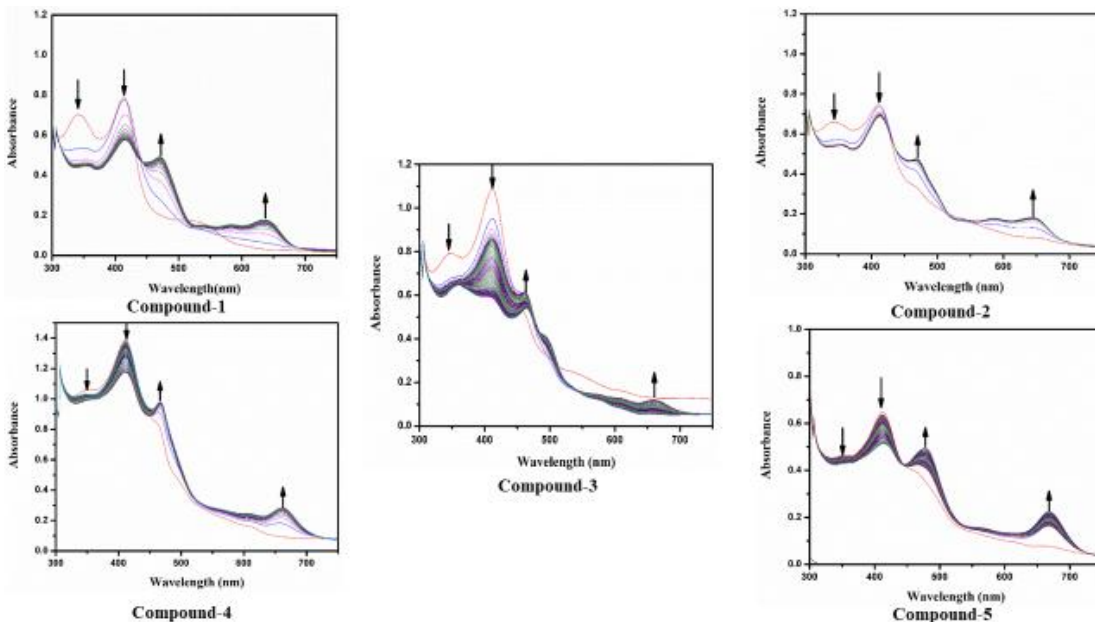


Fig. 3.10: UV-vis spectral changes upon oxygen atom transfers from (oxo)manganese(V) corrole to thioanisole (**1-Mn(O)** and **2-Mn(O)**) in ethyl acetate while **3-Mn(O)** to **5-Mn(O)** in acetonitrile)

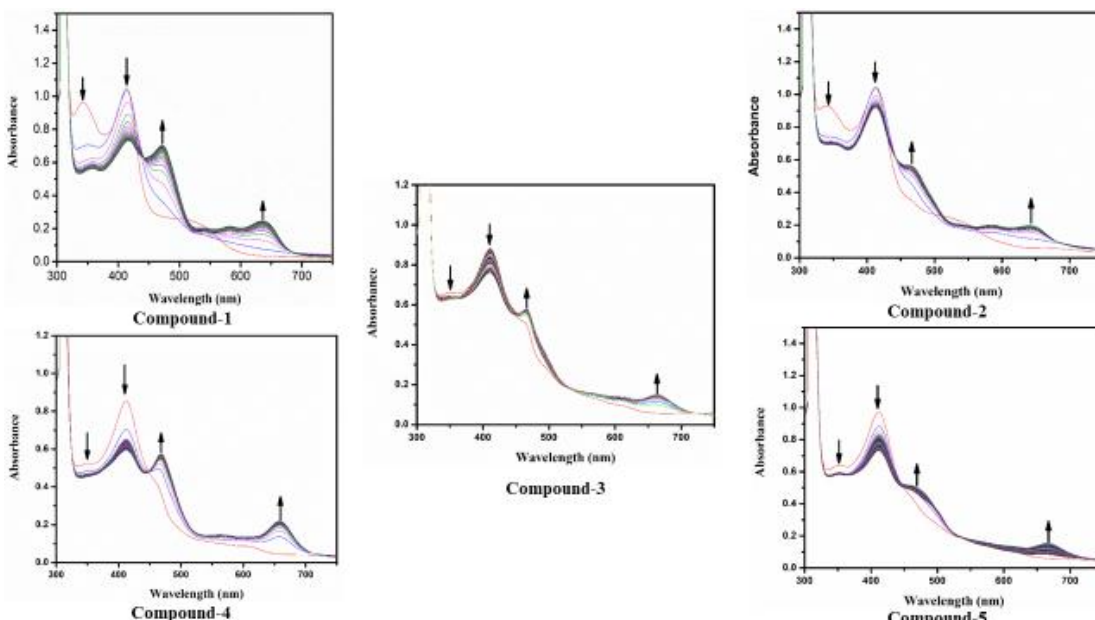


Fig. 3.11: UV-vis spectral changes upon oxygen atom transfers from (oxo)manganese(V) corrole to *para*-methoxy thioanisole (**1-Mn(O)**, **2-Mn(O)**) in ethyl acetate and **3-Mn(O)** to **5-Mn(O)** in acetonitrile)

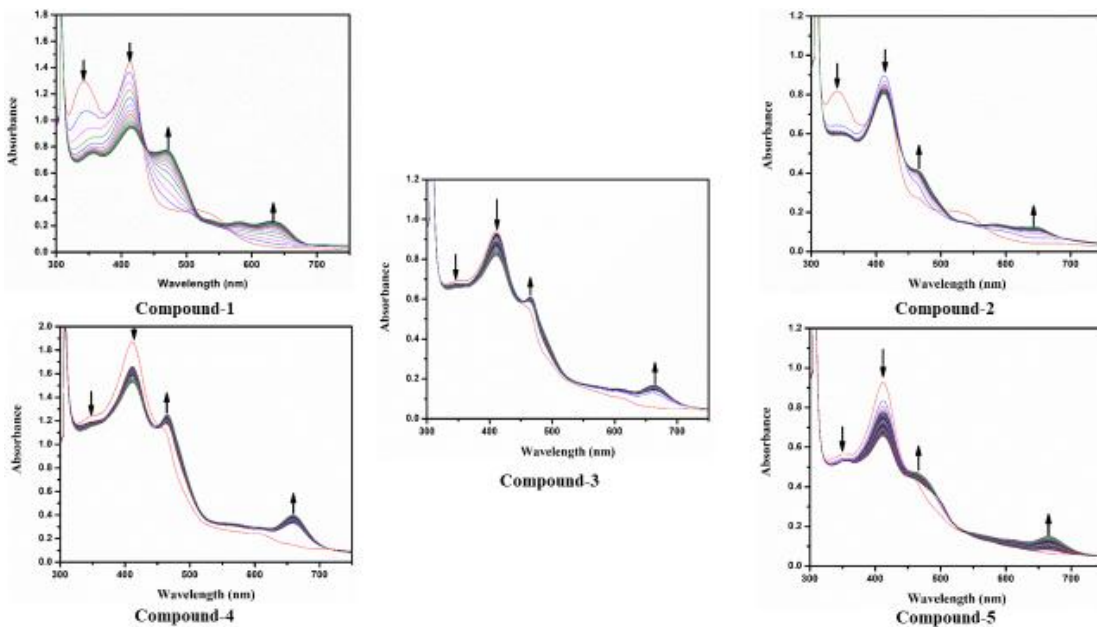


Fig. 3.12: UV-vis spectral changes upon oxygen atom transfers from (oxo)manganese(V) corrole to *para*-fluoro thioanisole (**1-Mn(O)**, **2-Mn(O)**) in ethyl acetate and **3-Mn(O)** to **5-Mn(O)** in acetonitrile)

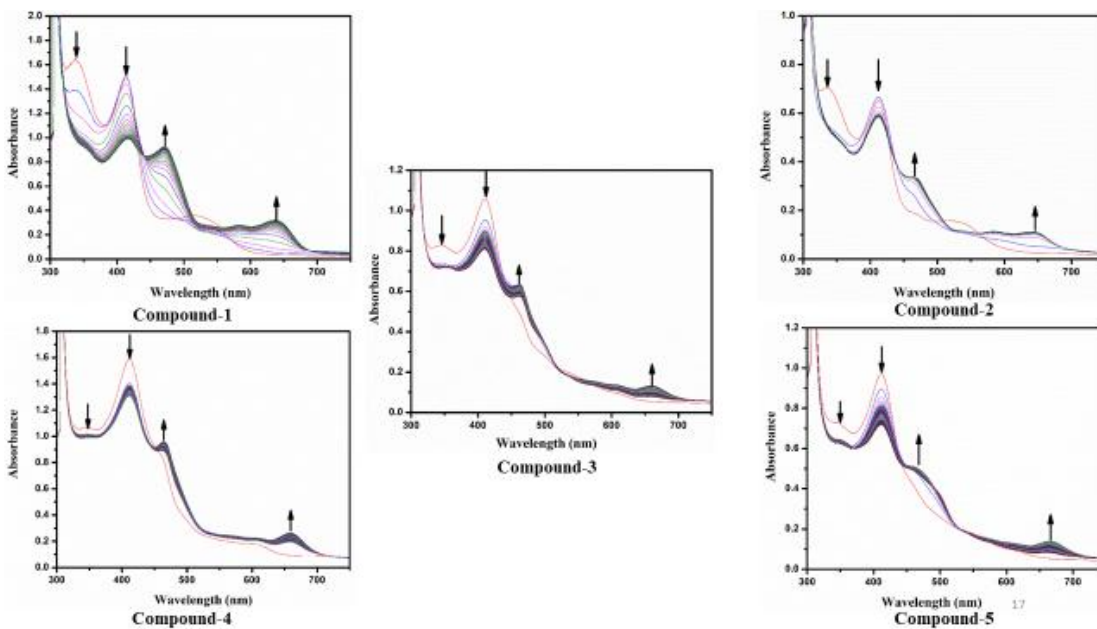


Fig. 3.13: UV-vis spectral changes upon oxygen atom transfers from (oxo)manganese(V) corrole to *para*-(methylthio) benzonitrile (**1-Mn(O)**, **2-Mn(O)**) in ethyl acetate and **3-Mn(O)** to **5-Mn(O)** in acetonitrile)

Table 3.2: First order rate constant (k) of self-decay and pseudo-first-order rate constants (k_{obs}) of oxygen atom transfer to thioanisole (**1-Mn^V(O)**, **2-Mn^V(O)** in ethyl acetate and **3-Mn^V(O)** to **5-Mn^V(O)** in acetonitrile).

Rate constant ($M^{-1}s^{-1} \times 10^4$)					
	Self-decay	H-C ₆ H ₄ -S-CH ₃	CH ₃ O-C ₆ H ₄ -S-CH ₃	F-C ₆ H ₄ -S-CH ₃	CN-C ₆ H ₄ -S-CH ₃
1-Mn ^V =O	3.21	4.34	7.18	12.78	14.60
2-Mn ^V =O	1.65	3.23	4.65	9.92	10.88
3-Mn ^V =O	0.12	1.21	2.51	3.73	7.44
4-Mn ^V =O	1.10	1.37	1.85	3.22	4.92
5-Mn ^V =O	2.23	3.16	4.83	4.03	8.13

Table 3.3: Concentration of thioanisole used for kinetic study

S.No.	Thioanisole derivatives used	Concentration (M)
1	H-C ₆ H ₄ -S-CH ₃	1.703
2	CH ₃ O-C ₆ H ₄ -S-CH ₃	0.719
3	F-C ₆ H ₄ -S-CH ₃	0.820
4	CN-C ₆ H ₄ -S-CH ₃	0.5

3.7 Density functional theory (DFT) calculations

We performed DFT calculations for the HOMO-LUMO gap identification and electronic distribution and compared the results with the reported manganese corroles [26]. DFT optimisation revealed a manganese atom in **1-Mn** to **5-Mn** corroles situated 0.04 above the mean plane of four pyrrolic nitrogens and 0.04 to 0.05 above the mean plane of the macrocycle (Table 3.4). The same pattern was observed in the single crystal structure of manganese corrole [2,5,48]. We found that **1-Mn** and **2-Mn** corroles have higher HOMO and LUMO gaps due to the presence of electron withdrawing groups on the periphery of their macrocycle. The phenomenon is supported by the $E_{1/2}$ values of **1-Mn** to **5-Mn** corroles (Table 3.1). If we look at the frontier molecular orbital, we can see that mainly LUMO's have 3d_{xz} orbital of the manganese metal ion and LUMO+1 is associated with the -NO₂ group (electron withdrawing group) at the A₂ meso position and 3d_{z²} of

manganese metal ion. These observations represent that Mn corrole initially undergoes reduction at manganese metal rather than the macrocycle ring (Fig.3.8) [49].

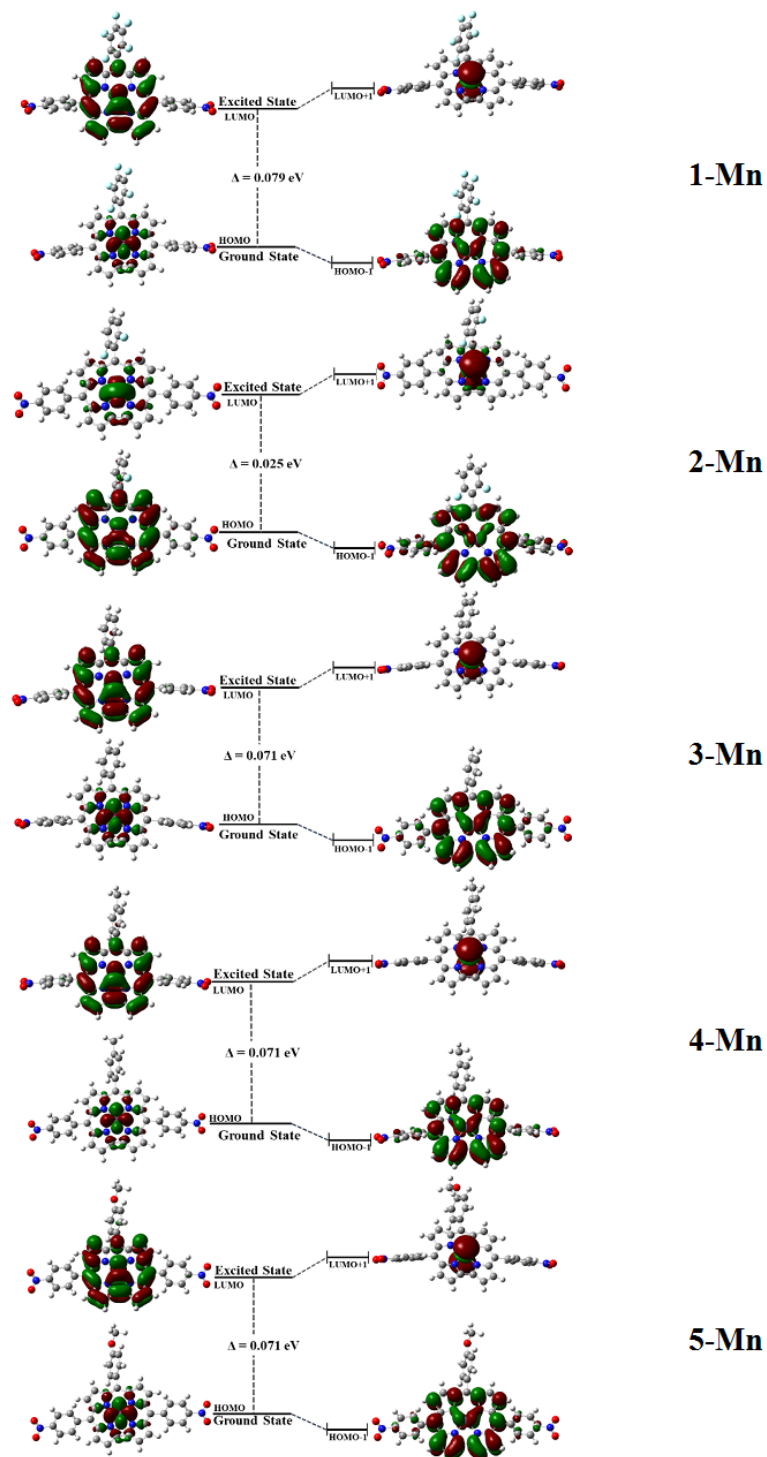


Fig. 3.14: FMO (frontier molecular orbital) of **1-Mn to 5-Mn** corrole, (Isosurface value= 0.02)

Table 3.4: DFT optimized molecules structural parameters and frontier molecular orbital energy

Molecule	Distance from the plane(Å)		Molecular orbitals (eV)			
	N ₄ /Mn	Mean plane/Mn	LUMO+1	LUMO	HOMO	HOMO-1
1-Mn	0.042	0.044	-6.35	-6.69	-6.77	-6.80
2-Mn	0.046	0.050	-6.08	-6.19	-6.21	-6.44
3-Mn	0.044	0.046	-6.35	-6.70	-6.77	-6.80
4-Mn	0.048	0.053	-6.35	-6.70	-6.77	-6.80
5-Mn	0.049	0.054	-6.35	-6.70	-6.77	-6.80

3.8 Conclusion

We have synthesised the 5 *trans*-A₂B maganese corroles and the oxo complexes of manganese corroles which are characterised by the ¹H NMR, UV-visible spectroscopy, mass spectroscopy and cyclic voltammetry. We determined the rate constant of self-decay and oxygen transfer reactions to thioanisole. The process of OAT to a derivative of *p*-thioanisoles followed the disproportionation path. The electron releasing and withdrawing group attached on phenyl group at C₁₀ position of corrole affected the oxygen transfer rate constant of the 1-Mn^V(O) to 5-Mn^V(O) corroles. Also, a new series of *trans*-A₂B free base corroles was synthesised and was characterised by UV-visible, ¹H NMR spectroscopy. Electrochemistry clearly described the substituent effect on the oxidation potential of manganese(III) complex of *trans*-A₂B corrole. Furthermore, DFT calculation also supported this phenomenon.

References

1. Gross, Z.; Golubkov, G.; Simkhovich, L. *Angew. Chem. Int. Ed. Engl.* **2000**, *39*, 4045-4047.
2. Kumar, A.; Goldberg, I.; Botoshansky, M.; Buchman, Y.; Z., G. *J. Am. Chem. Soc.* **2010**, *132*, 15233-15245.
3. Bose, S.; Pariyar, A.; Biswas, A. N.; Das P.; and Bandyopadhyay, P. *Catal. Commun.* **2011**, *12*, 1193–1197.
4. Bose, S.; Pariyar, A.; Biswas, A. N.; Das, P.; and Bandyopadhyay, P. *Catal. Commun.* **2011**, *12*, 446–449.
5. He, J.; Xu, Z. G.; Xu, X.; Mahmood, M. H. R.; and Liu, H. Y. *J. Porphyrins Phthalocyanines* **2013**, *17*, 1196-1203.
6. Yu, L.; Wang, Q.; Dai, L.; Ying, L. W.; Chen, R.; Mahmood, M. H. R.; Liu, H. Y.; and Chang, C. K. *Chinese Chem. Lett.* **2013**, *24*, 447-449.
7. Wang, Q.; Zhang, Y.; Yu, L.; Yang, H.; Mahmood, M. H. R.; and Liu, J. *Porphyrins Phthalocyanines*. **2014**, *18*, 316-325.
8. Ng, N.-C.; Mahmood, M. H. R.; Liu, H.-Y.; Yam, F.; Yeung, L.-L.; Chang, C.-K. *Chinese Chemical Letters* **2014**, *25*, 571–574.
9. Mahmood, M. H. R.; Wanga, H.-H.; Liu, H.-Y.; and Chang, C.-K. *J. Porphyrins Phthalocyanines*. **2015**, *19*, 1238-1250.
10. Kwong, K. W.; Lee, N. F.; Ranburger, D.; Malone, J.; Zhang, R.; *J. Inorg. Biochem.* **2016**, *163*, 39-44.
11. Guo, M.; Lee, Y.-M.; Gupta, R.; Seo, M. S.; Ohta, T.; Wang, H.-H.; Liu, H.-Y.; Dhuri, S. N.; Sarangi, R.; Fukuzumi, S.; Nam, W. *J. Am. Chem. Soc.* **2017**, *139*, 15858- 15867.
12. J.P. Zaragoza, M.A. Siegler, D. Goldberg, *J. Am. Chem. Soc.* **2018**, *140*, 4380–4390.

13. Tiffner, M.; Gonglach, S.; Haas, M.; Schöfberger, W.; Waser, M. *Chem. Asian J.* **2017**, *12*, 1048-1051.
14. Malik, M.; Kaur, R. *Polym. Adv. Technol.* **2018**, *29*, 1078-1085.
15. Caron, S.; Dugger, R. W.; Ruggeri, S. G.; Ragan, J. A.; Ripin, D. H. B. *Chem. Rev.* **2006**, *106*, 2943-2989.
16. Baeckvall, J. E. *Wiley-VCH Verlag: Weinheim*. **2004**.
17. Wojaczynska, E.; Wojacznski, J. *Chem. Rev.* **2010**, *110*, 4303-4356.
18. Hosseinpoor, F.; Golchubian, H. *Tetrahedron Lett.* **2006**, *47*, 5195-5197.
19. Kaczorowska, K.; Kolarska, Z.; Mitka, K.; Kowalski, P. *Tetrahedron* **2005**, *61*, 8315- 8327.
20. Surendra, K.; Krishnaveni, N. S.; Kumar, V. P.; Sridhar, R.; Rao, K. R. *Tetrahedron Lett.* **2005**, *46*, 4581-4583.
21. Paolesse, R.; Jaquinod, L.; Nurco, D.J.; Mini, S.; Sagone, F.; Boschi, T.; Smith, K. M. *Chem. Commun.* **1999**, *14*, 1307-1308.;
22. Paolesse, R.; Nardis, S.; Sagone, F.; Khoury, R. J. *J. Org. Chem.* **2001**, *66*, 550-556.
23. Gross, Z.; Galili, N.; Simkhovich, L.; Saltsman, I.; Botoshansky, M.; Blaser, D.; Boese, R.; Goldberg, I. *J. Org. Chem.* **1999**, *4*, 599-602.
24. Gross, Z.; Galili, N.; Saltsman, I. *Angew. Chem., Int. Ed.* **1999**, *38*, 1427-1429.
25. Yadav, O; Varshney, A; Kumar, A; Ratnesh, R. K.; and Mehata, M. S. *Spectrochimica Acta Part A: Molecular and Biomolecular Spectroscopy* **2018**, *202*, 207-213.
26. Yadav, O.; Varshney, A.; Kumar, A. *Inorganic Chemistry Communications* **2017**, *86*, 168-171.

27. Lu, G.; Li, J.; Jiang, X.; Ou, Z.; and Kadish, K. M. *Inorg. Chem.* **2015**, *54*, 9211-9222.
28. Liu, H. Y.; Lai, T. S.; Yeung, L. L.; Chang, C. K. *Org. Lett.* **2003**, *5*, 617-620.
29. (a) Paolesse, R.; Licoccia, S.; Fanciullo, M.; Morgante, E.; Boschi, T. *Inorg. Chim. Acta*. **1993**, *203*, 107-114; (b) Paolesse, R.; Licoccia, S.; Bandoli, G.; Dolmella, A.; Boschi, T. *Inorg. Chem.* **1994**, *33*, 1171-1176; (c) Adamian, V. A.; Souza, F. D.; Licoccia, S.; Di Vona, M. L.; Tassoni, E.; Paolesse, R.; Boschi, T.; Smith, K. M. *Inorg. Chem.* **1995**, *34*, 532-540; (d) Paolesse, R.; Pandey, R. K.; Forsyth, T. P.; Jaquinod, L.; Gerzevske, K. R.; Nurco, J.; Senge, M. O.; Licoccia, S.; Boschi, T.; Smith, K. M. *J. Am. Chem. Soc.* **1996**, *118*, 3869-3882; (e) Paolesse, R.; Macagnano, A.; Monti, D.; Tagliatesa, P.; Boschi, T. *J. Porphyrins Phthalocyanines* **1998**, *2*, 501-510; (f) Paolesse, R.; Sagone, F.; Macagnano, A.; Boschi, T.; Prodi, L.; Mantalti, L.; Zaccheroni, N.; Bolettaand, F.; Smith, K. M. *J. Porphyrins Phthalocyanines* **1999**, *3*, 364-370; (g) Paolesse, R.; Froiio, A.; Nardis, S.; Mastrianni, M.; Russo, M.; Nurco, D. J.; Smith, K. M. *J. Porphyrins Phthalocyanines* **2003**, *7*, 585-592; (h) Mandoj, F.; Nardis, S.; Pomarico, G.; Stefanelli, M.; Schiafinno, L.; Ercolani, G.; Prodi, L.; Genovese, D.; Zaccheroni, N.; Franczek, F. R.; Smith, K. M.; Xiao, X.; Shen, J.; Kadish, K. M.; Paolesse, R. *Inorg. Chem.* **2009**, *48*, 10346-10357; (i) Mandoj, F.; Stefanelli, M.; Nardis, S.; Mastrianni, M.; Franczek, F. R.; Smith, K. M.; Paolesse, R. *Chem. Commun.* **2009**, 1580-1582.
30. (a) Gryko, D. T. *Chem. Commun.* **2000**, 2243-2244; (b) Gryko, D. T.; Jadach, K. *J. Organomet. Chem.* **2001**, *66*, 4267-4275; (c) Gryko, D. T. *Eur. J. Org. Chem.* **2002**, 1735-1743; (d) Gryko, D. T.; Koszarna, B. *Synthesis* **2004**, *13*, 2205-2209; (e) Koszarna, B.; Gryko, D. T. *J. Organomet. Chem.* **2006**, *71*, 3707-3717.
31. Collman, J. P.; Zeng, L.; Decre'au, R. A. *Chem. Commun.* **2003**, *24*, 2974-2975.
32. Bröring, M.; Hell, C.; Brandt, C. D. *Chem. Commun.* **2007**, *18*, 1861-1862.
33. Mahammed, A.; Tumanskii, B.; Gross, Z. *J. Porphyrins Phthalocyanines* **2011**, *15*, 1275-1286.

34. Erben, C.; Will, S.; Kadish, K. M. In The Porphyrin Handbook; 1st ed.; Kadish, K. M., Smith, K. M., Guilard, R., Eds.; Academic Press: New York, 2000; Vol. 2, p 233-300.
35. Kadish, K.M. In Progress in Inorganic Chemistry, John Wiley, New York, 1986, p435.
36. Lucas, H. J.; Kennedy, E. R.; Formb, M. W. *Organic Syntheses* Vol. **1955**, 3, 483.
37. Conlon, M.; Johnson, A. W.; Overend, W. R.; Rajapaksa, D.; Elson, C. M. *J. Chem. Soc. Perkin Trans. 1973*, 1, 2281-2288.
38. Bendix, J.; Gray, H. B.; Golubkov, G.; Gross, Z. *Chem. Commun.* **2000**, 19, 1957-1958.
39. Kadish, K. M.; Adamian, V. A.; Van Caemelbecke, E.; Gueletii, E.; Will, S.; Erben, C.; Vogel, E. *J. Am. Chem. Soc.* **1998**, 120, 11986-11993.
40. Kadish, K. M.; Caemelbecke, E. V. *J. Solid State Electrochem.* **2003**, 7, 254-258.
41. Liang, X.; Fang, J.; Li, M.; Chen, Q.; Mack, J.; Molupe, N.; Nyokongc, T.; Zhua, W. *J. Porphyrins Phthalocyan.* **2017**, 21, 751-758.
42. Golubkov, G.; Bendix, J.; Gray, H. B.; Mahammed, A.; Goldberg, I.; DiBilio, A. J.; Gross, Z. *Angew. Chem. Int. Ed.* **2001**, 40, 2132-2134.
43. (a) Zdilla, M. J. Abu-Omar, M. M. *J. Am. Chem. Soc.* **2006**, 128, 16971-16979; (b) Zdilla, M. J.; Abu-Omar, M. M. *Inorg. Chem.* **2008**, 47, 10718-10722; (c) Zhang, R. Newcomb, M. *J. Am. Chem. Soc.* **2003**, 125, 12418-12419; (d) Liu, H. Y.; Yam, F.; Xie, Y. T.; Li, X. Y.; Chang, C.K. *J. Am. Chem. Soc.* **2009**, 131, 12890-12891; (e) Zhang, R.; Harischandra, D. N.; Newcomb, M. *Chem. Eur. J.* **2005**, 11, 5713-5720; (f) Wang, H.; Mandimutsira, B. S.; Todd, R.; Ramadhanie, B.; Fox, J. P.; Goldberg, D. P. *J. Am. Chem. Soc.* **2004**, 126, 18-19; (g) Gross, Z.; Nimri, S. *Inorg. Chem.* **1994**, 33, 1731-1732; (h) Czarnecki, K.; Nimri, S.; Gross, Z.; Proniewicz, L. M.; Kincaid, J. R. *J. Am. Chem. Soc.* **1996**, 118, 2929-2935; (i) Lansky, D. E.; Kosack, J. R.; Sarjeant, A. A. N.; Goldberg, D. P. *Inorg. Chem.*

- 2006**, *45*, 8477-8479; (j) Fryxelius, J.; Eilers, G.; Feyziyev, Y.; Magnuson, A.; Sun, L. C.; Lomoth, R. *J. Porphyrins Phthalocyan.* **2005**, *9*, 379-386; (k) Gao, Y.; Liu, J. H.; Wang, M.; Na, Y.; Akermark, B.; Sun, L. C. *Tetrahedron.* **2007**, *63*, 1987-1994; (l) Liu, H. Y.; Zhou, H.; Liu, L. Y.; Ying, X.; Jiang, H. F.; Chang, C. K. *Chem. Lett.* **2007**, *36*, 274-275; (m) De Visser, S. P.; Ogliaro, F.; Gross, Z.; Shaik, S. *Chem. Eur. J.* **2001**, *7*, 4954-4960.
44. (a) Tangen, E.; Ghosh, A. *J. Am. Chem. Soc.* **2002**, *124*, 8117-8121; (b) Zhao, H.; Pierloot, K.; Langner, E. H. G.; Swarts, J. C.; Conradie, J.; Ghosh, A. *Inorg. Chem.* **2012**, *51*, 4002-4006; (c) Zhang, R.; Newcomb, M. *Acc. Chem. Res.* **2008**, *41*, 468-477; (d) Leeladee, P.; Goldberg, D. P. *Inorg. Chem.* **2010**, *49*, 3083-3085; (e) Prokop, K. A.; Neu, H. M.; de Visser, S. P.; Goldberg, D. P. *J. Am. Chem. Soc.* **2011**, *133*, 15874-15877; (f) Mahammed, A.; Gross, Z. *J. Am. Chem. Soc.* **2005**, *127*, 2883-2887; (g) Etinger, I. N.; Mahammed, A.; Gross, Z. *Catal. Sci. Technol.* **2011**, *1*, 578-581; (h) Boss, S.; Pariyar, A.; Biswas, A.N.; Das, P.; Bandyopadhyay, P. *J. Mol. Catal. A: Chem.* **2010**, *332*, 1-6; (i) Privalov, T.; Sun, L. C.; Akermark, B.; Liu, J. H.; Gao, Y. Wang, M. *Inorg. Chem.* **2007**, *46*, 7075-7086; (j) Kim, S. H.; Park, H.; Seo, M. S.; Kubo, M.; Ogura, T.; Klajn, J.; Gryko, D. T.; Valentine, J. S.; Nam, W. *J. Am. Chem. Soc.* **2010**, *132*, 14030-14032; (k) Lansky, D. E.; Sarjeant, A. A. N.; Goldberg, D. P. *Angew. Chem. Int. Ed.* **2006**, *45*, 8214-8217; (l) Abu-Omar, M. M. *Dalton Trans.* **2011**, *40*, 3435-3444; (m) Lansky, D. E.; Goldberg, D. P. *Inorg. Chem.* **2006**, *45*, 5119-5125.
45. (a) Prokop, K. A.; de Visser, S. P.; Goldberg, D. P. *Angew. Chem. Int. Ed.* **2010**, *49*, 5091-5095; (b) Leeladee, P.; Baglia, R. A.; Prokop, K. A.; Latifi, R.; de Visser, S. P.; Goldberg, D. P. *J. Am. Chem. Soc.* **2012**, *134*, 10397-10400; (c) Han, Y.; Lee, Y.-M.; Mariappan, M.; Fukuzumi, S.; Nam, W.; *Chem. Commun.* **2010**, *46*, 8160-8162; (d) Fukuzumi, S.; Kotani, H.; Prokop, K. A.; Goldberg, D. P. *J. Am. Chem. Soc.* **2011**, *133*, 1859-1869.
46. Gao, Y.; Akermark, T.; Liu, J. H.; Sun, L. C.; Akermark, B. *J. Am. Chem. Soc.* **2009**, *131*, 8726-8727.
47. Zhu, C.; Liang, J.; Wang, B.; Zhuab, J.; Cao, Z. *PCCP* **2012**, *14*, 12800-12806.

48. Balazas, Y. S.; Saltsman, I.; Mahammed, A.; Tkachenko, E.; Golubkov, G.; Levine, J.; Gross, Z. *Magn. Reson. Chem.* **2004**, *42*, 624-635.
49. Liu, H.-Y.; Mahmood, M. H. R.; Qiu, S.-X.; Chang, C. K.; *Coord. Chem. Rev.* **2013**, *257*, 1306-1333.

CHAPTER 4

HALOGEN ATOM EFFECT ON THE SENSING OF BIS *p*-NITRO A₂B CORROLES TOWARDS Hg²⁺ ION

4.1 Introduction

In this work we have synthesised and characterised the four *trans*-A₂B corroles (where A = p-nitrophenyl, and B = o,m,p,m',o'-pentafluorophenyl, o,o'-difluoro, o,o'-dichloro and o,o' - dibromophenyl group). These corroles were tested as cation sensor towards Hg²⁺ ions selectively in toluene solution. We were reported the LoD of these compound and also compared with past Hg²⁺ ion sensor. These four *trans*-A₂B corroles have been shown the different fluorescence quenching for Hg²⁺ ion. Due to present of different number of halogen atom on phenyl ring and different halogen atom at 2,6 position on at C₁₀ position of corrole.

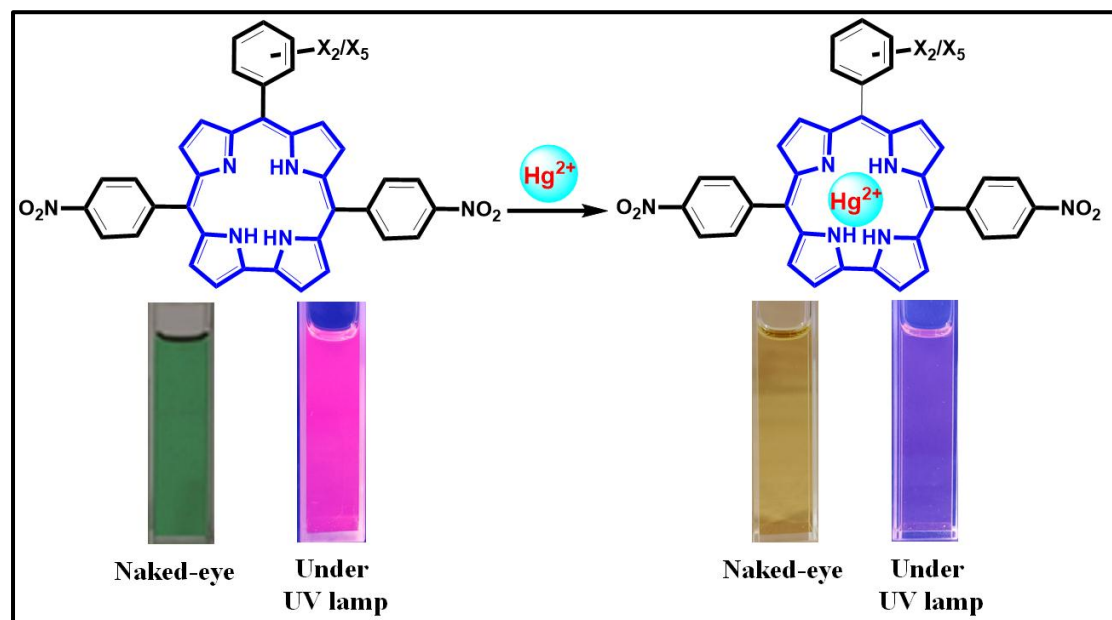


Fig. 4.1: Graphical representation of Hg²⁺ ion sensor by *trans*-A₂B free base corrole

Hg^{2+} ion sensor is worked due to cumulative effect of stationary and dynamic factor. Analyte recognised as signal transduction by the physical and chemical process [1]. To detect the analyte used the light emission process [2]. Fluorophore, receptor or spacer used as chemosensor for sensing [3]. One of the characteristic of good chemosensor have good photo stability, affinity and selectivity for analytes [4]. In previous years' literature, we have seen that many chemosensor employed to detect and quantify the cations in various field [5].

In addition, corroles used as chemosensor due to its photophysical and chemical properties [6,7]. Corrole have property to emit and absorb the visible region's light with good photo-stability and high fluorescent quantum yield [8,9]. Corrole is also used to recognise the metal ion in various oxidation state [10-12]. When we studied the previous year's literature then we found few reports. In this way, Zhang *et. al.* firstly corrole demonstrated as fluorescence quencher for Hg^{2+} ion [13]. Zhou et al. reported the phosphorous corrole Hg^{2+} ion sensor [14]. Bandyopadhyay and co-workers were introduced the free base A_2B corrole as metal ion sensor specially for Hg^{2+} ion [15]. Oliveira, Neves, Lodeiro and their co-workers were reported the gallium complex of corrole to investigation the sensing for Ag^+ , Cu^{2+} and Hg^{2+} ions via silica-based nanoparticles [16]. Srinivasan et al. were synthesised the newly free base A_2B corrole which shown fluorescence property towards Zn^{2+} ion [17]. Zhang and co-workers were prepared the corrole based covalent organic framework which have sensing ability towards Fe^{3+} , Cr^{3+} , Ga^{3+} , Al^{3+} , Cu^{2+} ions specially for Cu^{2+} [18]. Some metal ions are important for eco system and some metal ions are hazardous [3,19-26]. From general chemistry, Hg^{2+} ion one of the hazardous metal ion into several biological systems such

as damage to DNA, brain functions, chromosomal etc. So Hg^{2+} ion sensor more interesting target for environmental studies. In this manner, we report the four *trans*-A₂B free base corrole 10-(o,m,p,m',o'-pentafluorophenyl)-5, 15-bis(p-nitrophenyl)corrole (**1**), 10-(o,o'-Difluorophenyl)-5, 15-bis(p-nitrophenyl)corrole (**2**), 10-(o,o'-dichlorophenyl)-5, 15-bis(p-nitrophenyl)corrole (**3**), and 10-(o,o'-dibromophenyl)-5, 15-bis(p-nitrophenyl)corrole (**4**) and their synthesis method, spectroscopic characterisation, photophysical properties and its sensing ability for Hg^{2+} ion. We have been already demonstrated the corrole **1** and **2** as fluoride ion sensor [27]. We were synthesised and spectroscopically characterise the new *trans*-A₂B corrole **3** and **4**. Order of sensing ability towards Hg^{+2} ion is **4** > **3** > **1** > **2**. We have been evaluated the change in sensing ability for Hg^{+2} ion in the presence of different and number of halogen atom.

4.2 Experimental section

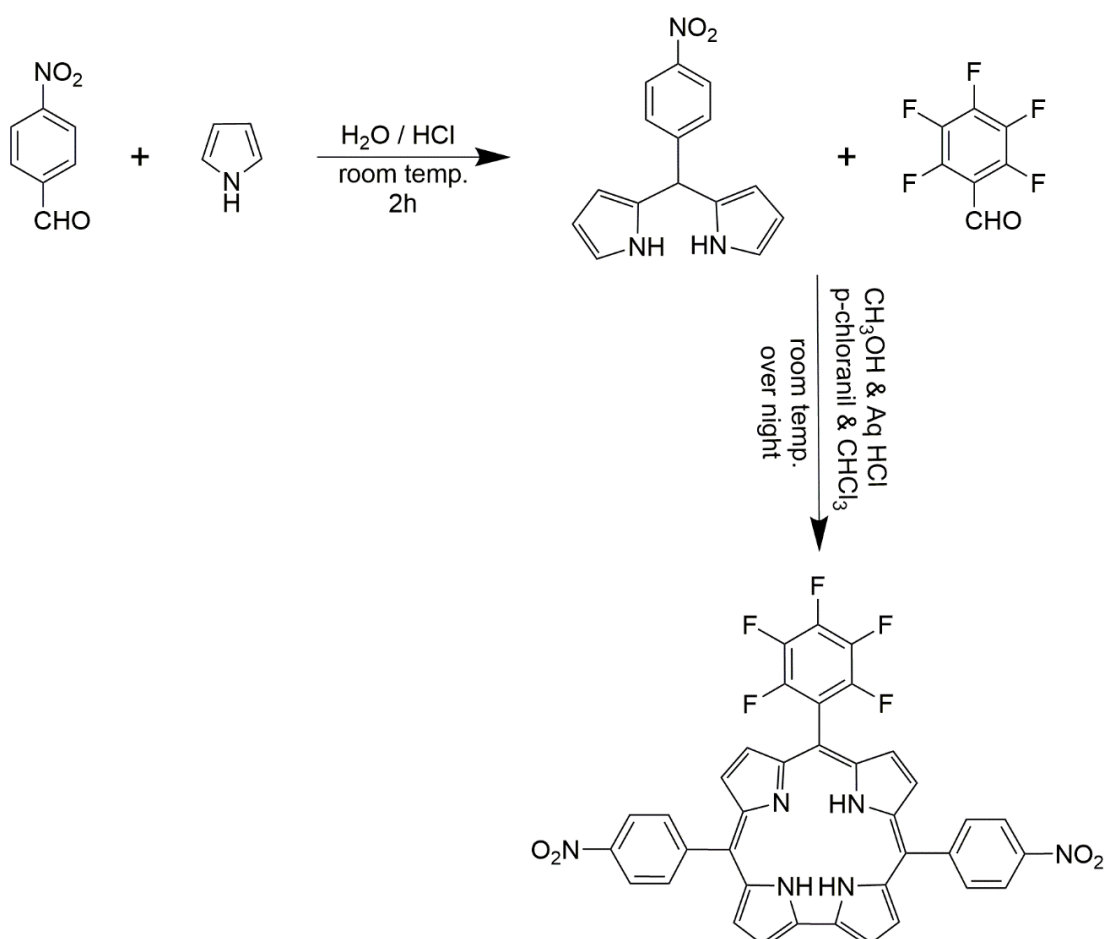
Purification of all synthesised the **1-4** *trans*-A₂B free base corrole through column chromatography by using silica gel as adsorbent. UV-1800 Shimadzu spectrophotometer was used to collect the UV-visible spectra of free base corroles. HORIBA spectrophotometer was used for fluorescence spectra of *trans*-A₂B corrole under 440 nm excitation wavelength. 1.5 mm entrance slit and 2 mm exit slit were used to fluorescence spectra. The measurement of quantum yield of **1-4** *trans*-A₂B corroles have done by experimentally using reference *meso*-tetraphenylporphyrin ($\Phi= 0.13$). Used the dry toluene solution for *trans*-A₂B free base corrole and methanolic solution for analyte (Hg^{2+} ion) in fluorescence quenching experiments.

4.3 Common method for the synthesis of *trans*-A₂B free base corrole

The synthesis method of *trans*-A₂B corroles followed the previous year's reports [10-12,15,16,27-29]. Firstly, 5-(*p*-nitophenyl)dipyrromethane (DPM) synthesised by the reaction of hydrochloric acid (36%, 1.5 mL) in 98.5 mL distilled water with *p*-nitophenyl benzaldehyde (1 equiv) stirring up to 2h at room temperature. The reaction mixture was filtered off and washed by distilled water with petroleum ether. After that we synthesised the *trans*-A₂B free base corrole by the reaction of 5-(*p*-nitophenyl)dipyrromethane (1 equi.) with respective benzaldehyde (0.5 equi.) in 100 mL CH₃OH and 5 mL of 36% HCl_{aq}. The reaction mixture stirring up to 2h at room temperature. The reaction mixture was extracted by the help of separating funnel using choloroform. Then reaction mixture was dried through anhydrous sodium sulphate (Na₂SO₄). The reaction mixture was stirred over night with *p*-chloranil (1.5 equi.) in choloroform at room temperature. The progress of reaction monitor by TLC in DCM/hexane solvent system. Then resultant reaction mixture was obtained though the evaporation process. At last, purification of crude *trans*-A₂B free base corrole by column chromatography using silica gel as adsorbent.

4.3.1 Synthesis of 10-(o,m,p,m',o'-Pentafluorophenyl)-5,15-bis(*p*-nitrophenyl) *trans*-A₂B corrole 1

The green colour solution was obtained by using column chromatography with 6:4; hexane: dichloromethane as eluent. UV-vis in toluene λ_{max} ($\text{\AA}/\text{M}^{-1} \text{ cm}^{-1}$) 442(6797), 598(2303). Rest analytical data of **1** corrole reported in our previous article [27].

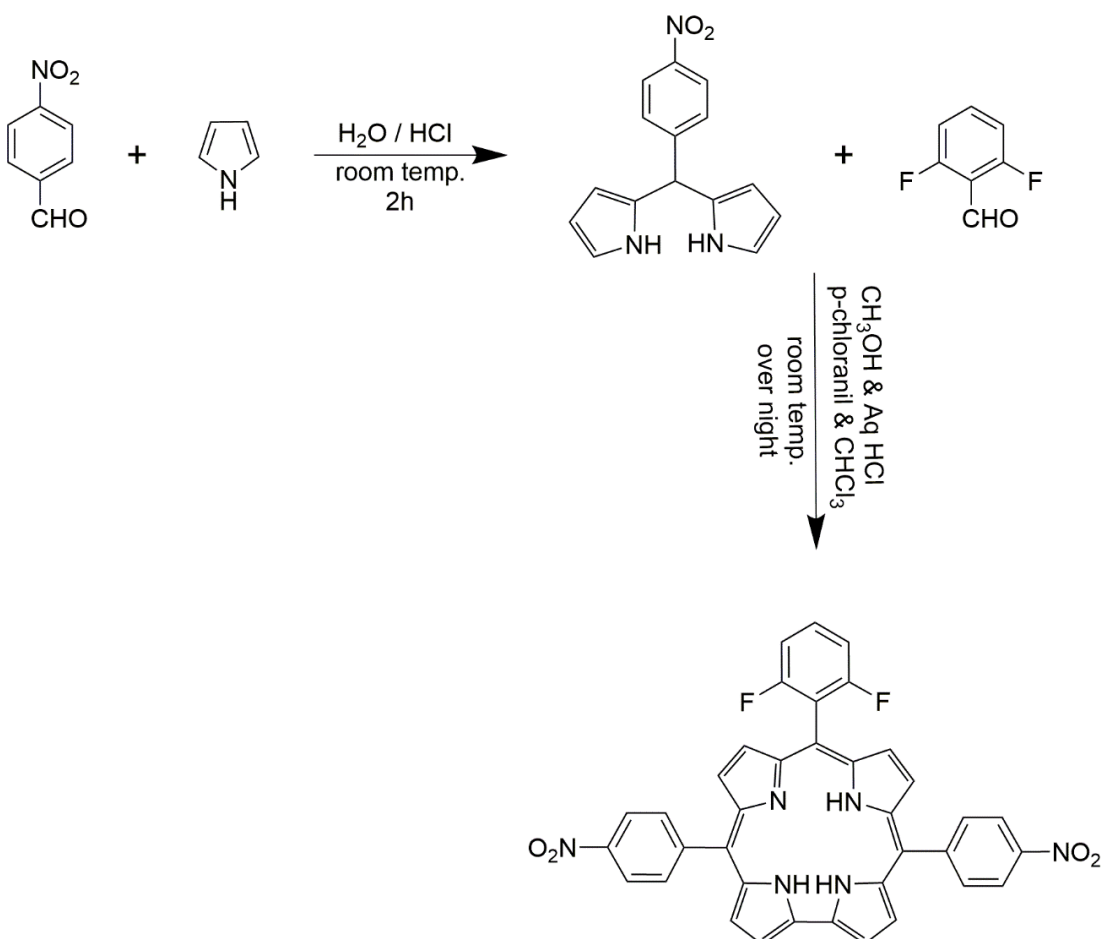


Scheme 4.1: Synthesis of 10-(o,m,p,m',o'-Pentafluorophenyl)-5,15-bis(p-nitrophenyl)corrole

4.3.2 Synthesis of 10-(o,o'-difluorophenyl)-5,15-bis(p-nitrophenyl) *trans*-A₂B corrole 2

The green color solution was obtained by column chromatography with 1:1; hexane: dichloromethane as eluent. UV-vis in toluene $\lambda_{\text{max}} (\text{\AA})$ 442(5272), 598(1505).

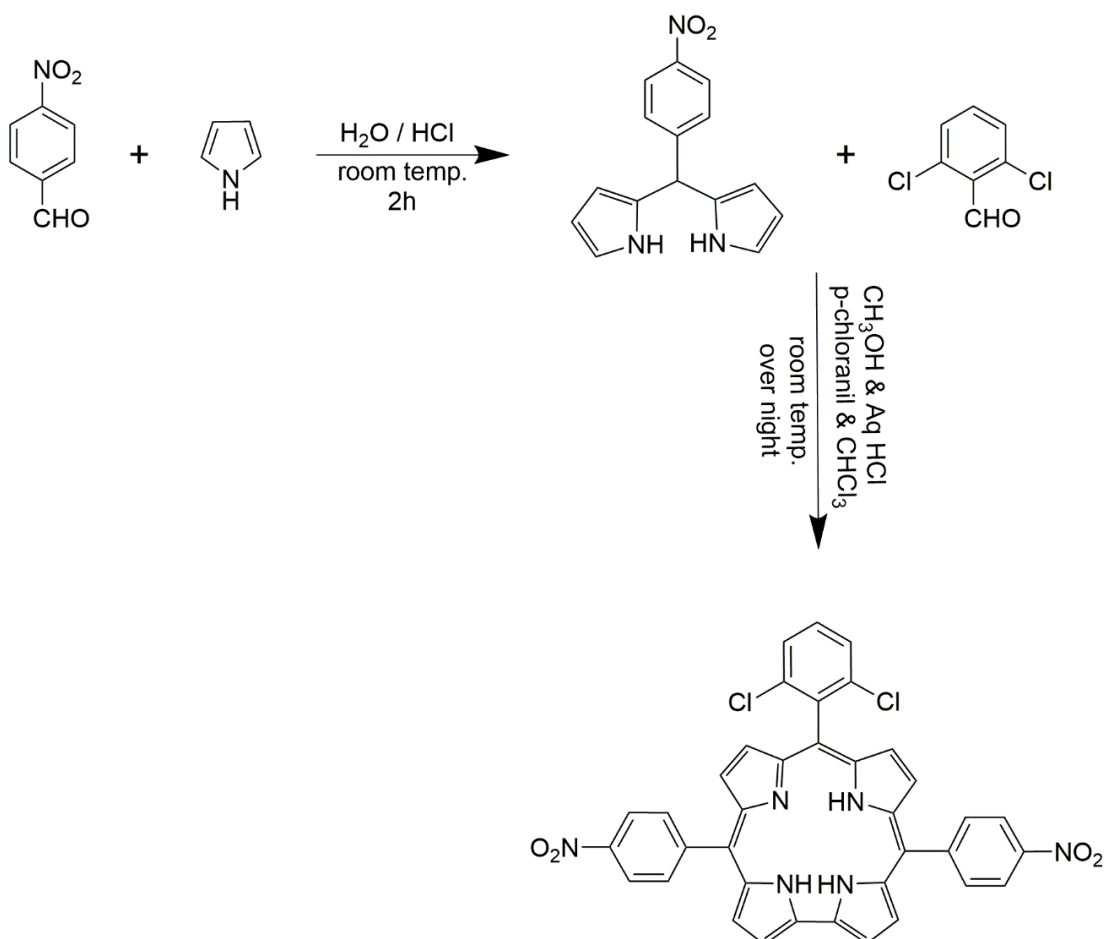
Rest analytical data of **2** corrole reported in our published article [27].



Scheme 4.2: Synthesis of 10-(o,o'-difluorophenyl)-5,15-bis(p-nitrophenyl)corrole

4.3.3 Synthesis of 10-(o,o'-dichlorophenyl)-5,15-bis(p-nitrophenyl) *trans*-A₂B corrole 3

The green color solution was obtained by column chromatography with 3:7; hexane: dichloromethane as eluent. UV-vis in toluene λ_{max} ($\text{M}^{-1} \text{cm}^{-1}$) 429(9090), 598(2404). ^1H NMR (400 MHz, CDCl_3) δ 9.08 (d, $J = 4.2$ Hz, 2H), 8.91 (d, $J = 4.7$ Hz, 2H), 8.74 (d, $J = 8.7$ Hz, 4H), 8.64 (d, $J = 2.3$ Hz, 2H), 8.59 (d, $J = 8.7$ Hz, 4H), 8.49 (d, $J = 4.7$ Hz, 2H), 7.85 (d, $J = 8.7$ Hz, 2H), 7.77 – 7.72 (m, 1H) (**Fig. 4.2**). HRMS: Calcd for $\text{C}_{37}\text{H}_{22}\text{Cl}_2\text{N}_6\text{O}_4$ m/z found 684.107, m/z theo 684.108 (**Fig. 4.4**).



Scheme 4.3: Synthesis of 10-(o,o'-dichlorophenyl)-5,15-bis(p-nitrophenyl)corrole.

4.3.4 Synthesis of 10-(o,o'-dibromophenyl)-5,15-bis(p-nitrophenyl) *trans*-A₂B corrole 4

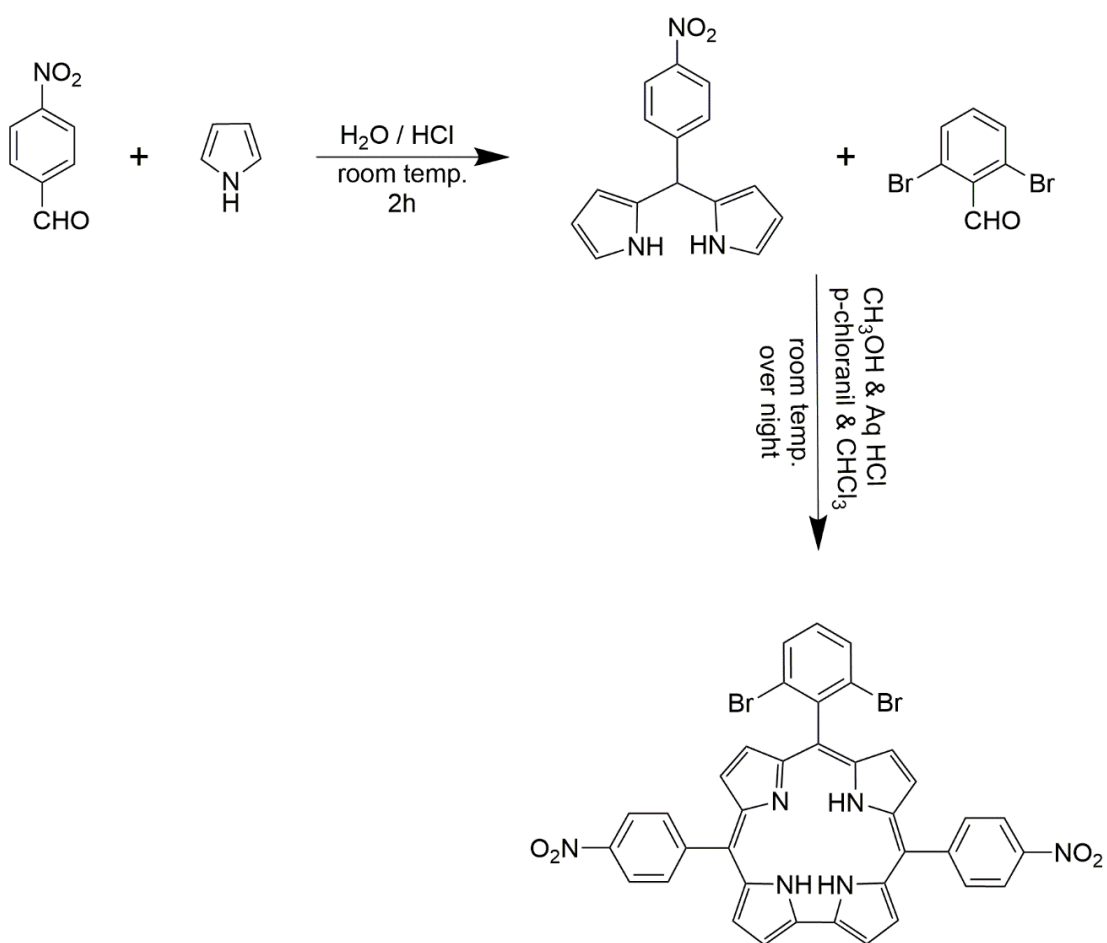
The intense green color solution was obtained by column chromatography with 1:9;

Hexane: dichloromethane as eluent. UV-vis in toluene $\lambda_{\text{max}} (\text{M}^{-1} \text{cm}^{-1})$ 430(47731),

596(14070). ¹H NMR (400 MHz, CDCl_3) δ 9.07 (d, 2H), 8.91 (d, 2H), 8.74 (d, 4H),

8.63 (d, 2H), 8.60 (d, 4H), 8.48 (d, 2H), 8.07 (d, 2H), 7.58 (t, 1H) (**Fig. 4.3**). HRMS:

Calcd for $\text{C}_{37}\text{H}_{22}\text{Br}_2\text{N}_6\text{O}_4$ m/z found 772.999, m/z theo 772.007 (**Fig. 4.5**).



Scheme 4.4 Synthesis of 10-(o,o'-dibromophenyl)-5,15-bis(p-nitrophenyl)corrole

4.4 Characterization

4.4.1 ^1H NMR spectrum of 10-(o,o'-dichlorophenyl)- 5,15-bis(p-nitrophenyl) *trans*-A₂B corrole 3 & 10-(o,o'-dibromophenyl)-5,15-bis(p-nitrophenyl) *trans*-A₂B corrole 4

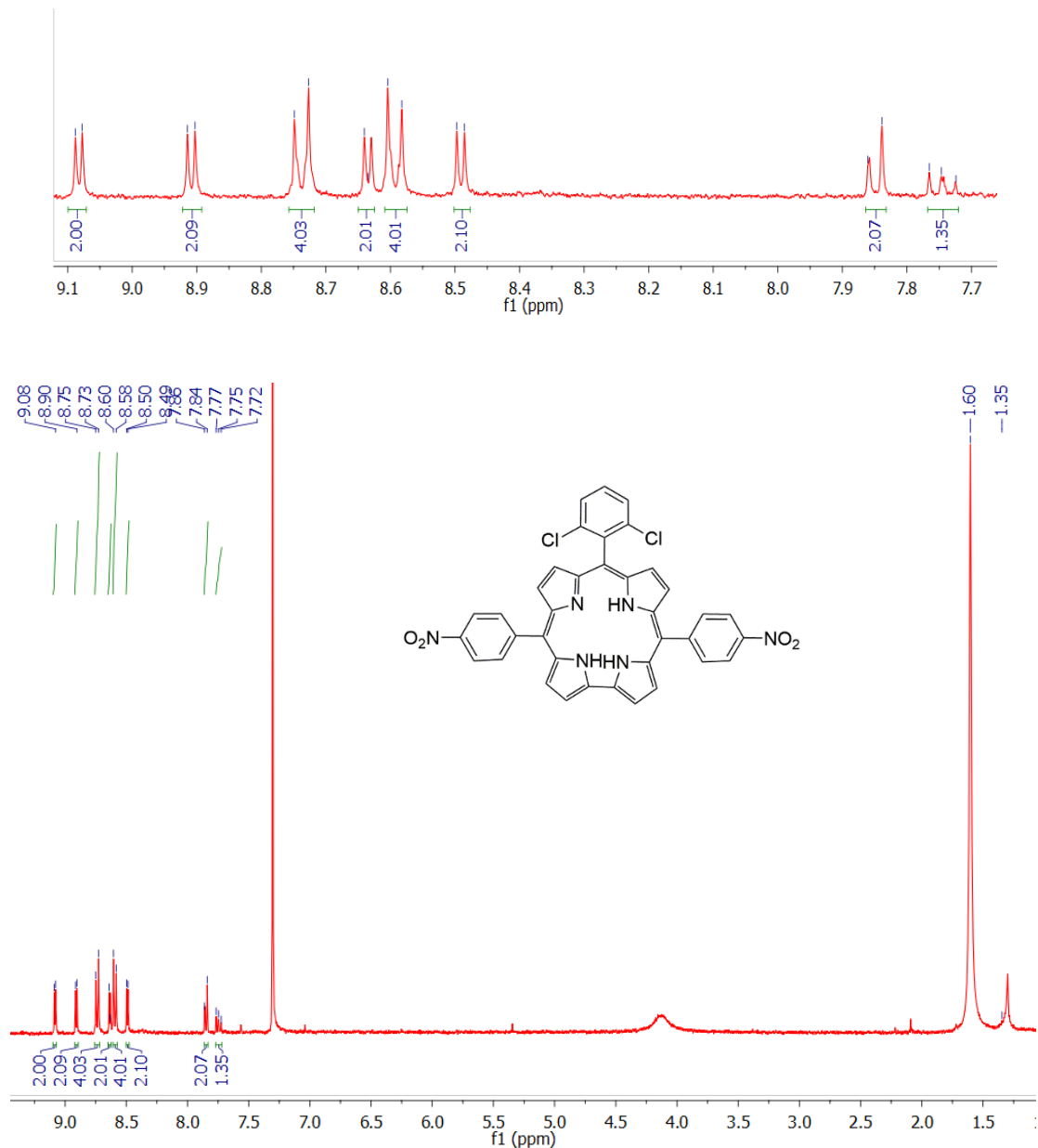


Fig. 4.2: ^1H NMR spectrum of 10-(o,o'-dichlorophenyl)- 5,15-bis(p-nitrophenyl) *trans*-A₂B corrole 3 in CDCl_3

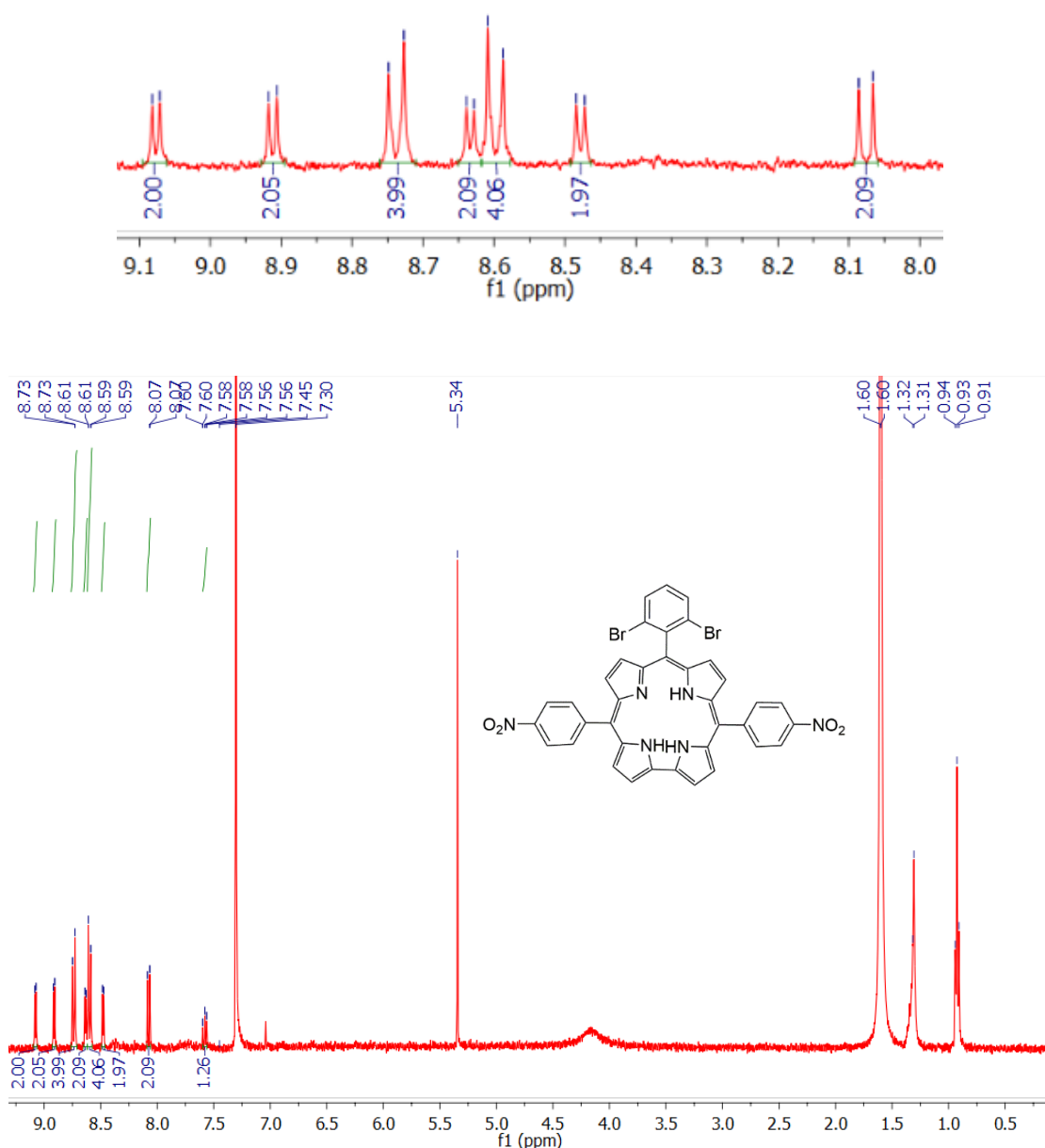


Fig. 4.3: ^1H NMR spectrum of 10-(o,o'-dibromophenyl)- 5,15-bis(p-nitrophenyl) *trans*-A₂B corrole **4** in CDCl₃

4.4.2 Mass spectra of 10-(o,o'-dichlorophenyl)-5,15-bis(p-nitrophenyl) corrole **3** & 10-(o,o'-dibromophenyl)- 5,15-bis(p-nitrophenyl) corrole **4**

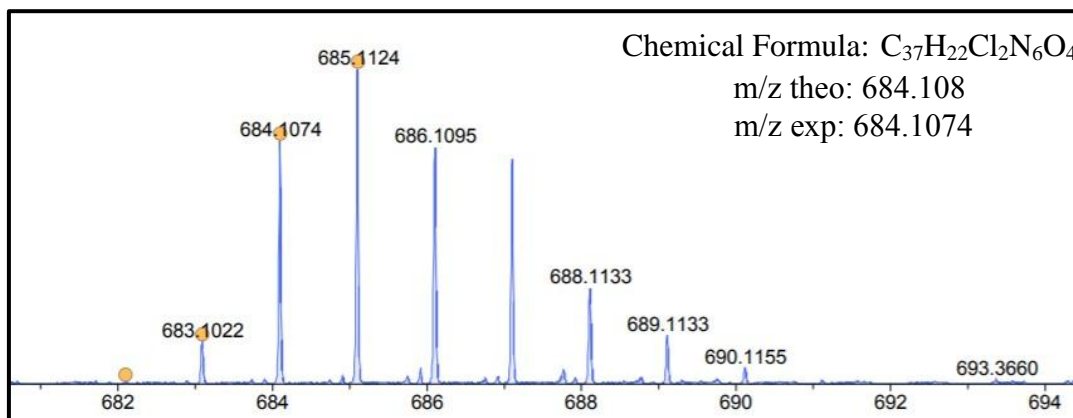


Fig. 4.4: HRMS Spectra of 10-(o,o'-dichlorophenyl)- 5,15-bis(p-nitrophenyl) *trans*-A₂B corrole **3**

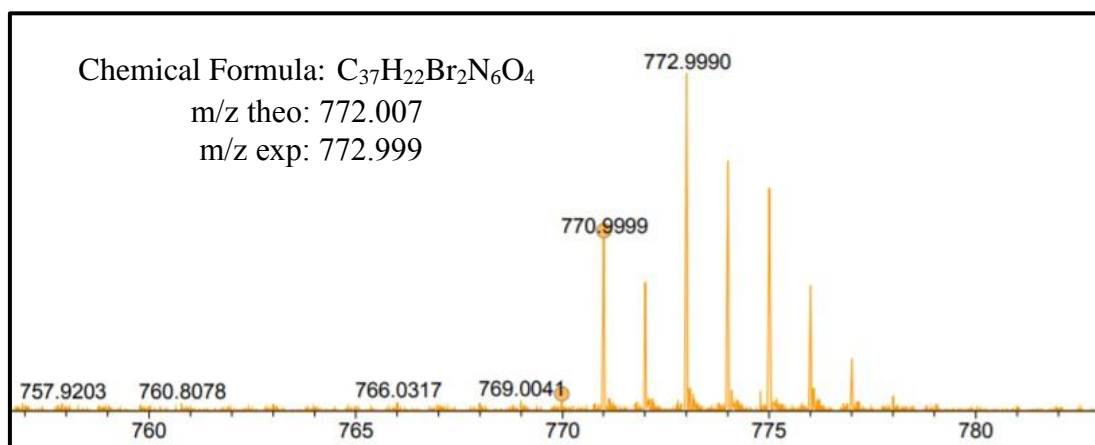


Fig. 4.5: HRMS Spectra of 10-(o,o'-dibromophenyl)- 5,15-bis(p-nitrophenyl) *trans*-A₂B corrole **4**

4.5 Results and discussion

We have been already reported the corrole **1** and **2** as fluoride ion sensor in our previous article [27]. For synthesis of corrole **3** and **4** used the previous year's synthetic protocols [29]. The corrole **1** has 5 fluorine atoms at both ortho, both meta and para positions of phenyl ring at C₁₀ position of corrole. Corrole **2**, **3**, **4** have fluorine, chlorine, bromine atom respectively at both ortho positions of phenyl ring at C₁₀ position of corrole. So the corrole **1** differs from corrole **2** by the number of fluorine atom and corrole **2**, **3**, **4** differ

by the different halogen atom. We were characterised the *trans*-A₂B corroles using the different spectroscopic techniques. Due to presence of halogen atom, all *trans*-A₂B corroles, **1-4**, have different electronic density. So this electronic effect of halogen atoms was examined for the sensing ability of *trans*-A₂B corrole towards Hg²⁺ ion.

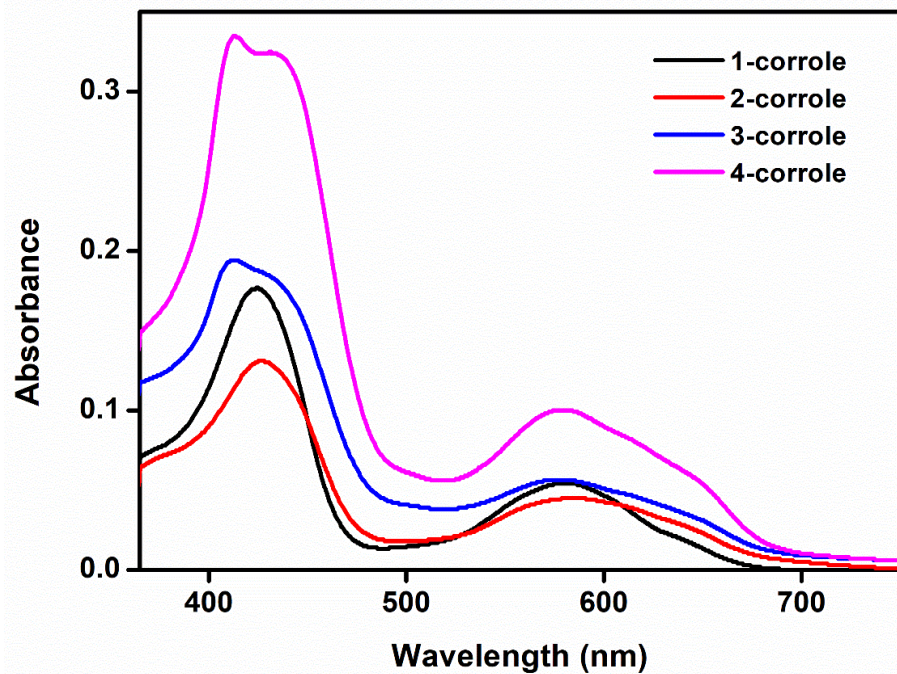


Fig. 4.6: UV-visible spectra of **1-4** *trans*-A₂B corroles in toluene (9.9 μ M)

We have done photophysical characterisation of A₂B corroles **1-4** in toluene at room temperature which shown in Table 4.1. We were observed B bands at 428- 444 nm and Q bands at 594-598 nm in toluene solution (Fig. 4.6). Whenever we have taken UV-visible spectra of **1-4** A₂B corroles with same concentration, we found highest molar absorption coefficient of corrole **4** and lowest molar absorption coefficient of corrole **2**. In general, if increasing the dielectric constant of the solution then bathochromic shift occurred. But bis(nitro) substituted corroles have opposite trend [10-12]. So, bis(nitro) substituted corroles have unique property compare to other substituted corroles i.e.

without nitro group. We have been recorded steady state fluorescence emission spectra of **1-4** *trans*-A₂B corroles in toluene. We were observed the strong emission bands within the range of 673-687 nm (Fig. 4.7). We were calculated Stoke's shift with the help of emission spectra of **1-4** *trans*-A₂B corroles. And we found Stoke's shift range 7743-8733 nm. This may be because of change in the electronic nature of excited state as compared to the ground state.

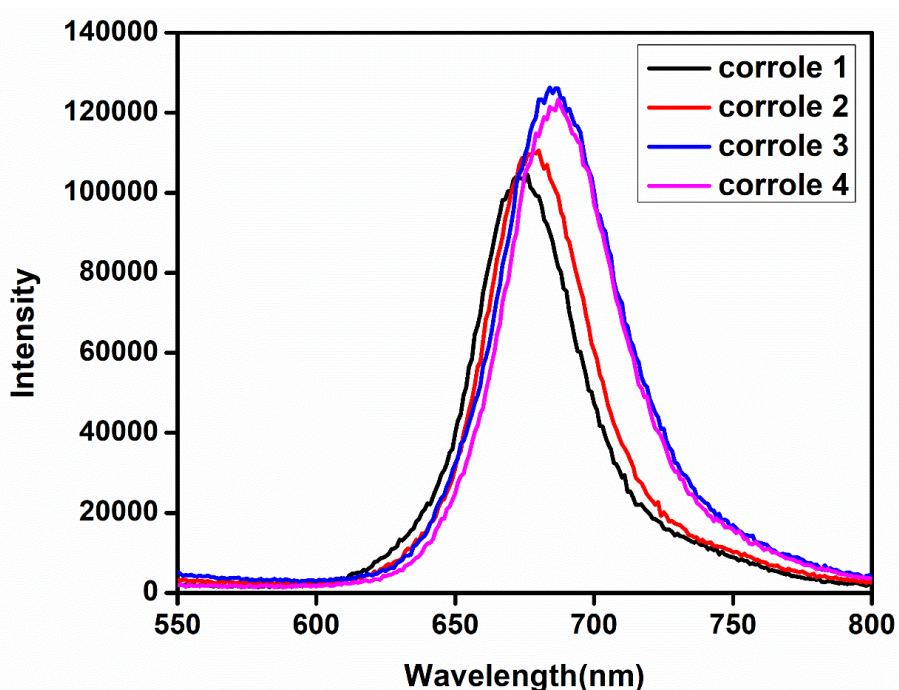


Fig. 4.7: Emission spectra of **1-4** A₂B corroles in toluene at 440 nm excitation

Further, we calculated the quantum yield of *trans*-**1-4** A₂B corroles by employing the Eq. (1). In which, tetraphenylporphyrin was used as a reference material.

$$QY_S = QY_R \times \left(\frac{I_S}{I_R} \right) \times \left(\frac{A_R}{A_S} \right) \times \left(\frac{\eta_S}{\eta_R} \right)^2 \quad (1)$$

Where, QY_S and QY_R are the quantum yields of sample and reference (Quantum yield of tetraphenylporphyrin = 0.13). I_S and I_R are the integrated area under the PL spectrum

of sample and reference (*meso*-tetraphenylporphyrin). A_R and A_S are the absorbance, η_R and η_S are the refractive indexes of the solvents and reference (*meso*-tetraphenylporphyrin) and sample respectively. The quantum yields of corrole **3** and **4** were higher than reported 5,15-bis(nitrophenyl) A₂B corroles due to stronger charge transfer [11,27,30].

Table 4.1: Photophysical data of **1-4** *trans*-A₂B corroles in toluene at room temperature.

Probe	$\lambda_{\text{max}}/\text{nm}$ ($\epsilon/\text{M}^{-1}\text{cm}^{-1}$)	λ_{em} (nm)	Stoke's shift (nm)	FWHM	QY%
1	442(6797), 598(2303)	672	7743	46.06	0.10
2	442(5272), 598(1505)	680	7919	45.34	0.11
3	429(9090), 598(2404)	686	8733	52.97	0.12
4	430(47731), 596(14070)	687	8700	50.85	0.13

5,15-Bis(nitrophenyl) A₂B corroles have ability to sense the metal ions but highly sensing ability towards for Hg²⁺ ion even at lower concentration (i.e. $<10^{-6}$ – 10^{-9}M) [15]. The fluorescence quenching of *trans*-A₂B corroles towards Hg²⁺ ion with the change in halogen atom at phenyl ring at C₁₀ position of corrole was also examined. For fluorescence study, we have chosen toluene as solvent for corroles and methanol for analyte [15]. The photo-stability of corroles, **1-4**, and remarkable solubility in toluene made it better choice for fluorescence study.

The fluorescence response of **1-4** A₂B corroles were determined for different cations in order to check the specific sensing of **1-4** by carrying out fluorescence titration. The results obtained from fluorescence titration are shown in the Fig. 4.8 which clearly indicates that quenching of fluorescence intensity is lesser influenced by these cations

relative to that of Hg^{2+} ion. The corroles, **1–4** shows peculiar selectivity and high affinity for Hg^{2+} ion.

Hypsochromic shift of ICT transition occurred whenever solution of Hg^{2+} ion prepared in methanol added and into the toluene solution of *trans*-A₂B corroles. Because of the binding of Hg^{2+} ion through lone pair of inner nitrogen atom of corrole. Hg^{2+} ion serves as quencher through spin-orbital coupling effect [31].

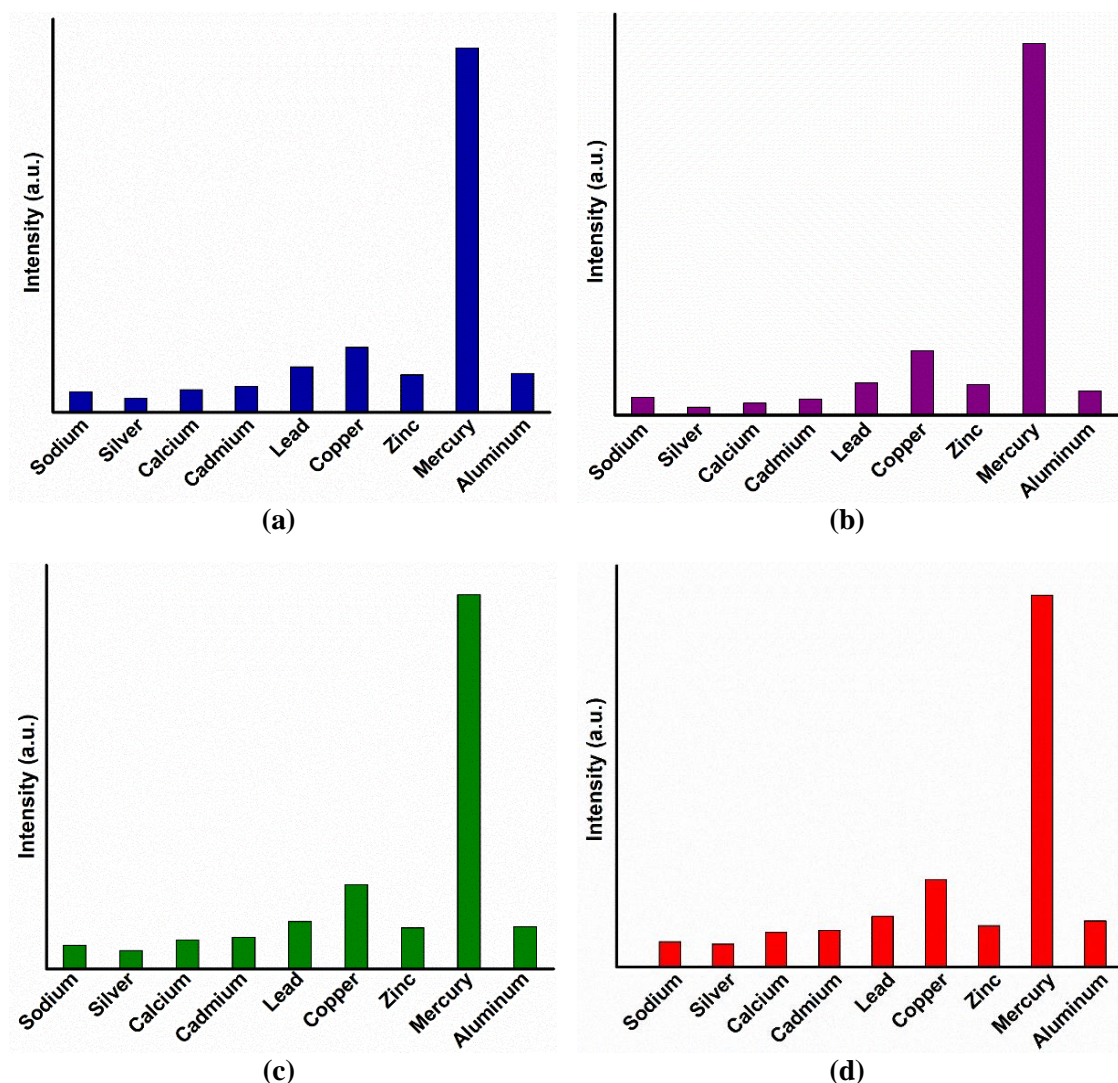


Fig. 4.8: Fluorescence response of, **1–4** of 9.9×10^{-6} M to various cations (3.3×10^{-7} M) in toluene represented as **a–d**, respectively.

We were easily observed the process of binding phenomena of Hg^{2+} ion with **1-4 A₂B** corroles via color change of toluene solution of free base A₂B corrole by naked eye and also UV-lamp. We saw by the naked eye the change of green color of **1-4 trans-A₂B** corroles in to yellowish brown color. In UV-lamp, before addition of Hg^{2+} ion, free base A₂B corroles looked highly fluorescent pink color also. But after addition of Hg^{2+} ion, free base A₂B corroles became colourless without any fluorescent in UV-lamp. We also obtained the trend of molar absorption coefficient of **1-4 A₂B** corroles, which was continuously decreases with increasing the concentration of Hg^{2+} ion as shown Fig.4.9.

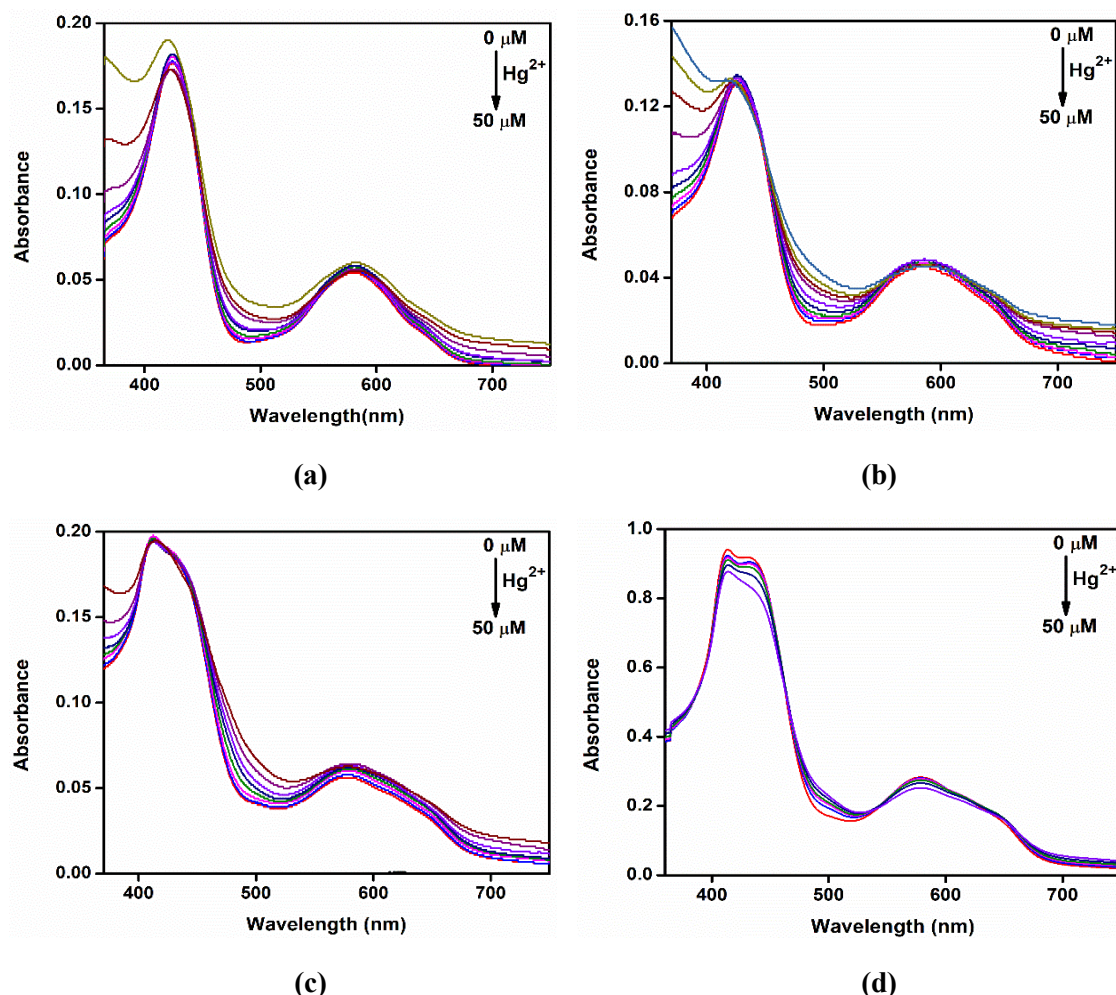


Fig. 4.9: Change in UV-visible spectrum during the addition of ethanol solution of Hg(II) acetate in toluene solution of **1-4 A₂B** corroles in aerobic condition represented as **a, b, c, d** respectively.

We have been also recorded the fluorescence spectra of titration between different concentration of methanol solution of Hg^{2+} ion into toluene solution of **1-4 A₂B** corroles. Then we observed the quenching of fluorescence emission intensity continuously decrease as shown Fig. 4.10.

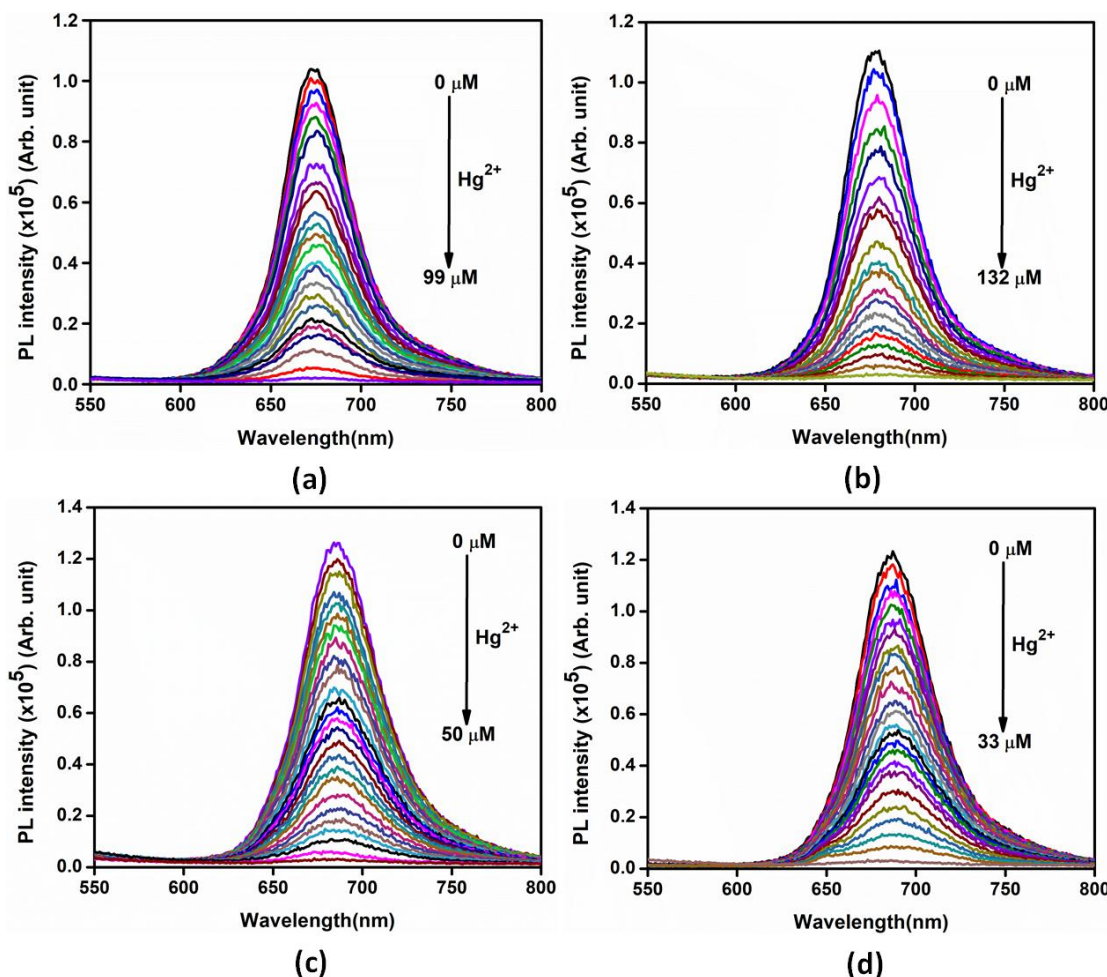


Fig. 4.10: The decay in fluorescence emission intensity during the titration of methanolic solution of $\text{Hg}(\text{II})$ acetate (3.3×10^{-7} M) in toluene solution of **1-4 A₂B** corroles (9.9×10^{-6} M) respectively under the excitation at $\lambda=440$ nm in aerobic condition.

This is due to the non-radiative relaxation path from excited state to ground state, which signifies absence of emission band and represent the new fluorophore formation of $\text{Hg}(\text{II})$ -corrole. Excessive addition of Hg^{2+} ion, the saturation point was observed. It is evident that all the **1-4 A₂B** corrole have different saturation point because of number of

halogen atoms and different halogen atom present on phenyl ring at C₁₀ position of corrole. Saturation point of **1**, **2**, **3**, **4** corrole are 99 μM, 132 μM, 50 μM, 33 μM respectively (Fig. 4.10). Corrole **4** showed the highest quenching ability towards Hg²⁺ ion out of **1-4** A₂B corroles. We observed the quenching order **4>3>1>2** A₂B corroles towards Hg²⁺ ion under identical condition. It is well shown in Fig. 4.10, the order of quenching through the increasing concentration of Hg²⁺ ion used for titration.

In general, for quenching the PL intensity in the presence of quencher are occurred due to static interaction or dynamic interaction or both [32]. But in this case of *trans*-A₂B corrole static as well as dynamic interactions are responsible for quenching in the presence of Hg²⁺ ion [15]. Further, investigations by the well-known Stern-Volmer relationship (Eq.2) examined. The S-V plot for the quenching of PL intensity of *trans*-A₂B corrole in the presence of various concentration of Hg²⁺ ion (Fig. 4.11).

$$\frac{I_0}{I} = 1 + K_{SV} [\text{Hg}^{2+}] \quad (2)$$

Where I₀ represent the initial PL intensity without Hg²⁺ ion and I represent final PL intensity in the presence of quencher (Hg²⁺ ion), [Hg²⁺] signifies the molar concentration of methanol solution of Hg²⁺ ion added into toluene solution of A₂B corrole and K_{SV} represent the PL quenching constant [M⁻¹]. We observed linear relation with positive deviation between (I₀/I)-1 and molar concentration of Hg²⁺ion in the S-V plot for particular range of concentrations (Fig. 4.11) which is similar to earlier reported in literature for quenching by metal ions [33].

From the Stern–Volmer plot, we were calculated the K_{SV} (10⁵ M⁻¹) for **1**, **2**, **3**, **4** *trans*-A₂B corroles are 0.39, 0.81, 0.49, 0.40 respectively. The limit of detection (LoD) of **1-4** A₂B corroles were found 21.93μM, 38.61 μM, 8.72 μM, 2.64 μM respectively using

formula $3\sigma/K$, which is comparable to other reported sensors in the literature for Hg^{2+} ions and tabulated in the Table 4.2. Where σ represent the standard deviation and K represent the slope of the Stern–Volmer plot. The linear detection ranges for **1**, **2**, **3** and **4** A_2B corroles are 6.6×10^{-6} to 69.3×10^{-6} M, 9.9×10^{-6} to 75.9×10^{-6} M, 8.25×10^{-6} to 56.1×10^{-6} M and 9.9×10^{-6} to 44.55×10^{-6} M, respectively. The value of linearity constant (R^2) for **1**–**4** A_2B corrole are 0.97, 0.98, 0.97, 0.99 respectively. The values of K_{SV} , LoD, linearity range and R^2 tabulated in Table 4.3. We observed the order of LoD for **1**–**4** A_2B corroles towards Hg^{2+} ion is **4** > **3** > **1** > **2**.

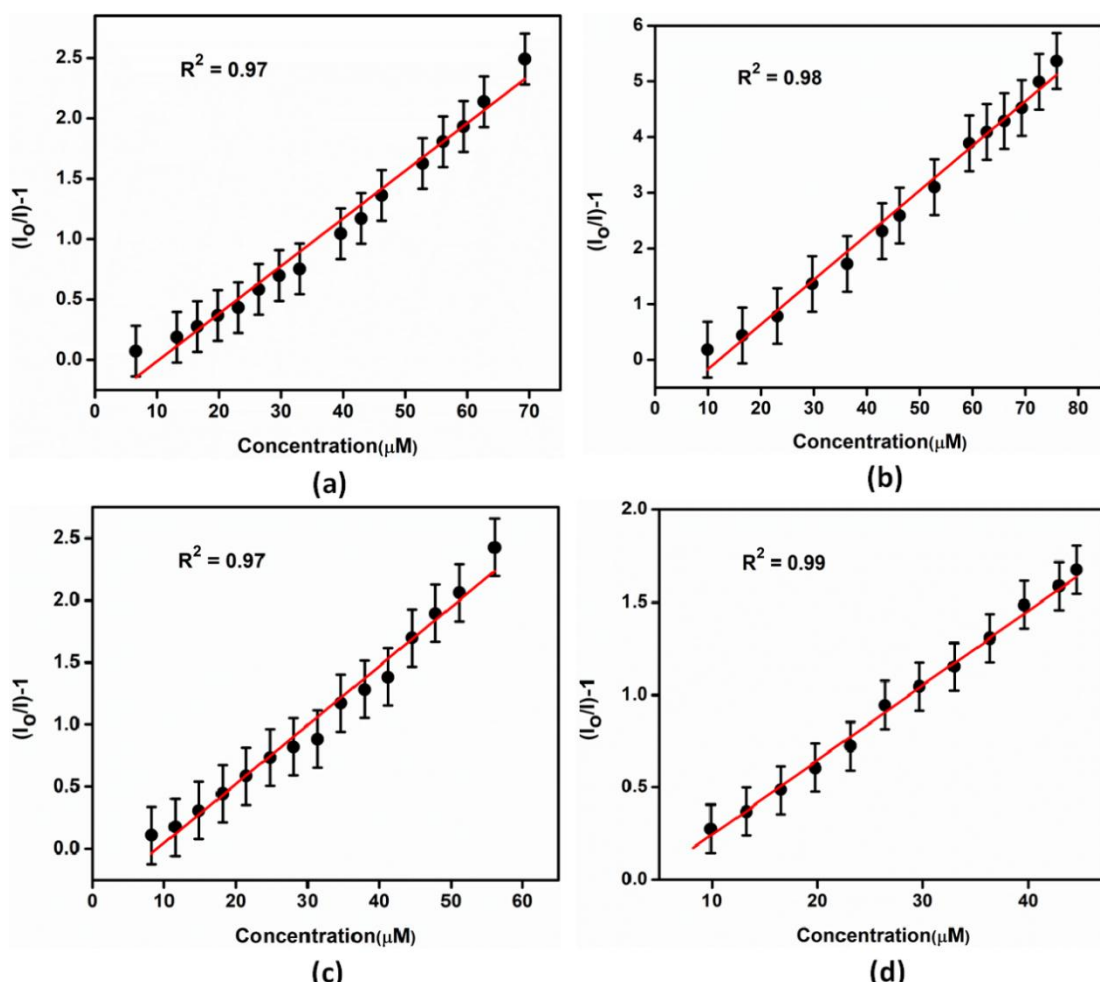


Fig. 4.11: The Stern–Volmer plot of compounds **1**–**4** A_2B corroles respectively with positive deviation during increasing the concentration of methanolic solution of $\text{Hg}(\text{II})$ acetate inset the value of linearity constant (R^2).

Table 4.2: Comparison of the LoD with other reported sensors

S. No.	LoD towards Hg^{2+}	Used conc. of Hg^{2+} for sensing	Reference
1.	-	1.2×10^{-7} to 1.0×10^{-4} M	[13]
2.	-	0 to 60×10^{-9} M	[14]
3.	-	2.49×10^{-6} M	[15]
4.	0.02 (ppm)	10^{-4} - 10^{-6} M	[16]
5.	2.64-38.61 (μM)	3.3×10^{-7} M	this work

Table 4.3: Comparison of **1-4** probes for Hg^{2+} sensing

Probe	K_{SV} (M^{-1})	LoD (μM)	Linearity range (μM)	R^2
1	0.39×10^5	21.93	6.6-69.3	0.97
2	0.81×10^5	38.61	9.9-75.9	0.98
3	0.49×10^5	8.72	8.25-56.1	0.97
4	0.40×10^5	2.64	9.9-44.55	0.99

We have been done the fluorescence titration for A_2B corroles, 1-4 with the addition of Hg^{2+} ion. The significant quenching of fluorescence intensity of corroles were observed and in the presence of higher concentration of Hg^{2+} ion, quenching is more appreciable. The S-V plot (Fig. 4.10) signifies the dynamic and static interactions through $(I_0/I)-1$ and concentration of Hg^{2+} ion. The formation of long-lived charge-separated states in nonpolar solvents also quenches the fluorescence in corrole-fullerene [34]. This is the reason that in the presence of Hg^{2+} ion, electronic spectral changes occurred in A_2B corrole. The order of sensing depends on the electron donating property of halogen atom which is present at C_{10} position of corrole. The increasing order of electron donating efficiency of halogen atom is $\text{F} < \text{Cl} < \text{Br}$ [35]. It is clear from above discussion that sensing efficiency of A_2B corrole depend upon the behaviour of halogen atom.

4.6 Conclusion

In this work, we have been synthesised the **1-4** *trans*-A₂B free base corroles which were explored as Hg²⁺ ion sensor. We were studied the quenching of the fluorescence emission intensity during the addition of different concentration of Hg²⁺ ion. We obtained the sensing order of **1-4** *trans*-A₂B corrole towards Hg²⁺ ion is **4>3>1>2**. This order confirmed the electronic effect of halogen atoms present on the phenyl ring of C₁₀ position of corrole. The value of LoD as well as amount of Hg²⁺ ion also followed the sensing order. So we concluded that sensing efficiency of **4** higher than **3** corrole and sensing efficiency of **3** corrole higher than not only for **2** corrole but also higher than **1** towards Hg²⁺ ion. Because of increase in halogen atom on phenyl group will increases the sensing efficiency of substituted 5,15-bis(nitrophenyl) free base corrole as in case of **1** corrole and **2** corrole. And in case of **2**, **3**, **4**, halogen atom fluorine(F), chlorine(Cl), bromine(Br) present at 2,6 position of phenyl ring respectively at C₁₀ position of corrole. So the reason may be electron donating property of halogen atom increase the sensing ability of *trans*-A₂B corrole towards Hg²⁺ ion. These result will help to scientific community to design new chemosensors for detection of Hg²⁺ in the environment.

References

1. (a) Bell, T.; Hext, *Chem. Soc. Rev.* **2004**, *33*, 589–598; (b) De Silva, A. P.; Gunaratne, H. Q. N.; Gunnlaugsson, T.; Huxley, A. J. M.; McCoy, C. P.; Rademacher, J. T.; Rice, T. E. *Chem. Rev.* **1997**, *97*, 1515–1566; (c) Desvergne, J. P.; Czarnik, A.W.; Eds; *Kluwer Academic: Dordrecht, The Netherlands*, **1997**, 492; (d) Czarnik, A.W. Ed; *American Chemical Society: D. C. Washington*, **1993**; (e) Czarnik, A. W. *Acc. Chem. Res.* **1994**, *27*, 302–308; (f) Rudzinski, C. M.; Hartmann, W. K.; Nocera, D. G. *Coord. Chem. Rev.* **1998**, *171*, 115–123; (g) Rudzinski, C. M.; Nocera, D. G.; Ramamurthy, V.; Schanze, K. S. Eds.; *Marcel Dekker: New York*, **2001**, 1–91; (h) Rudzinski, C. M.; Young, A. M.; Nocera, D. G. *J. Am. Chem. Soc.* **2002**, *124*, 1723–1727; (i) Swager, T. M. *Acc. Chem. Res.* **1998**, *31*, 201–207; (j) Mohr, G. J. *Chem. Eur. J.* **2004**, *10*, 1082–1090; (k) De Silva, A. P.; Fox, D. B.; Moody, T. S.; Weir, S. M. *Trends Biotechnol.* **2001**, *19*, 29–34.
2. (a) Dahan, M.; Levi, S.; Luccardini, C.; Rostaing, P.; Riveau, B.; Triller, A. *Science* **2003**, *302*, 442–445; (b) Shimizu, K. T.; Neuhauser, R. G.; Leatherdale, C. A.; Empedocles, S. A.; Woo, W. K.; Bawendi, M. G. *Phys. Rev. B* **2001**, *63*, 205316/1–5; (c) Deniz, A. A.; Dahan, M.; Grunwell, J. R.; Ha, T.; Faulhaver, A. E.; Chemla, D. S.; Weiss, S.; Schultz, P. G. *Proc. Natl. Acad. Sci. U.S.A.* **1999**, *96*, 3670–3675; (d) Ha, T.; Ting, A. Y.; Liang, J.; Caldwell, W. B.; Deniz, A. A.; Chemla, D. S.; Schultz, P. G.; Weiss, S. *Proc. Natl. Acad. Sci. U.S.A.* **1999**, *96*, 893–898.
3. Lodeiro, C.; Capelo, J. L.; Mejuto, J. C.; Oliveira, E.; Santos, H. M.; Pedras, B.; Nunez, C. *Chem. Soc. Rev.* **2010**, *39*, 2948–2976.
4. Xu, Z.; Yoon, J.; Spring, D. R. *Chem. Soc. Rev.* **2010**, *39*, 1996–2006.
5. (a) Chen, P.; He, C. *J. Am. Chem. Soc.* **2004**, *126*, 728–729; (b) Henary, M. M.; Fahrni, C. J. *J. Phys. Chem. A* **2002**, *106*, 5210–5220; (c) Walkup, G. K.; Imperiali, B. *J. Am. Chem. Soc.* **1996**, *118*, 3053–3054.
6. Aviv, I.; Gross, Z. *Chem. Commun.* **2007**, 1987–1999.

7. Santos, C. I. M.; Barata, J. F. B.; Calvete, M. J. F.; Vale, L. S. H. P.; Dini, D.; Meneghetti, M.; Neves, M. G. P. M. S.; Faustino, M. A. F.; Tome, A. C.; and Cavaleiro, J. A. S. *Curr. Org. Synth.* **2014**, *11*, 29-41.
8. Lodeiro, C.; Capelo, J. L.; Mejuto, J. C.; Oliveira, E.; Santos, H. M.; Pedras, B.; Nunez, C. *Chem. Soc. Rev.* **2010**, *39*, 2948-2976.
9. (a) Chen, P.; He, C. *J. Am. Chem. Soc.* **2004**, *126*, 728-729; (b) Henary, M. M.; Fahrni, C. *J. Phys. Chem. A* **2002**, *106*, 5210-5220; (c) Walkup, G. K.; Imperiali, B.; *J. Am. Chem. Soc.* **1996**, *118*, 3053-3054.
10. Ventura, B.; Degli Esposti, A.; Koszarna, B.; Gryko, D. T.; Flamigni, L. *New J. Chem.* **2005**, *29*, 1559-1566.
11. Ding, T.; Aleman, E. A.; Modarelli, D. A.; Ziegler, C. *J. Phys. Chem. A* **2005**, *109*, 7411-7417.
12. Paolesse, R.; The Porphyrin Handbook, ed. Kadish, K. M.; Smith, K. M.; Guilard, R. Academic Press, New York. **2000**, vol. 2, ch. 11, pp. 202-203.
13. He, C. L.; Ren, F. L.; Zhang, X. B.; and Han, Z. X. *Talanta* **2006**, *70*, 364-369.
14. Zhou, Y.; Deng, M.; Du, Y.; Yan, S.; Huang, R.; Weng, X.; Yang, C.; Zhang, X.; and Zhou, X. *Analyst* **2011**, *136*, 955-961.
15. Pariyar, A.; Bose, S.; Chhetri, S. S.; Biswas, A. N.; and Bandyopadhyay, P. *Dalton Trans.* **2012**, *41*, 3826-3831.
16. Santos, C. I. M.; Oliveira, E.; Fernandez-Lodeiro, J.; Barata, J. F. B.; Santos, S. M.; Faustino, M. A. F.; Cavaleiro, J. A. S.; Neves, M. G. P. M. S.; and Lodeiro, C. *Inorg. Chem.* **2013**, *52*, 8564-8572.
17. Adinarayana, B.; Thomas, A. P.; Yadav, P.; Kumar, A.; and Srinivasan, A. *Angew. Chem. Int. Ed.* **2016**, *55*, 969-973.
18. Li, Y.; Chen, M.; Han, Y.; Feng, Y.; Zhang, Z.; and Zhang, B. *Chem. Mater.* **2020**, *6*, 2532–2540.

19. Aviv-Harel, I.; Gross, Z. *Coord. Chem. Rev.* **2011**, *255*, 717-736.
20. (a) Hussain, S. M.; Hess, K. L.; Gearhart, J. M.; Geiss, K. T.; Schlager, J. J. *Toxicol. In Vitro* **2005**, *19*, 975-983. (b) Landsdown, A. B. G. *Crit. Rev. Toxicol.* **2007**, *37*, 237-250.
21. Donnell, E. E.; Han, S.; Hilty, C.; Pierce, K. L.; Pines, A. *Anal. Chem.* **2005**, *77*, 8109–8114.
22. Lione, A. *J. Gen. Pharmacol.* **1985**, *16*, 223-228.
23. Crisponi, G.; Nurchi, V. M.; Bertolas, V.; Remelli, M.; Faa, G. *Coord. Chem. Rev.* **2012**, *256*, 89-104.
24. (a) Chen, X.; Nam, S.-W.; Jou, M.; Kim, Y.; Kim, S.-J.; Park, S.; Yoon, J. *Org. Lett.* **2008**, *10*, 5235-5238. (b) Nolan, E. M.; Lippard, S. J. *Chem. Rev.* **2008**, *108*, 3443-3480. (c) Tamayo, A.; Pedras, B.; Lodeiro, C.; Escriche, L.; Casabo, J.; Capelo, J. L.; Covelo, B.; Kivekas, R.; Sillampaa, R. *Inorg. Chem.* **2007**, *46*, 7818-7826. (d) Mameli, M.; Lippolis, V.; Caltagirone, C.; Capelo, J. L.; Nieto-Faza, O.; Lodeiro, C. *Inorg. Chem.* **2010**, *49*, 8276-8286.
25. (a) Rocha, A.; Marques, M. M. B.; Lodeiro, C. *Tetrahedron Lett.* **2009**, *50*, 4930-4933. (b) Jou, M. J.; Chen, X.; Swamy, K. M. K.; Kim, H. N.; Kim, H.-J.; Lee, S.; and Yoon, J. *Chem. Commun.* **2009**, 7218-7220. (c) Park, C. S.; Lee, J. Y.; Kang, E.-J.; Lee, J.-E.; Lee, S. S. *Tetrahedron Lett.* **2009**, *50*, 671-675. (d) Tamayo, A.; Oliveira, E.; Covelo, B.; Casabo, J.; Escriche, L.; Lodeiro, C. Z. *Anorg. Allg. Chem.* **2007**, *633*, 1809-1814.
26. (a) Capelo, J. L.; Maduro, C.; Mota, A. M. *Ultrason. Sonochem.* **2006**, *13*, 98-106. (b) Nolan, E. M.; Lippard, S. J. *Chem. Rev.* **2008**, *108*, 3443-3480.
27. Yadav, O.; Varshney, A.; Kumar, A.; Ratnesh R. K.; and Mehata, M. S. *Spectrochimica Acta Part A: Molecular and Biomolecular Spectroscopy* **2018**, *202*, 207–213
28. (a) Yadav, O.; Varshney, A.; Kumar, A. *Inorg. Chem. Commun.* **2017**, *86*, 168-171; (b) Varshney, A.; Kumar, A.; Yadav, S. *Inorganica Chimica Acta* **2021**, *514*, 120013.

29. (a) Gross, Z.; Galili, N.; Saltsman, I. *Angew. Chem. Int. Ed.* **1999**, *38*, 1427–1429; (b) Paolesse, R.; Jaquinod, L.; Nurco, D. J.; Mini, S.; Sagone, F.; Boschi, T.; Smith, K.M. *Chem. Commun.*, **1999**, *14*, 1307–1308; (c) Paolesse, R.; Nardis, S.; Sagone, F.; Khoury, R. G. *J. Organomet. Chem.* **2001**, *66*, 550–556. (d) Rohand, T.; Dolusic, E.; Ngo, T. H.; Maes, W.; and Dehaen W. *ARKIVOC* **2007**, (x) 307-324.
30. Mahammed, A.; Weaver, J. J.; Gray, H. B.; Abde las, M.; Gross, Z. *Tetrahedron Lett.* **2003**, *44*, 2077–2079.
31. McClure, D. S. *J. Chem. Phys.* **1952**, *20*, 682–686.
32. Fraiji, L. K.; Hayes, D. M.; Werner, T. C. *J. Chem. Educ.* **1992**, *69*, 424–428.
33. (a) Sharma, P.; Mehata, M. S. *Optical Materials* **2020**, *100*, 109646; (b) Sharma, P.; Mehata, M. S. *Materials Research Bulletin* **2020**, *131*, 110978; (c) Sharma, V.; Mehata, M. S.; *Spectrochimica Acta Part A: Molecular and Biomolecular Spectroscopy* **2021**, *260*, 119937; (d) Sharma, V.; Mehata, M. S. *Materials Research Bulletin* **2021**, *134*, 111121.
34. D’Souza, F.; Chitta, R.; Ohkubo, K.; Tasior, M.; Subbaiyan, N. K.; Zandler, M. E.; Rogacki, M. K.; Gryko, D. T.; and Fukuzumi, S. *J. Am. Chem. Soc.* **2008**, *130*, 14263-14272.
35. Clark, D. T.; Murrell, J. N.; and Tedder, J. M. *J. Chem. Soc.* **1963**, 1250-1253.

CHAPTER 5

CONCLUSION AND FUTURE SCOPE

5.1 Conclusions

Corrole has contracted core than porphyrin and similar to corrin ring of vitamin B₁₂. Corrole has characteristic to stabilise the metal ion in various oxidation state. In many applications, Corrole has superiority over porphyrin. So corrole has major attention in recent years. Many research groups have given synthesis method of corrole and metallocorrole and explored its applications in different fields such as sensing, solar cell, catalysis, medicinal etc. But there are some fields which are not yet explored. This thesis contains some of the less explored field in corrole chemistry. The first chapter of thesis is about the basic, type of corroles and its synthetic protocols and also discussed the application of corroles in various fields. The second chapter of thesis contain my objectives which are completed in my PhD journey. In the third chapter, Catalytic acitivity of bis p-nitro A₂B (oxo)Mn(V) corroles towards sulfides was discussed. We synthesised the series of five *trans*-A₂B corrole and its manganese complex of corrole and also its oxo complex of manganese corrole. Out of five **1**, **2**, **3** A₂B corrole and its manganese corrole already reported in earlier reports, so matched the analytical data of these compounds with literature. But **4**, **5** A₂B corroles and its manganese complex and also all five (oxo)manganese(V) corrole are newly synthesised which are characterised by UV-visible spectroscopy, mass spectroscopy ¹H NMR spectroscopy and CHN analysis. We studied the kinetic rate of self-decay of (oxo)manganese complexes and kinetic rate of oxygen atom transfer from (oxo)manganese complexes to sulfides. The oxygen atom transfer reaction followed two pathways first one is disproportionation

mechanism and second is direct pathway. We studied the electrochemistry of all five Mn-corroles. We were calculated the HOMO-LUMO gap using the DFT calculations. After the all study, when change the substituent of phenyl ring at C₁₀ position of corrole then we obtained different quantitative data. So we concluded that the reactivity of bis p-nitro A₂B (oxo)Mn(V) corroles affected by the negative electro inductive effect (-I effect). These result will motivate to scientist of medicinal field for utilisation of sulfoxides. In next chapter, we were explored the sensing ability of *trans*-A₂B free base corrole towards the metal ions. We were studied over the four *trans*-A₂B free base corrole in which **1**, **2** *trans*-A₂B free base corrole already reported in our previous research article and **3**, **4** *trans*- A₂B corrole newly synthesised and characterised. We were characterised by using different spectroscopic techniques such as UV-visible, ¹H NMR and mass spectrometry. We were collected the photo physical data of *trans*- A₂B corroles during the addition of metal ions. Then we found that all four *trans*- A₂B corroles have high sensing ability towards Hg²⁺ ion, which was proved by the value of LoD and required Hg²⁺ ion for completing the fluorescence quenching of the *trans*- A₂B corroles. We were obtained the differ value of LoD and required of analyte for complete quenching of the *trans*- A₂B corrole, when we changed the halogen atom or its number at phenyl ring of C₁₀ position of corrole. These interesting results will motivate for designing new chemosensor which have sensing ability towards hazardous cation and anion.

5.2 Future scope

Ultimately, the first aim of this thesis improve the method of oxidation reaction by using (oxo)manganese(V) corrole. The intermediates of high valent oxo manganese

corrole can be used as catalyst for biomimetic oxidation reactions. Currently, investigations are under proceed in our laboratory to better define mechanistic pathways with the application scope of (oxo)manganese(V) corrole and eco-friendly oxidant for oxidation of organic reactions. In photochemistry, we will try to produce the high valent oxo manganese corrole using the visible light, which is working as eco-friendly catalyst. Eco-friendly catalyst has significant application in medicinal and environmental field. Second aim of the thesis design the fluorescent chemosensors, which is highly sensitive towards ions. These chemosensors have applications in different fields such as analytical chemistry, biomedical analysis, environmental science. Currently in our lab, explored the corrole by change of halogen derivative for sensing the hazardous anions like as cyanide, fluoride, phosphate etc. And also we will monitor the analytes either *vitro* or *in vivo*.

LIST OF PUBLICATIONS

1. Atul Varshney and Anil Kumar; A₂B corroles: fluorescent signalling system for Hg²⁺ ion; *J. Chem. Sci.*; 2022, **134**:124.
2. Atul Varshney, Deepali Ahluwalia, Ritika Kubba, Jyoti, Anil Kumar; Recent developments in corroles as an ion sensor; *Journal of the Indian Chemical Society*; 2022, **99**, 100708.
3. Atul Varshney, Anil Kumar, Sunil Yadav; Catalytic activity of bis p-nitro A2B (oxo)Mn(V) corroles towards oxygen transfer reaction to sulphides; *Inorganica Chimica Acta*; 2021, **514**, 120013.
4. Deepali Ahluwalia, Atul Varshney, Sachin Kumar, Anil Kumar, Sudhir Gopalrao Warkar, Narendra Singh, and Prashant Dubey; One-pot synthesis of magnetic iron phosphide nanoparticles; *Inorganic and Nano-Metal Chemistry*; 2020, **2**.
5. Omprakash Yadav, Atul Varshney, Anil Kumar, Ratneshwar Kumar Ratnesh, Mohan Singh Mehata; A₂B corroles: Fluorescence signaling systems for sensing fluoride ions; *Spectrochimica Acta Part A: Molecular and Biomolecular Spectroscopy*; 2018, **202**, 207–213.
6. Usha Raju, Atul Varshney and Anil Kumar; Mesoporous Multi-Metal Citrates as Scavengers for Organic Dyes; *J. Surface Sci. Technol.*; 2018, **34**(1–2), 50–57.
7. Omprakash Yadav, Atul Varshney, Anil Kumar; Manganese(III) mediated synthesis of A2B Mn(III) corroles: A new general and green synthetic approach and characterization; *Inorganic Chemistry Communications*; 2017, **86**, 168–171.

LIST OF CONFERENCES AND WORKSHOP

1. **Atul Varshney**, Narendra Singh and Anil Kumar “One-pot Synthesis of Magnetic Iron Phosphide Nanoparticles” International conference on Bio and Nano Technologies for Sustainable Agriculture, Food, Health, Energy and Industry (ICBN-2018), 21-23 February 2018, Department of Bio & Nano Technology, GJU & ST, Hisar, India. (Poster presentation)
2. Om Prakash Yadav, **Atul Varshney** and Anil Kumar “A new Synthetic Methodology for A₂B Manganese(III) corroles”, International conference on advances in analytical sciences (ICAAS -2018), 15-17 March 2018, CSIR – Indian Institute of petroleum, Dehradun, India. (Poster presentation)
3. **Atul Varshney**, Anil Kumar “Catalytic Property of Bis p-Nitro A₂B Mn(III) Corrole” Tenth International conference on Porphyrins & Phthalocyanines, 1-6 July 2018, Munich, Germany. (Poster presentation).
4. “**Workshop on Molecular Modelling**” held on 23 January **2018**, organized by ARSD College, University of Delhi, Delhi, India.

ABOUT THE AUTHOR

Name: **Atul Varshney**

Father's Name: Rakesh Kumar Varshney

Mother's Name: Reeta Varshney

Nationality: Indian



The author completed his bachelor's and master's degree in Chemistry from D. S. college, Aligarh. He pursued his M.Sc. in inorganic chemistry as specialization. He joined DTU in the year 2016 as a JRF under Prof. Anil Kumar at the Department of Applied Chemistry, DTU. His research work revolves around the applications of free base corrole and manganese corrole. During his Ph.D. he has received Commendable research excellence award in 2017, 2022, 2023 by Delhi Technological University. In 2018, he joined Basic Education Department, Uttar Pradesh as assistant teacher at Composite school Nagla Govind, Hasayan, Hathras.